STRENGTH AND BEHAVIOR OF REINFORCED CONCRETE TWO-WAY IRREGULAR JOIST FLOORS UNDER CONCENTRATED LOAD

Aristide Nicolopoulos

A Thesis

in

The Faculty

of

Engineering

Presented in Partial Fulfillment of the Requirements
for the degree of Doctor of Philosophy at
Concordia University
Montreal, Quebec, Canada

November 1982

ABSTRACT

ABSTRACT

STRENGTH AND BEHAVIOR OF REINFORCED CONCRETE TWO-WAY IRREGULAR JOIST FLOORS UNDER CONCENTRATED LOAD

Aristide Nicolopoulos, Ph.D.
Concordia University, 1982

Economic trends necessitate the introduction of structural systems which use less material and are simpler in erection. Reinforced concrete ribbed structural systems are recognized as a means of achieving the above economic objectives.

The irregularly-ribbed joist floor is a particular case of ribbed floors characterised by orthogonally unevenly distributed ribs of the same or different geometry. These floors, in addition to the above-mentioned economic advantages, have the potential to contribute structural efficiency and architectural flexibility.

The construction of such floors is economically feasible today, due to the introduction of a new versatile plastic formwork system, developed with the author's participation. Since these floors represent a relatively new concept in the building industry, the need for the development of appropriate design guidelines is apparent. The objective of this thesis is to study experimentally the strength and behavior of these floors and to develop basic criteria and procedures required in design practice.

For the purpose of analysis, the joist floors are approximated in this study, by an equivalent open grid of T-beams. Both elastic and collapse analysis of grillages are examined as prerequisites of a refined design process. The elastic analysis is done by the matrix-displacement method using an appropriate commercially available computer program. The collapse analysis is accomplished by the use of appropriate "upper" and "lower bound" limit analysis techniques.

A class of methods of limit design for reinforced concrete frames, presented by M.Z. Cohn and referred to as "equilibrium (serviceability)" methods, is used as the basis for the development of a trial-and-error limit design procedure appropriate for the conceptual design of irregular joist floors.

A series of joist floor models is studied analytically and experimentally. The study is limited however, to ribbed single-panel models simulating several types of two-way irregular joist floors, subjected to a single concentrated load (aiming at applications in industrial buildings.)

The analytical investigation of the models is made on the basis of the proposed limit design procedure. The experimental program provides information on the elastic and elasto-plastic behavior of the models and helps the understanding of the collapse mechanisms and the evaluation of the "true" collapse load. Also, an assessment of the accuracy of the analytical procedure is made. The effect of reinforcement transfer from the middle to the edge strips of the models is also studied in order to explore the different possibilities of distribution of reinforcement between the ribs.

Several recommendations for the design of two-way irregular joist floors are presented, as a result of this research program.

ACKNOWLEDGEMENTS

ACKNOWLEDGEMENTS

The author wishes to express his sincere appreciation to his supervisor, Dr. Zenon A. Zielinski, Professor of Civil Engineering, for his encouragement and advice during the course of this work.

Thanks are also due to personnel of the Structures Laboratory of Concordia University, where the experimental work was carried out.

Special thanks to Miss M. Stredder for her concerned work in typing this manuscript.

The financial support provided by NSERC (National Science and Engineering Research Council) of Canada under Grant A-1017 and by BEER Construction Company of Montreal, is gratefully acknowledged.

TABLE OF CONTENTS

TABLE OF CONTENTS

LIST OF TABLES

LIST OF TABLES

LIST OF FIGURES

LIST OF FIGURES

NOTATION

NOTATION

The letter symbols throughout this study are defined as follows:

A_s	Provided area of tension reinforcement
A_s^{req}	Required area of tension reinforcement
$A_{s,total}$	Total area of tension reinforcement in each direction
b	Width of compression face of equivalent T-beam
b_w	Minimum width of joist web
c	Clear concrete cover for main reinforcement
d	Effective depth of equivalent T-beam
d_{av}	Assumed average effective depth
E_c	Modulus of elasticity of concrete
E_s	Modulus of elasticity of steel
E_i	External work done by the ultimate loads in the mechanism i
$f(\ )$	A function of the variables shown in parenthesis
f_c	Stress in concrete
f'_c	Specified compressive strength of concrete
f_c^t	Tensile strength of concrete
f_s	Stress in steel reinforcement

f_y	Specified yield strength of reinforcement
h	Overall thickness of joist floor
h_f	Thickness of the top slab
h_w	Depth of the joist web
i	Index referring to a loading scheme or collapse mode (i=1,2,...)
I	Moment of inertia about the centroidal axis of a member cross-section
g	Indicator referring to a gross concrete section
cr	Indicator referring to a cracked transformed reinforced concrete section
I_x	Torsional rigidity factor in the application of the "STRESS" program
I_y	Moment of inertia in the application of the "STRESS" program
J	Torsional rigidity factor of a member cross-section
j	Index referring to a critical section (j=1,2,...)
L	Span length measured from center-to-center of supports
ℓ	Length module of the equivalent grid
M	Moment at the center of the ribs
M_j	Elastic envelope moment value at section j, due to service load
$\bar{M}_j$	Elastic envelope moment value at section j, due to ultimate load
$\bar{M}_k$	Elastic envelope moment value at section k, due to ultimate load

M_o Total one-way static moment

$M_{o,u}$ Total one-way static moment, due to ultimate load

$M_{p,j}$ Plastic moment at section j

M_p^n Plastic moment at a critical section of rib n

M_u Ultimate moment capacity of a rib section

M_w Working moment capacity of a rib section

M_x Moment in the ribs of the x-direction

M_y Moment in the ribs of the y-direction

n Modular ratio = E_s/E_c

P Concentrated load applied at the center of the test-panels

P_u Ultimate load capacity of the test-panels

P_w Working load capacity of the test-panels

q Net reinforcement index of a critical section

s Spacing of joists

U_i Energy dissipated by plastic hinges in the mechanism i

W Specified or experimental service load

W_u Specified or experimental ultimate (limit state) load

$W_{u,i}$ Ultimate load for collapse mode i, based on plastic analysis

x Distance of the neutral axis from the extreme compression fibre

x_i	Serviceability index associated with mechanism i
$\bar{x}_i$	Balanced yield safety parameter associated with mechanism i (all x_j's equal)
x_j	Yield safety parameter of section j
x_j^{all}	Admissible yield safety parameter of section j
x_k	Yield safety parameter of section k
x_θ	The maximum x_j value that ensures rotation compatibility
x^n	Yield safety parameter at a critical section of rib n
y_i	Percentage of elastic moment redistribution associated with mechanism i
δ	Deflection recorded or estimated
δ^{all}	Maximum allowable deflection
ε'_c	Recorded strain in concrete at the lower face of the top slab
ε_s	Recorded strain in steel reinforcement
∂_j	Inelastic rotation of section j
∂_{pj}	Rotation capacity of section j
λ_o	Overall load factor (safety against structural collapse)
λ_1	First yield load factor (safety against local section failure)
λ_{1j}	Yield load factor at section j
λ_i	Collapse load factor in failure mode i

ΣM	Total one-way moment
ΣM_{av}	Average total ultimate moment capacity in the two directions
ΣM_x	Total moment in the x-direction
$\Sigma M_{x,u}$	Total ultimate moment capacity in the x-direction
ΣM_y	Total moment in the y-direction
$\Sigma M_{y,u}$	Total ultimate moment capacity in the y-direction
ϕ	Diameter of chosen rib reinforcement

CHAPTER 1

INTRODUCTION

CHAPTER 1

INTRODUCTION

1.1 GENERAL

Reinforced concrete ribbed slabs are recognized as a means of maximizing structural efficiency, while minimizing the weight and cost in floor construction.

These structures often are also chosen by architects to create large floor spans at comparatively reduced headroom and for their aesthetic advantages.

The construction of such structures has been simplified by the introduction of removable form-pans made from steel, plastics and other suitable material.

However, the choice of types of ribbed slabs which are appropriate for floor applications, may be limited by such structural restraints as geometry and loading, as well as by practical and economical considerations such as availability of the appropriate formwork system, appearance, etc.

Two-way ribbed floor systems can be generally classified according to the criteria shown in Figure 1.1.

A ribbed floor system can be considered to be either a joist system or a slab and beam system, depending on whether

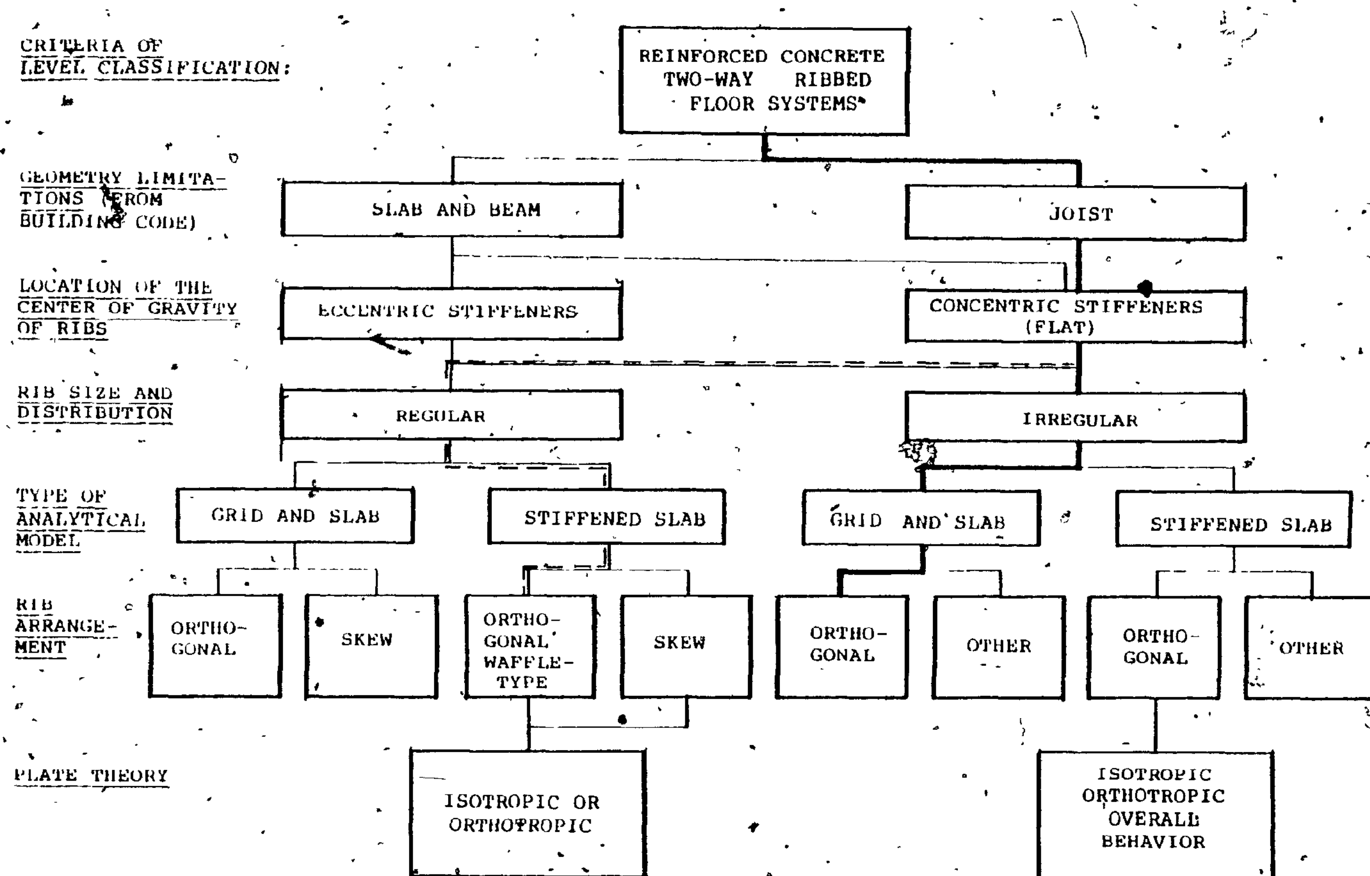

FIG. 1.1 PROPOSED CLASSIFICATION OF THE TWO-WAY RIBBED FLOORS

or not the geometry limitations specified by the "Code for the Design of Concrete Structures for Buildings" (CAN3-A23.3-M77, Section 6.9) are met.

Joist floors usually have ribs of the same depth, whereas slab and beam systems may have either ribs of the same depth or sets of ribs of different depths (eccentrically stiffened systems).

Furthermore, ribbed floor systems can be distinguished as regular and irregular. As irregular systems, those having stiffeners of the same or different geometry, unevenly distributed in orthogonal directions may be specified. Skew or other type arrangements of ribs are also possible. Regular systems with non-uniform loading may also be classified as irregular for design purposes.

Ribbed systems may also be subdivided for the purpose of analysis into equivalent grid and slab systems, or equivalent stiffened slab systems, according to the relative proportions of slab and ribs, or according to the theoretical interpretation of their overall behavior.

Orthogonally ribbed systems may be further distinguished as isotropic or orthotropic. In the case of orthotropic ribbed systems the cause of the orthotropy may be the different geometry and/or the different spacing of ribs in the two orthogonal directions.

As an example of this classification, waffle-type or coffered slab floors can be specified as regular, orthogonally ribbed joist floor systems, which are usually treated as stiffened slabs (identification shown in dashed line in Fig. 1.1).

Irregularly ribbed joist floor systems defined according to the above classification represent a wide range of possible rib patterns which can be used to provide additional flexibility and efficiency in the design of floor structures. These floor systems may be particularly useful in structures where geometrical discontinuities such as large openings, mixed boundary conditions, unusual slab shapes, etc., or non-uniform loading conditions exist. All these cases usually require a design outside the code rules for two-way slab systems.

Irregularly ribbed joist floor systems with rib concentrations and orientations, corresponding to the actual loading conditions and geometrical characteristics of particular individual applications, can provide proper structural behavior and good serviceability. Such irregular joist floor systems can be formed by a subdivision of the slab structure into strong or supporting zones (strips or bands) and weak or middle zones. In such irregular systems a degree of regularity in the arrangement of their ribs is still desirable; thus a uniform distribution of ribs within each zone but different concentrations of ribs in different zones may be considered.

1.2 APPLICATION OF TWO-WAY IRREGULAR JOIST FLOORS

A new plastic formwork system suitable for the construction of reinforced concrete two-way, orthogonally ribbed joist floor systems has been developed with the author's participation (Zielinski and Nicolopoulos 1980) [1]. The system was developed at the conception stage of this research program, to fulfil the need for a versatile formwork, appropriate for practical applications of irregularly ribbed joist floors.

With this system, joist floors can be constructed using segmental plastic form-pans made up as assemblies of modular replaceable end and filler units, as illustrated in Figure 1.2. The system has the flexibility enabling the forming of regular and irregular joist floors of various orthogonal grid patterns. By matching two end units, square base domes are formed, suitable for waffle-like floor structures with square voids. By combining two end units with several filler units, long-domes of rectangular bases and of different modular lengths are formed, suitable for irregular joist floor systems.

The development of the formwork system was sponsored by Beer Construction Co. The system is now marketed under the trade mark of BEER-ZAZ. The development of the system included laboratory tests at Dupont Canada, and structural tests and design work by the author at Concordia University. Different joist floor system applications have also been developed. Example applications are demonstrated in Figures 1.3 and 1.4, showing the placing of concrete on the formwork

FIG. 1.2 THE BEER-ZAZ SEGMENTAL FORM-PAN SYSTEM

FIG. 1.3 PLACING CONCRETE ON FORMWORK MADE WITH BEER-ZAZ PAN SEGMENTS

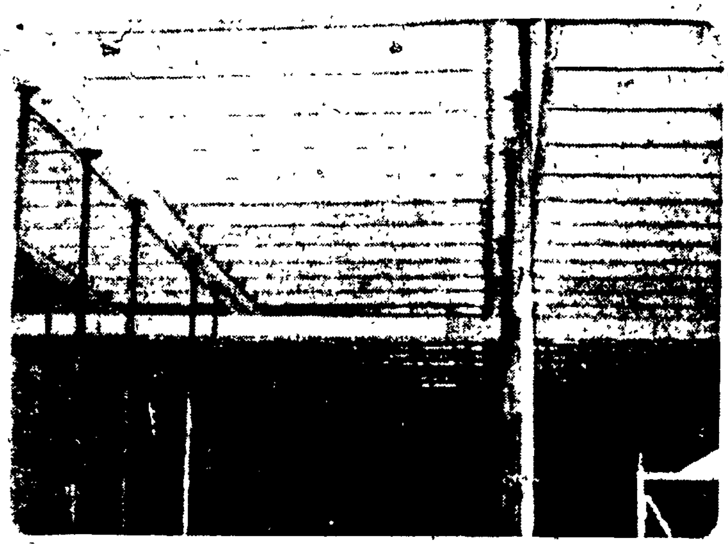

FIG. 1.4 FINISHED CEILING AFTER FORMWORK REMOVAL

and the finished ceiling after the stripping of the formwork.

A series of joist system examples for square and rectangular multi-bay floors with uniformly or unevenly distributed ribs, based on the modular dimensions of the BEER-ZAZ formpans is shown in Figure 1.5. These example floors are designed for residential or commercial buildings where uniformly distributed loads prevail.

Irregularly ribbed joist floors can have a wide range of applications. However, the present study is limited to the investigation of the orthogonally, irregularly ribbed joist floors (identification shown in thick line in Figure 1.1), subjected to a single concentrated load, as is often encountered in the design of reinforced concrete slabs in industrial buildings.

The flexural behavior and bending moments are of prime importance in the design of such structures. Shear and torsion are usually less significant factors. In most cases of joist systems, the ribs have flexural cracks under the service load, which is acceptable in reinforced concrete design practice. The neutral axis of the rib T-sections in bending, normally falls within the flange, and the torsional rigidity of the cracked ribs becomes practically negligible. In this way, the concrete area in the web of the ribs under load remains practically inactive for the purpose of flexural resistance. By recognizing that the flexural rigidity of the top slab itself, is very small, the joist system can be

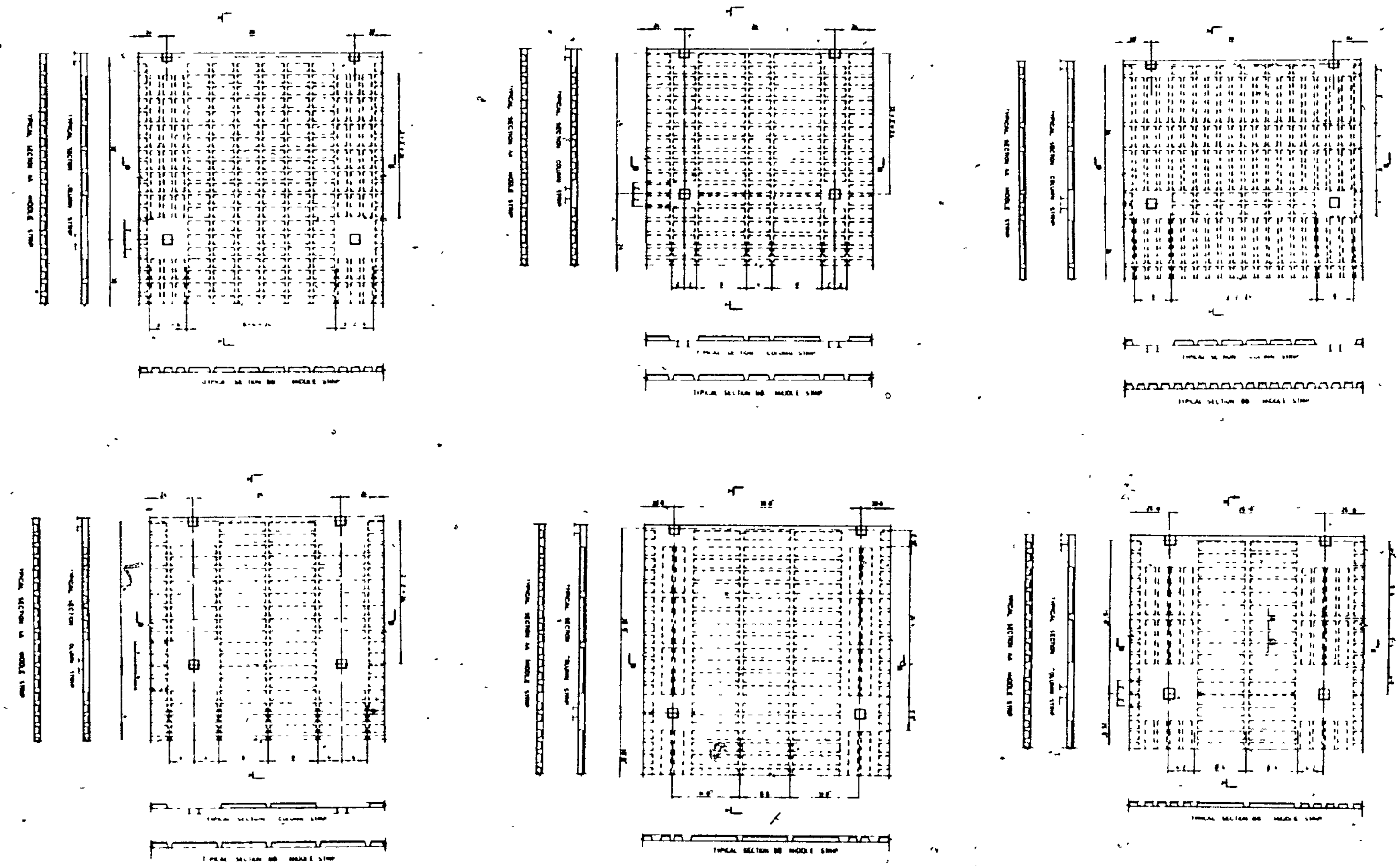

FIG. 1.5 EXAMPLES OF TWO-WAY JOIST FLOOR SYSTEMS

considered as an open grid of T-beams with flexural rigidities as provided by the concrete area in the flange of the T-beam in compression and the steel area in the web in tension.

This assumption allows an important simplification in the analysis of irregularly ribbed joist floors by treating them as equivalent grids. Also, in this way, the collapse behavior of these floors can easily be rationalized.

The distribution of reinforcement is an important factor exerting influence on the behavior and strength of the shallow ribbed reinforced concrete joist floors in post cracking stages. Research has shown that satisfactory serviceability can be achieved when reinforcement is distributed between the ribs according to the distribution of elastic moments. It can also be stated that, since flexural rigidities of the transformed rib sections are proportional to the amount of reinforcement in the ribs, the pattern of the ribs is of limited importance and the ribs should be rather regarded as a means for accommodating the required tension reinforcement with respective concentration in the heavily loaded zones.

1.3 SCOPE OF THE STUDY

Reinforced concrete two-way irregular joist floors may have a wide application in building construction because of their potential advantages offered, which include architectural flexibility and construction economy, as well as structural adaptibility and efficiency.

The application of these floors is to be checked mainly for geometrical inadequacies in the rib arrangements. There may be circumstances where the reinforcement needed, according to an elastic analysis, and the available concrete area in the ribs cannot be matched. A solution to this problem may be to transfer the reinforcement which cannot be accommodated in the ribs of strips considered, to the neighboring strips where more concrete area may be available, as in the case of column strips where larger ribs or solid concrete zones are usually provided. The feasibility of this solution remains to be checked.

The purpose of this study is to investigate experimentally the behavior and strength of two-way irregular joist floors subjected to a single concentrated load, and subsequently, to develop those design criteria and procedures required to facilitate their application in building practice.

The study includes strength tests on square, single panel joist floor models with differently orthogonally distributed and reinforced ribs, where various percentages of reinforcement have been transferred from the middle to the edge strips.

CHAPTER 2

STATE OF THE ART REVIEW

CHAPTER 2

STATE OF THE ART REVIEW

2.1 GENERAL

Theoretically speaking, for a precise elastic analysis of reinforced concrete irregularly ribbed floors, probably the best results can be obtained by an analytical procedure in which the ribs and top slab are treated as separate elements. The procedure would take into account the bending and membrane action in the slab, axial forces, biaxial bending and torsional moments in the ribs, while satisfying the equilibrium and compatibility requirements at the joints between the slab and rib portions. Similarly, for a detailed limit analysis of these floor systems, various combinations of grid and slab yielding mechanisms must be examined in order to predict the "true" collapse load.

For practical engineering applications, the reinforced concrete two-way irregularly ribbed joist floors may be analysed by using either an equivalent slab, or an equivalent grid theoretical model. In the case of an equivalent slab, irregularities in the stiffening system may cause difficulties in the analytical formulation of the problem and in the derivation of generalized procedures. Thus, the equivalent grid model is considered more appropriate.

Another alternative is the application of the finite element method. Various modelling techniques have been used in the past to study different problems. Such techniques may use plate finite elements for the representation of the slab and offset unidimensional beam elements at the centroidal lines of the ribs, which are joined by elements of infinite stiffness with the slab elements. In this way, the effect of T-beam action can be closely approximated. Some other techniques may instead use plate elements for the slab in combination with three-dimensional solid elements for the modelling of the ribs. Also, for the elastoplastic finite element analysis of ribbed systems, some different modelling techniques have been devised, such as the ones using layered systems of beam and plate elements, or plate elements for the slab and a combination of solid element and hollow rebar elements for the ribs.

However, because of the geometry of the ribbed slabs, a large number of elements are required to obtain an accurate solution. Therefore, it may not be an economical procedure for this type of structure.

For the elastic analysis of an equivalent grid system, the matrix-displacement method can be used. This method utilizes the matrix formulation of slope-deflection equations, one of the classic methods of structural analysis.

Various computer programs are commercially available today for this type of analysis, which are considered fast and inexpensive. One of these programs is STRESS (Structural Engineering System Solver), which is capable of analysing any type of two or three-dimensional frame. Another similar program especially created for grid analysis is the GRIDSAP. This program is one of the SAP (Structural Analysis Programs) group of programs available as part of the STRU-PAK library.

For the limit analysis of grids, the "true" collapse load may be approached either by an "upper bound" solution, based on the virtual work method and a kinematically admissible mode of failure, or by a "lower bound" solution, based on the plastic equilibrium method and a statically admissible mode of failure. If the upper and lower bound results coincide, this is a confirmation for the uniqueness of the collapse load ("unique" solution of limit analysis). The collapse load corresponding to the lower bound solution is always a conservative assumption for design purposes.

One program currently available commercially for the elasto-plastic limit analysis of three-dimensional frames, is the LAGS (Limit Analysis of General Structures), which is one of the programs of the SDRC (Structural Dynamics Research Corporation) library.

All the above-mentioned computer programs are available from most of the major data centers in Canada.

2.2 ANALYSIS AND DESIGN OF TWO-WAY RIBBED FLOORS

Previous studies, which are relevant to two-way ribbed flat floor systems, have been concerned mainly with the analysis and design of regular (uniform) orthogonal or skew systems.

Studies on these structures in the elastic range include the grid analogy, the orthotropic plate approximation and an "exact" solution for ribbed plates.

Lightfoot and Sawko (1960) [2] presented a matrix-displacement computerized procedure for the grid-type analysis of various structures, including ribbed floor systems.

In a manual procedure proposed by Ray (1960) [3] for the analysis of building grid floors, the deflections are worked out by orthotropic plate theory, and for these deflections, the moment and torque distribution are calculated using an iteration method.

In a similar procedure suggested by Mase and Jain (1970) [4], the moments and torques, being the functions of second derivatives of deflections, are worked out by a finite difference method.

A matrix-displacement computerized procedure was presented by Harris (1972) [5], which, as he stated, "is particularly suited to the analysis and design of regular two-way concrete joist floors."

Reiss and Socal (1972) [6], used the orthotropic plate theory to analyse ribbed flat slabs. In their treatment, the torsional stiffness of ribs is neglected and the resulting plate equation is solved by an energy method.

Anisotropic skew ribbed slabs were studied by Goldberg, Tatsa and Levy (1977) [7]. In this investigation, the orthotropic plate theory is used and the plate equations are transformed to a skew axis system. The resulting general differential equation is then solved by an energy approach.

A computerized procedure for the analysis and design of cross-ribbed (waffle) floors as equivalent torsionless grids of T-beams, was reported by Gilardi (1978) [8]. By equating the deflections of cross-ribs at each intersection, a system of equations in matrix form is obtained.

Ribbed flat slabs were investigated also by Tebbett and Harrop (1979) [9]. In their work, an "exact" ribbed plate analysis is used which provides three simultaneous partial differential equations, and a finite difference method computer program is applied to solve these equations.

The orthotropic rigidities of concrete waffle-type slab structures were studied by Kennedy and Bali (1979) [10], for both precracking and postcracking stages.

Studies of the regular ribbed floor systems in the elasto-plastic range include both the upper and lower bound solutions.

Moreira da Rocha (1964) [11], outlined a procedure for the analysis of bridge grillages. He suggested the use of an elastic analysis to secure the serviceability requirements of the structure and then the use of a plastic[1] analysis for the structural safety against failure. In the plastic analysis, which is based on the virtual work principle, the plastic moments are proportioned to the maximum elastic moments under service loads (moment envelope), and the coefficients of proportionality are calculated on the basis of an assumed mode of failure.

Das (1966) [12], used the plastic theory to study building grid floors. In his procedure, the lowest upper bound collapse load is calculated on the basis of several trial collapse mechanisms and the virtual work principle. The collapse loads are calculated as functions of an assumed plastic moment, which applies to all critical sections for all the mechanisms. Under

[1]The term "plastic" is associated with the formation of plastic hinges in rigid, perfectly plastic materials; thus plastic analysis is a particular case of limit analysis. In the present study, the term "limit" will be used in the narrow sense, on an equal basis with the term "plastic" although it could be more appropriate to be used in relation to specific limit states of structural behavior.

the lowest collapse load, a trial statically admissible moment distribution pattern is established to ensure that nowhere is the assumed plastic moment exceeded. Thus, this collapse load satisfying both the upper and lower bounds, is defined as the true collapse load.

Regular building grid floors were also investigated by Petcu (1968) [13]. This study considers the combination of simultaneous grid and slab failure mechanisms consisting of plastic hinges in the ribs and yield lines in the slab panels. Various elementary collapse mechanisms are considered, as well as combinations of elementary mechanisms. The plastic moments which are the same for all ribs in each direction and proportional to the maximum elastic moments of the same direction, are calculated on the basis of virtual work of the external forces and of the plastic moments acting on the plastic hinges and along the yield-lines. It is shown that the maximum values of plastic moments under given uniform load are obtained in the case of a combination of all elementary mechanisms, considered to be the case of the true collapse mechanism.

Finally, Pillai and Lash (1969) [14] conducted a study on the strength and behavior of medium-span reinforced concrete grid and slab bridges. In their work, they use the plastic theory for the analysis of the equivalent grids, considering both the upper and lower bound theorems and including the plastic torsional strength of the grid members. On the basis of experimental results, they concluded that plastic theory gives a reasonably good estimate of the mode of failure and of the collapse load for this type of structure.

Although no complete treatment for the full range elastic, elasto-plastic analysis and design of reinforced concrete joist floors has been proposed and research information concerning concentrated loads is scarce, past investigations have provided enough background to adequately treat the regularly ribbed floors. Elastic procedures are well established, and the principles of plastic theory are well developed.

Moreover, for certain types of regularly ribbed floor structures, load factors have been established experimentally, allowing the estimation of service load limit from the collapse load calculated according to the plastic theory. These load factors are established on the assumption that the service load limit corresponds to the limit of the allowable deflections. These load factors also allow a realistic estimation of service load deflections by means of an elastic analysis, based on the cracked concrete sections.

On account of the fact that irregular joist floors have been chosen to be studied as equivalent grids, previous studies on the limit analysis of grillages are presented next.

2.3 LIMIT ANALYSIS OF EQUIVALENT GRID MODELS

Regular and irregular grillages in the elasto-plastic range or in the fully plastic limit state, have been studied for various loading and support conditions.

In an early paper by Heyman (1952) [15], square grids were analysed on the basis of kinematic and static principles. The procedure described consisted of the calculation of an upper bound of the collapse load and a static analysis under this load, to find the corresponding moment distribution, with all moments being proportional to an assumed plastic moment. By multiplying all moments by the ratio of the assumed moment - to - the maximum moment occurring in the distribution, moments lesser or equal to the assumed moment are established in all cross-sections and a statically admissible system results. Furthermore, by multiplying the upper bound collapse load by the same ratio, a lower bound is obtained. The true collapse load is assumed to be the average of the two bounds. It is interesting to note that in the static analysis, the torsional stiffness of the grid members has been considered, but its effect on the flexural plastic hinges of the kinematic approach has been neglected.

An analytical incremental procedure for torsionless grids was presented by Reddy and Hendry (1960) [16], based on slope-deflection equations given in matrix form. A manual iterative static equilibrium method was also presented by the same authors (1961) [17]. The method is based on an elasto-plastic moment distribution procedure using the principle of successive shear corrections.

Shaw (1963) [18], advanced the procedure of limit analysis of grillages by clarifying and generalizing the moment-balancing technique used to obtain a statically admissible moment field. He used this technique in conjunction with the mechanism technique (kinematic principle) to analyse grids of any configuration. By neglecting the torsional stiffness of the grid members and by using "unit" loads on the joints, he presented a "simple" moment balancing process,and a "systematic" one similar to the numerical relaxation process. He suggested that one should start the procedure with some possible mechanism and use the process to correctly locate flexural hinges and then to modify the chosen mechanism as many times as it is necessary in order to obtain a lower bound and at the same time, to produce an improved upper bound.

Sawko (1964) [19], presented a computerized matrix analysis procedure, based on static equilibrium, in which the torsional stiffness was included. The procedure is repeated iteratively under incremental loading, treating the elastic analysis as a special case and inserting hinges wherever the flexural moments exceed the plastic moment capacity of the members. The procedure provides continuity in the elasto-plastic range and allows a good estimation of deflection for the complete range of loading.

A method for analyzing the piecewise linear behavior of elastic-plastic grid systems was presented by Hongladaromp, Rossow and Lee (1968) [20]. By this method, torsionless grids of general form, with different flexural rigidities, plastic moment capacities and member spacing can be analysed for various loading and support conditions. The method combines static equilibrium and compatibility equations to produce a system of governing equations in matrix form, appropriate for computer programming. The use of this method with an incremental loading technique can provide a complete load-deformation history of the grid system.

Finite difference calculus was used by Wah (1969) [21], to analyse regular, torsionless, elastic-plastic grillages under arbitrary loadings. The method is programmable and is based on the lower bound theory. The use of the method enables the determination of the deflection and bending moments at all stages of the loading, until the formation of a collapse mechanism.

A numerical method for the limit analysis of grillages, based on the lower bound theorem, was presented by Sonoda and Kurata (1970) [22]. This computerized method uses non-linear convex programming on account of the convexity of yield surface, and can be applied to the analysis of anisotropic and arbitrary-shaped grillages and plates.

Walsh (1970) [23], used a successive elastic analysis procedure, similar to the one used by Sawko, to estimate the collapse load in grids, taking into account their torsional stiffness. The method is based on the lower bound theorem and consists of two phases. In the first phase of successive analysis, torsional stiffness is zero and flexural hinges are inserted at the sections where the plastic moment is reached. In the second phase of successive analysis, both the flexural and torsional hinges are inserted wherever the plastic flexural moment and plastic torsional moment are reached, respectively. The collapse load is calculated as a linear combination of the two solutions. The method is programmable and gives an elastic analysis solution in each intermediate step. For torsionless grids, the first phase is sufficient to provide an accurate solution.

Askari (1976) [24], developed a computerized procedure for the analysis of torsionless grids to produce a "unique" collapse load, based on both the upper and lower bound solutions. Using the static method, he presents a system of simultaneous equations in matrix form, aiming to maximize a parameter multiplier of the forces and thus, to define the number and location of the critical sections and the corresponding lower bound collapse mechanism. Then, using the kinematic method, he obtains a system of equations corresponding to possible collapse mechanisms. Subsequently linear programming is used to calculate the minimum value for the forces multiplier parameter and to obtain the corresponding lowest, upper bound collapse mechanism.

Corner-supported square grillages and point-supported continuous grillages were studied by Marsh (1977) [25]. On the basis of the results from the incremental collapse analysis of space trusses, he suggested that the absence of torsional stiffness in grillages may lead to the creation of unidirectional yielding in certain zones, rather than to the formation of flexural hinges along hypothetical yield lines. Assuming a particular collapse mode, he is using the energy method to provide theoretical evidence.

Various types of torsionless regular grids have been studied by Grigorian, and generalized unique collapse load formulae have been established on the basis of upper and lower bound theorems of limit analysis, using finite difference calculus. In one of his papers (1973) [26], corner-supported rectangular grillages under uniform load are treated, with special attention focused on the critical strength of the edge beams. In another paper (1977) [27], the case of concentrated loads is studied, using techniques developed in his previous studies.

In an extension of the work of Grigorian, Massonnet and Save (1980) [28], presented a procedure for the analysis of irregular grillages with unequal spacing of beams suitable for application in hydrostatically-loaded structures.

This short description of the available literature in the area of the limit analysis of grillages, gives a good picture of the developments accomplished in this field over the past thirty years, and offers guidance for the choice of the appropriate procedures to be used in the different problems, according to the precision required and the availability of resources.

Shaw's method will be used in this study to analyse the experimental program test-panels, as equivalent grids of T-beams. His method has been chosen because it offers a simple and comprehensive manual procedure, appropriate for treating concentrated loads.

2.4 LIMIT DESIGN OF EQUIVALENT GRID MODELS

The progress report on code clauses for limit design, presented by the ACI-ASCE Committee 428 (1968) [29], provides some basic information and guidance for the limit design of reinforced concrete frames.

A class of methods of limit design, referred to as "equilibrium (serviceability)" methods, were presented by Cohn (1972) [30]. Their mathematical formulation expresses the satisfaction of equilibrium and serviceability by explicitly considering the limit states of global and local failures (structural collapse and yielding of any section). Satisfaction of the compatibility condition requires a separate analysis. These methods are appropriate for a direct limit design of reinforced concrete frames, and some of their principles will be used in this study.

The methods are supplemented with an appendix on draft code provisions. Although these provisions are restricted to continuous one-way slabs, continuous beams and one-storey frames, an extension into grid structures may be considered as a starting point.

The basic procedure followed in the above class of methods has been summarized in a flowchart form by the author of this thesis using Cohn's notation, and is illustrated in Figure 2.1. Application of the procedure for the limit design of the equivalent grid models, which are discussed in the experimental program, is demonstrated in Appendic C.

A thorough study on the structural standards relative to the inelasticity in reinforced concrete was also presented by Cohn (1979) [31]. Various aspects are treated in this investigation, such as load factors, understrength factors, and elastic moment redistribution. The existing compatibility and equilibrium methods of limit design are reviewed, and he concludes with the remark that on the basis of the equilibrium methods, the formulated draft code provisions are simple and may be beneficial to the practice of structural concrete design.

START

DATA FOR LOADS, MEMBER PROPERTIES AND OTHER PARAMETERS

$W, W_u, I, J, E_c, b, d, f'_c, f_y, \gamma_1 = 1.2, \min x_j^{all} = 0.70, \delta^{all}$

DETERMINE THE MINIMUM YIELD SAFETY PARAMETER ($\min x_j$)

$\min x_j^{all} \le \min x_j = \gamma_1 \gamma_0 = 1.2 (W_u / W) \ge 1.0$

CHECK DEFLECTIONS AND OTHER SERVICEABILITY REQUIREMENTS

$\delta = f(W, I, J, E_c) \le \delta^{all}$

DETERMINE THE ELASTIC MOMENT ENVELOPE FOR THE SPECIFIED ULTIMATE LOAD

$\bar{M}_j = f(W_u, I, J, E_c)$

WRITE LIMIT EQUILIBRIUM EQUATIONS AND ADDITIONAL SERVICEABILITY CONDITIONS

$U_i [(x_j \bar{M}_j), \theta_j] \ge E_i [W_u, \theta_j]$

$x_j = x_k = \bar{x}_b$ OR $x_j \bar{M}_j = x_k \bar{M}_k = (x\bar{M})_b$.

(NOTE: ALTERNATIVE SERVICEABILITY CONDITIONS WITH EQUAL OR ASSIGNED x_j VALUES FOR CERTAIN SECTIONS, MAY BE CONSIDERED)

BY SOLVING THE ABOVE SYSTEM OF EQUATIONS AND INEQUALITIES CALCULATE THE BALANCED YIELD SAFETY PARAMETERS OR THE BALANCED PLASTIC MOMENTS AND DETERMINE THE SCALE FACTORS (x_j)

$\bar{x}_i = \bar{x}_b$ OR $(x\bar{M})_i = (x\bar{M})_b$

$\min x_j \le x_j = \max \bar{x}_i \le 1.0$ OR (THE ASSIGNED AND DERIVED VALUES)

DETERMINE THE DESIGN PLASTIC MOMENTS (M_{pj})

$M_{pj} = x_j \bar{M}_j$ OR $\min x_j \bar{M}_j \le M_{pj} = \max (x\bar{M})_i \le \bar{M}_j$

DETERMINE THE REQUIRED FLEXURAL STEEL ACCORDING TO U.S.D. METHOD AND CALCULATE THE NET REINFORCEMENT INDEX

$A_s^{req} = f(M_{pj}, b, d, f'_c, f_y)$, $q_i = (A_s^{req}/bd) \cdot (f_y / f'_c)$

DETERMINE THE WEB REINFORCEMENT FOR THE ELASTIC SHEARS CALCULATED FOR THE ULTIMATE LOAD

IN CASE THAT $\min x_j < 0.85$ AND/OR $q_j > 0.3$ CHECK THE ROTATION COMPATIBILITY OF SECTION j AND INCREASE ITS DUCTILITY IF REQUIRED (I.E., BY PROVIDING SOME COMPRESSION REINFORCEMENT)

$\theta_j \le \theta_{pj}$ OR $x_j \ge x_j'$

END

FIG. 2.1 SYNOPSIS OF COHN'S "EQUILIBRIUM (SERVICEABILITY)" METHODS OF LIMIT DESIGN FOR CONCRETE FRAMES

2.5 DESIGN PROCEDURE FOR TWO-WAY IRREGULAR JOIST FLOORS

Two-way, irregularly-ribbed joist floors may be analysed as equivalent grids of T-beams. The complete design problem of such systems involves the optimum (feasible) selection of the structural configuration and member proportions to transmit safely the various loads to the structural supports. "Optimum" may include esthetics, cost, structural efficiency, etc., while "safely" may require serviceability checks, as well as a factor of safety against collapse. The difficulties in the formulation of an explicit solution lay in the fact that it is not possible for someone to anticipate in advance the required number of ribs or the total concrete area in the ribs in each zone needed to accomodate the reinforcement required, neither is it possible to predict the performance of the system before the choice of reinforcement is made. Thus, the process of design by trial and error seems to be the most appropriate for this type of floor.

A trial and error design procedure may be accomplished in a step-by-step manner. The flowchart of such a design procedure is presented in Figure 2.2, showing the sequence of required steps and possible iterations. First, the grid is analysed in the elastic state under the factored load assuming gross concrete sections, and then the required reinforcement for the ribs, is calculated according to the U.S.D. method.

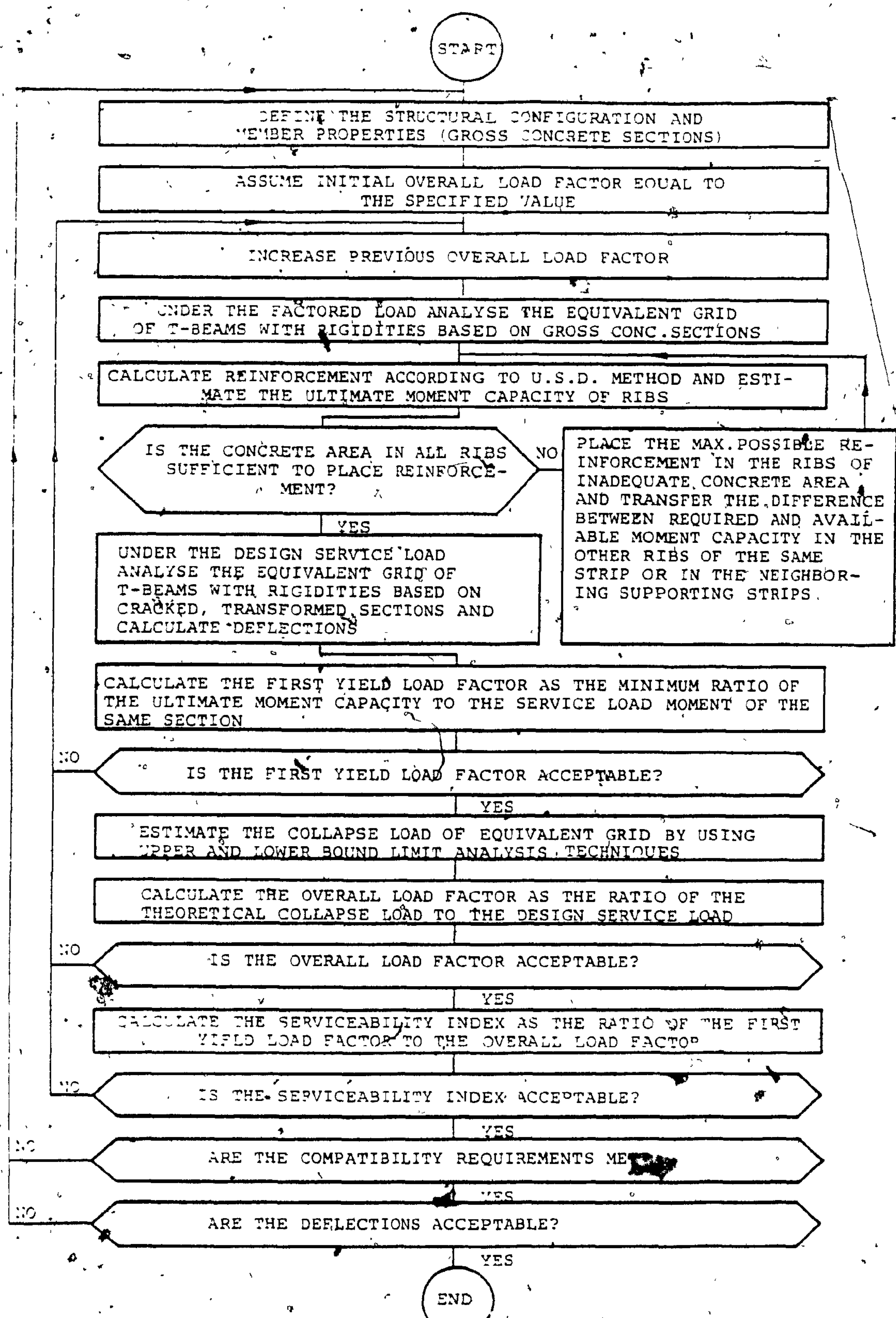

FIG. 2.2 FLOWCHART OF THE PROPOSED TRIAL-AND-ERROR LIMIT DESIGN PROCEDURE FOR TWO-WAY IRREGULAR JOIST FLOORS

It may be discovered that in certain ribs, it is impossible to place the reinforcement required because of inadequate concrete area. In that case, the maximum possible amount of reinforcement is placed in these ribs and their ultimate moment capacity is evaluated accordingly. The difference between the required and available moment capacities of the overloaded ribs is then added onto the other ribs of the same strip. If this is also impossible, the total difference in the moments of all ribs of a weak strip is transferred and distributed between the ribs of the neighboring strong strips. Larger ribs, suitable for accommodating more reinforcement, can be provided in supporting zones. On the basis of the modified moment distribution, the reinforcement is calculated in all the ribs and the ultimate moment capacity of all the ribs is estimated. Next, the properties of the cracked transformed sections of all the ribs are calculated, and the elastic analysis is repeated, under the design service load, assuming cracked transformed concrete sections, to calculate the moments and deflections. Then the first yield load factor, representing a safety factor against local section failure, is estimated as the minimum value between all critical sections, of the ratio of the ultimate moment capacity to the service load moment of the same section. Finally, a complete plastic analysis is performed to evaluate the collapse load, from which the overall load factor representing a safety factor against structural collapse, is obtained as the ratio of the collapse-to-design service load. If the various design criteria are met, the design is considered satisfactory, otherwise a higher load factor is used, which results in more reinforcement, and in the case that this measure does not produce an acceptable solution, the structural configuration of the ribbed floor is modified.

The procedure is based on the same design criteria as the "equilibrium (serviceability)" methods of limit design, and it can be presented using the same notation given by Cohn. A synopsis of the basic mathematical statements of the procedure in a flowchart form is shown in Figure 2.3. The refinement of this procedure consists of the fact that in this case, the calculated values of the various design criteria (i.e., factors and indices) are based on the final reinforcing arrangement and the rigidities of cracked transformed concrete sections, and they can be checked against some assumed minimum values.

In this procedure, the design problem is reversed, being an analytical investigation rather than a direct design. The plastic moments in the critical sections are calculated according to the chosen reinforcing arrangement for each "assumed" value of the overall load factor (λ_o^g). The subsequently calculated "actual" overall load factor (λ_o^{cr}) is the problem's variable and is successively corrected in each iteration.

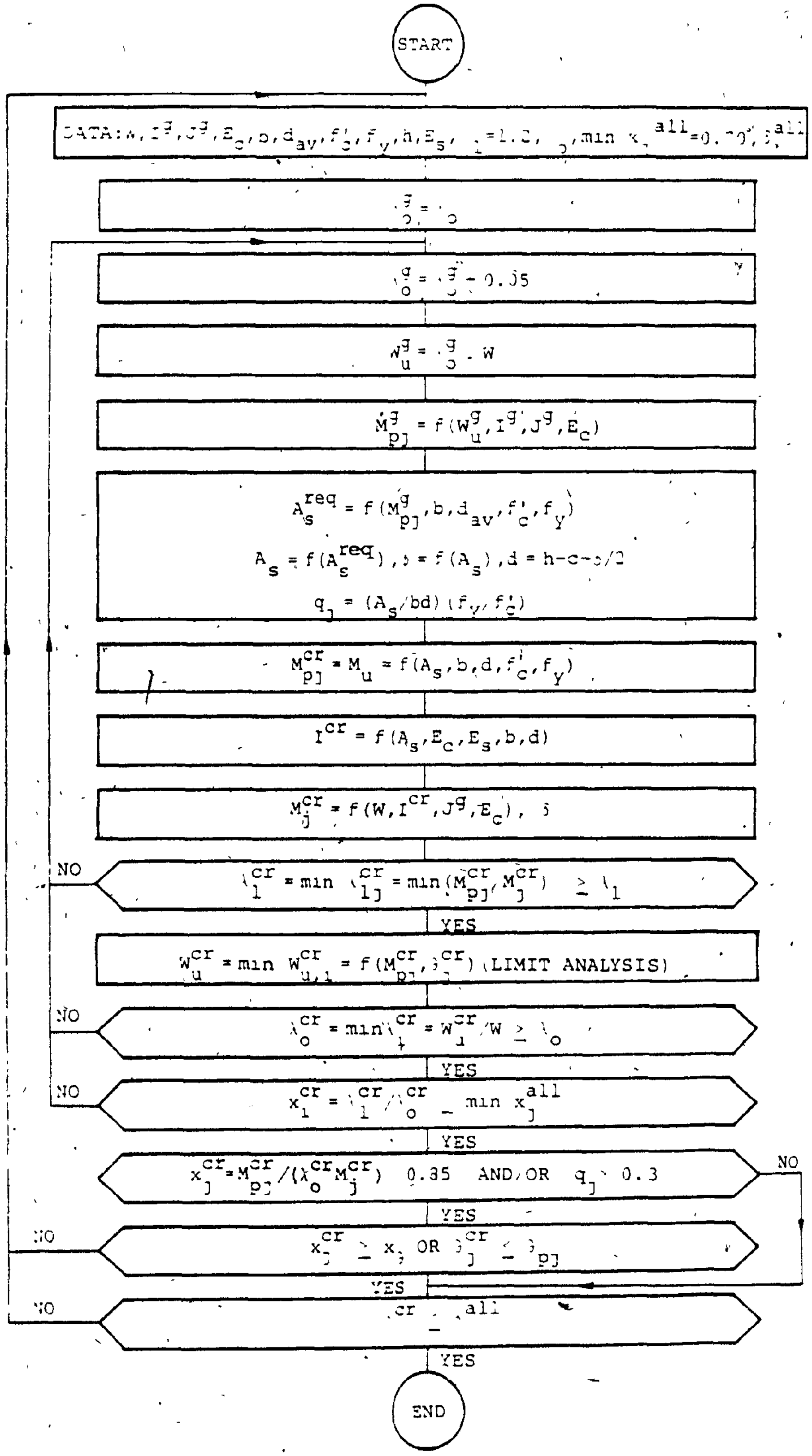

FIG. 2.3 SYNOPSIS OF THE BASIC STATEMENTS OF THE PROPOSED LIMIT DESIGN PROCEDURE FOR TWO-WAY IRREGULAR JOIST FLOORS

The system of limit equilibrium equations and serviceability conditions previously used to produce the scale factors (x_j), is substituted here by the trial-and-error process aiming at the definition of an appropriate value of the "actual" overall load factor.

An example application of the proposed trial-and-error limit design procedure in the case of test-panel I_A, which is studied in the experimental program, is demonstrated in Appendix D.

CHAPTER 3.

EXPERIMENTAL PROGRAM

CHAPTER 3

EXPERIMENTAL PROGRAM

3.1 GENERAL

Simple models representing characteristic irregular ribbed floor patterns were examined in the experimental program. These models were subjected to a single concentrated load at the center, to simulate actual joist floor applications in industrial buildings.

The basic requirements considered in the choice of models was manageability in size and simplicity in erection. Regular design and construction practices were followed in their realization, considered to be the appropriate procedure for the scale of models and for the type of tests.

A theoretical investigation of the models on the basis of those analytical procedures discussed earlier was included with the objective to predict the behavior of the models in the elastic and elasto-plastic range and to estimate the collapse load. The assumed reinforcement distribution was also examined, and compared to the distribution required according to the elastic analysis.

3.2 DESIGN OF THE MODELS

Tests were made on four 1/3-scale models of actual single-bay, square, four-corner supported, two-way joist floors, having a span length of 7.32 m and a depth of 0.51 m (approx. L/15).

Four such models with different rib patterns and reinforcing arrangement were designed on the assumption that each rib of the model was equivalent to three ribs of the actual structure, both made on the basis of a modular grid of 0.61 x 0.61 m, by using the BEER-ZAZ plastic form-pans. This assumption corresponds to the scale factor of 1/3 in the total cross-sectional area of the ribs and simulates closely the overall floor behavior.

Figures 3.1, 3.2 and 3.3, show the shape of the test-panels, designed as equivalent models, superimposed over the corresponding actual floors.

The test panels were 2.59 m x 2.59 m in plan and 171.5 mm in depth. The average rib width was 152.4 mm with a slope of 1/5.

Two of the panels, namely I_A and I_B were made with the same rib pattern but with different reinforcement distribution between the individual ribs. Panel II was chosen as an isotropic model with polar symmetry in the arrangement of the ribs. Panel III was designed to have edge ribs only in the one direction; thus a limited two-way action was expected to occur provided by the top slab and the edge ribs in the one direction. This model was included for the purpose of compari-

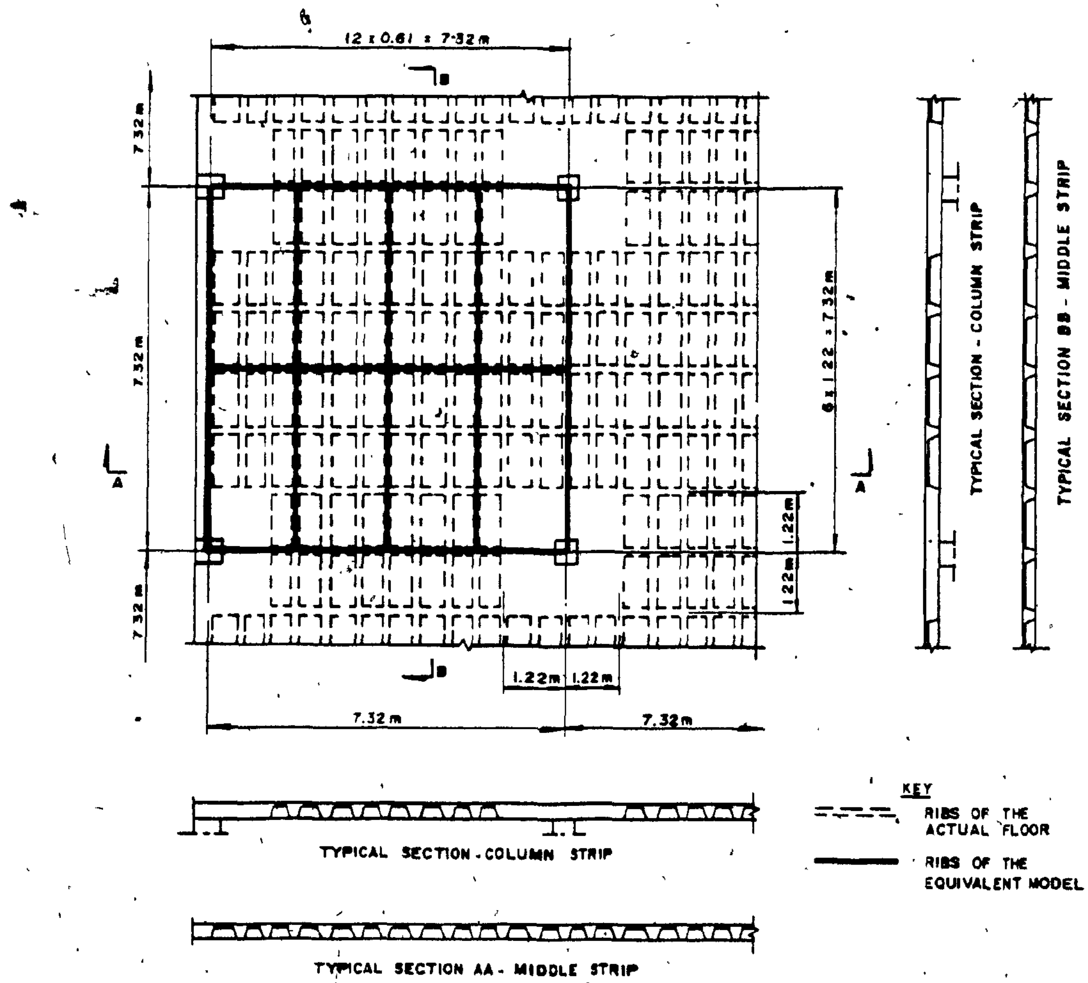

FIG. 3.1 EQUIVALENT MODEL USED FOR THE DESIGN OF THE TEST-PANELS I_A AND I_B

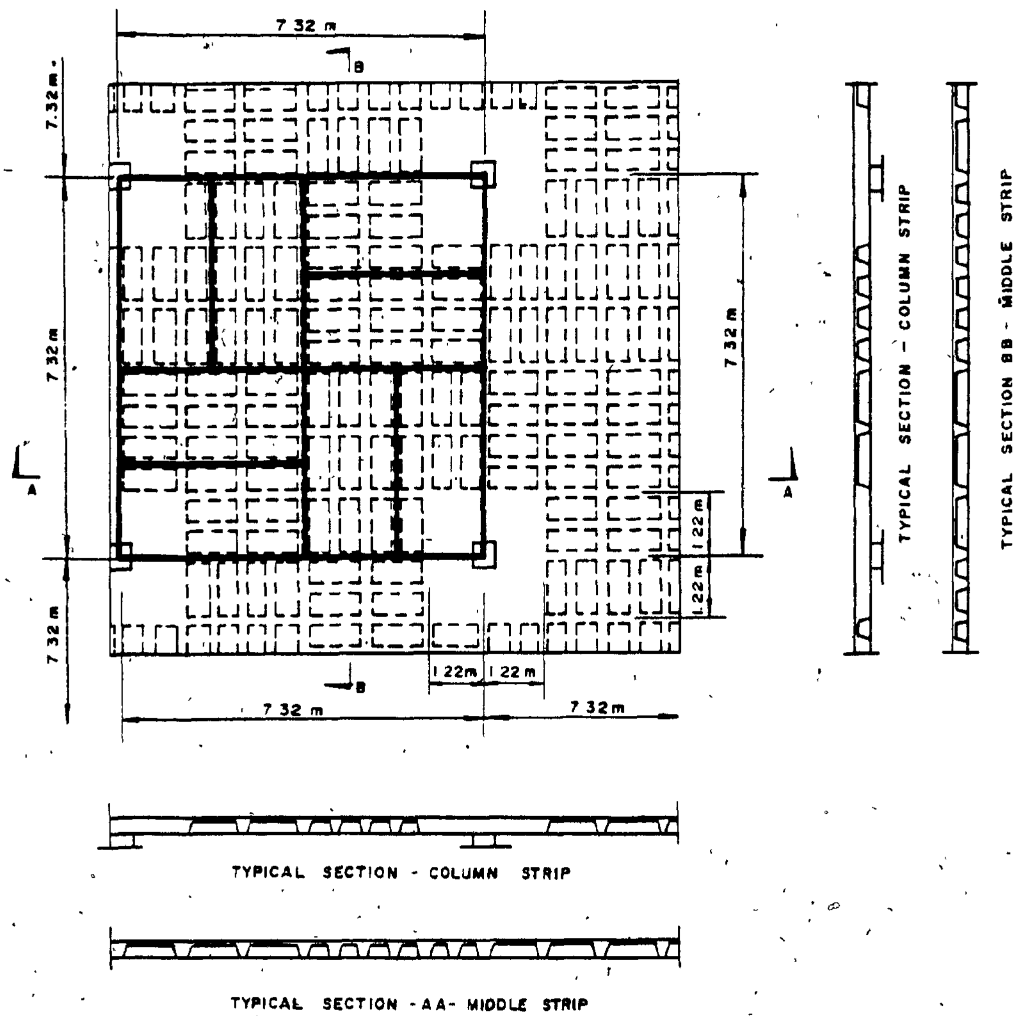

FIG. 3.2 EQUIVALENT MODEL USED FOR THE DESIGN OF THE TEST-PANEL II

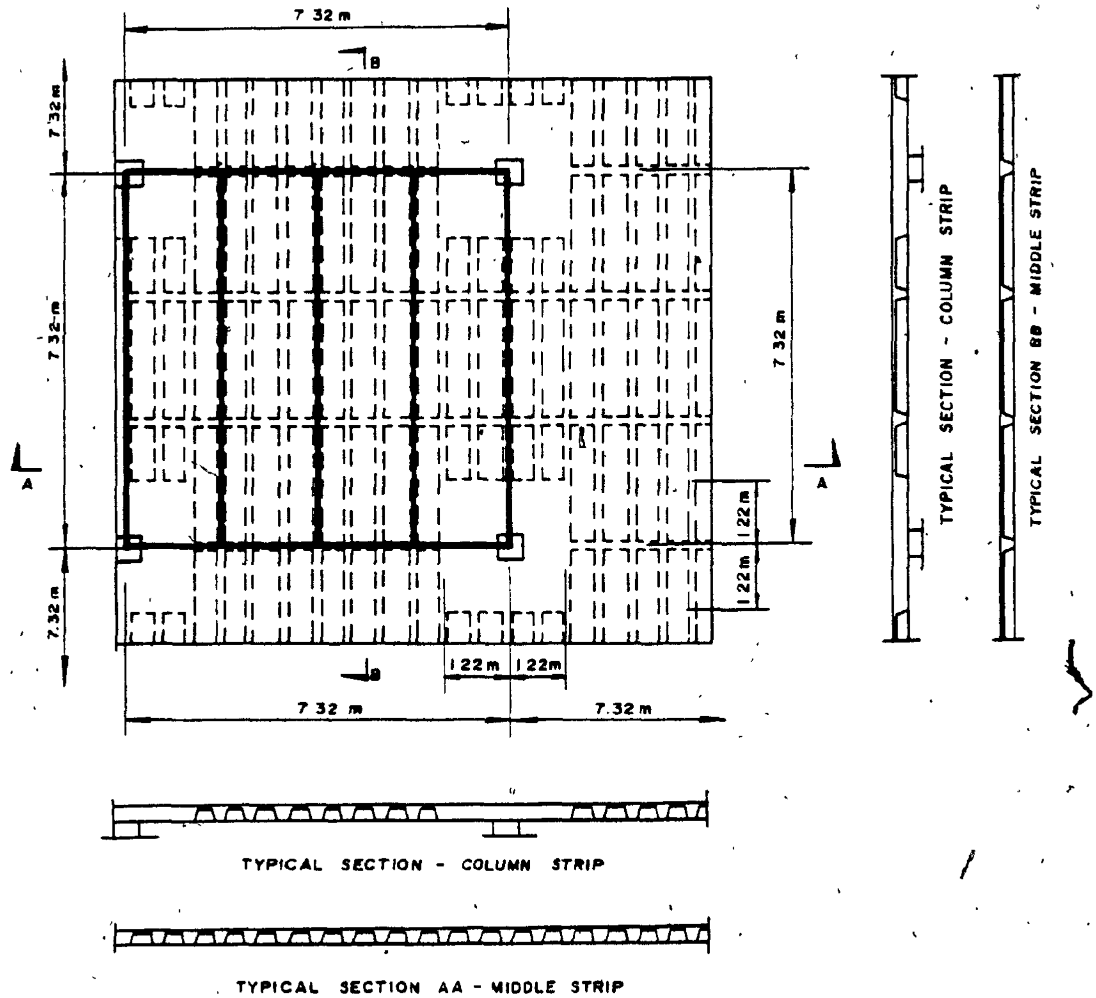

FIG. 3.3 EQUIVALENT MODEL USED FOR THE DESIGN OF THE TEST-PANEL III

son and observation of the local failure mechanism of a system which cannot redistribute effectively the elastic moments in the two perpendicular directions under increasing load.

The dimensional requirements for joist floors and typical sections of the actual floors and the models, are shown in Figures 3.4, 3.5 and 3.6.

The design live load was assumed equal to 70 kN concentrated at the center of the panels. The panels' own weight was not accounted for, having relatively insignificant effect compared to the effect of the concentrated load. (i.e., the weight of the heaviest panel is equal to (D.L.) = $0.64\ m^3 \times 2.4\ Mg/m^3 \times 9.807\ m/sec^2 \simeq 15$ kN and the total static moment due to this load, considered as uniformly distributed, is $M_{o,D}$ = (D.L.) $\times$ L/8 = $15 \times 2.44/8 = 4.58$ kN·m. This value is only 10% of the corresponding value due to the concentrated load of 70 kN: $M_{o,L} = 70 \times 2.44/4 = 42.7$ kN.m).

A load factor of 1.7 was assumed for the proportioning of the concrete sections according to the ultimate strength design theory. The ultimate design load was

$$P_u = 1.7 \times 70 = 119 \text{ kN}$$

and the required total moment capacity of the panels in each direction was

$$M_{o,u} = P_u \times L/4 = 119 \times 2.44/4 = 72.59 \text{ kN.m}$$

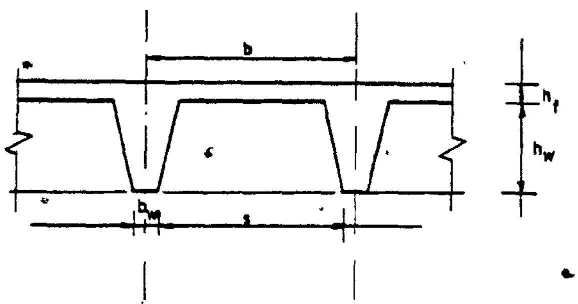

$s \leq 800$ mm
$b_w \geq 100$ mm
$h_f \geq 50$ mm
$b_w \geq (1/3.5)\,h_w$
$h_f \geq (1/12)\,s$

FIG. 3.4 DIMENSIONAL REQUIREMENTS FOR JOIST FLOORS

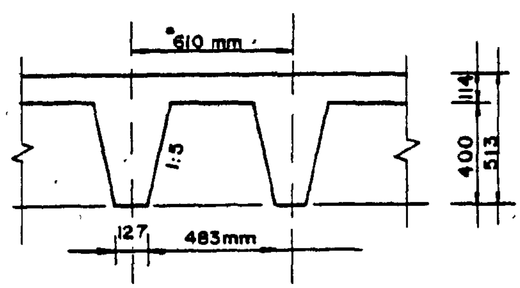

$s = 483 < 800$
$b_w = 127 > 100$
$h_f = 114 > 50$ mm
$b_w > (1/3.5)\,400 = 114$
$h_f > (1/12)\,483 = 40$

FIG. 3.5 TYPICAL SECTION OF ACTUAL FLOORS

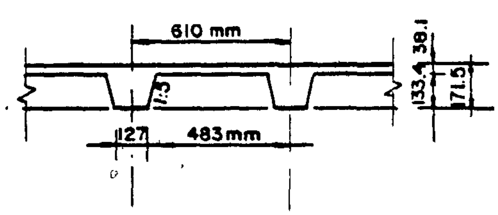

$b_w = 127 > 100/3 = 33$
$h_f = 38.1 > 50/3 = 17$
$b_w > (1/3.5)\,133.4 = 38$
$h_f \approx (1/12)\,483 = 40$

FIG. 3.6 TYPICAL SECTION OF EQUIVALENT SCALE MODELS

The above moment was apportioned between the middle and column (edge) strips and the corresponding ribs, according to the following assumptions:

A distribution of 50% was assigned to both the middle and column strips for panels I_B,II and III, with the exception of the weak direction of panel I_B, where 41.67% (50/2+50/3) was assigned to the column strip, and 16.67% (50/3) to the middle strip for the purpose of allowing a higher moment redistribution between the two perpendicular directions. In panel I_A, 60% of the total one way moment was assigned to the column strip and 40% to the middle strip, as recommended by the "Code for the Design of Concrete Structures for Buildings" (CAN 3-A23.3-M77, Section 11.4.4.3) for the distribution of positive moments of an interior panel,according to the direct design method for flat slabs.

The middle strip was assumed to consist of all the interior ribs available in each direction and the column strip of only the edge ribs.

According to the above assumptions, the distribution percentages of the total one-way static moment and the corresponding moments per rib, as well as the required area of steel reinforcement and the sizes of those bars chosen for the rib reinforcement were calculated, and are shown in Fig. 3.7.

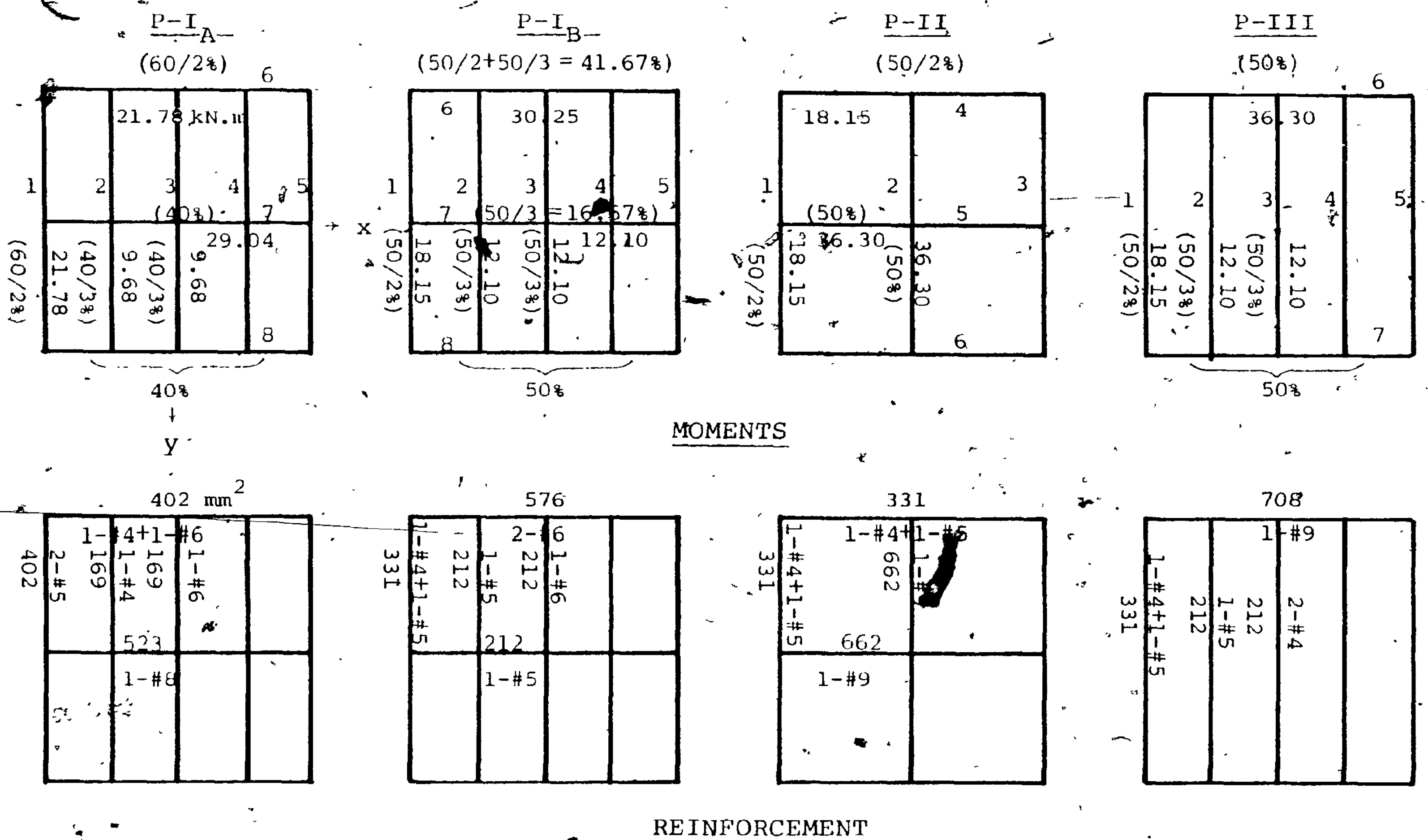

$M_{o,u} = 72.59$ kN.m

$A_{s,total} = 1333$ mm^2 (Average)

$$A_s = 0.85b\, d\frac{f'_c}{f_y} - \sqrt{\left\{\left[0.85b\, d\frac{f'_c}{f_y}\right]^2 - 1700\, M_u\, b\frac{f'_c}{f_y^2}\right\}}$$

(where: b,d in mm, M_u in kN.mm, f'_c, f_y in MPa)

(Data: b = (304.8, or 609.6 mm), d = d_{av} = 140 mm,
f'_c = 34.5 MPa, f_y = 414 MPa)

FIG. 3.7 DISTRIBUTION OF MOMENTS AND CORRESPONDING REINFORCEMENT IN THE TEST-PANELS

The total amount of reinforcement provided in each of the two perpendicular directions of each panel was approximately equal to $A_{S,total} = 1,333\ mm^2$, and was the same for all the panels.

The test-panels were designed, assuming the concrete compressive strength to be $f'_c = 5$ ksi (34.5 MPa) and the reinforcement yield strength $f_y = 60$ ksi (414 MPa). Slightly higher strengths were recorded for both materials during the tests. The calculation of reinforcement was based on an average effective depth of d = 140 mm, and was done using the formula shown in Figure 3.7. The choice of reinforcing bars was made according to Table 3.1.

3.3 THEORETICAL INVESTIGATION OF THE TEST-PANELS

The panels were analysed assuming a four-corner supported grid of T-beams equivalent model. For the analysis of the grid models in the elastic range, the "STRESS" computer program was used. The computer output for the analysis of the grid model of a waffle square panel, based on gross concrete sections, which is similar to the analysis of all test-panels, is listed in Appendix A.

The results of the analysis of the grid models of the above waffle panel as well as of the test-panels are presented in Figure 3.8, showing the moments in the ribs as percentages of the total one-way moment for each direction. Two of the panels were

TABLE 3.1 REINFORCING BAR COMBINATIONS AND TOTAL STEEL AREAS

BAR NO. (IMPERIAL)	BAR NO. (METRIC)	AREA (MM^2)
# 4	~10M	129
# 5	15M	200
# 6	~20M	284
# 7	~20M	---
# 8	25M	510
# 9	~30M	645

BAR COMBINATIONS	AREA (MM^2)
1-#4	129
1-#5	200
2-#4	258
1-#6	284
1-#4+1-#5	329
2-#5	400
1-#4+1-#6	413
1-#5+1-#6	484
1-#8	510
2-#6	568
1-#9	645

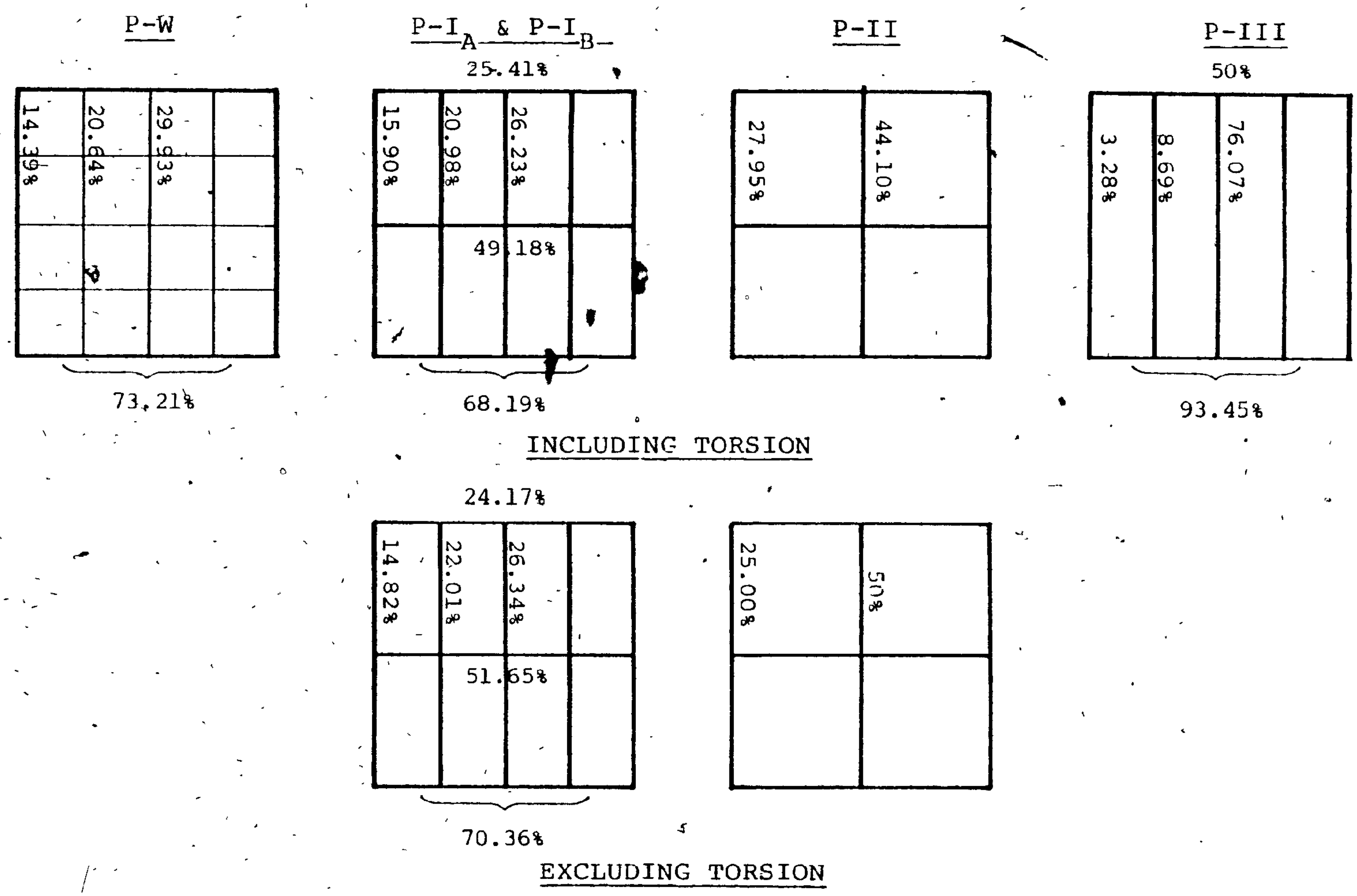

FIG.3.8 DISTRIBUTION OF MOMENTS ACCORDING TO THE ELASTIC ANALYSIS BASED ON GROSS CONCRETE SECTIONS

also analysed without considering the torsional stiffness in the T-beam members of the grid. The difference in the results with the case where torsion was included, was found to be relatively small.

A comparison of the moment percentages given in Figures 3.7 and 3.8 shows the deviation between the moment distribution assumed for the design of reinforcement, and the distribution calculated according to the elastic analysis based on gross concrete sections. Because of the small deviation in the case of panel II, it can be assumed that this panel is designed according to the elastic analysis.

Assuming a proportional relation between the moments and the corresponding areas of reinforcement (see the formula in Figure 3.7), the percentage of reinforcement transferred from the middle to the edge strips in the test-panels can be calculated. In panel I_A, this percentage is 9.8 in the one direction, and 28.19 in the other. Since the ribs are intersecting and two-way action is considered, an average transfer of 18.69 (≃20%) is assumed for the panel. Similarly, in panel I_B, these percentages are 32.51 and 18.19, with an average transfer of 25.35 (≃25%). The average transfer for panel II is - 5.9 (≃0%) and for panel III is 43.45 (≃40%), (one-way action). On the basis of provided reinforcement in the ribs and its location, which was verified after completion of the tests and the breaking of the panels, the moment of inertia of cracked transformed sections of the ribs, as well as the working and ultimate moment capacity of the ribs were calculated. The results of these calculations are summarized in Table 3.2. The formulae and other information used in the calculations are also shown in this table.

In order to obtain a better analytical approximation of the distribution of the bending moments in the initial post-cracking stages, the elastic analysis of the equivalent grids was performed again, assuming the calculated flexural rigidities of the cracked transformed sections of the ribs. In this analysis, the torsional rigidity of the ribs was kept the same as that for the uncracked sections, although it may be reduced substantially after cracking, on the assumption that its influence is very small for the purpose of this investigation. The results of the analysis are illustrated for all panels in Figure 3.9, for both cases with and without torsional rigidity in the ribs.

The elastic analysis of the equivalent grids was also used to predict the deflection characteristics of the panels. These results are shown later, in comparison with the experimental values. The ultimate moment capacity of the ribs, calculated in Table 3.2, as well as their corresponding moment percentages per rib, and the total ultimate moment capacity of the panels in each direction, are shown in Figure 3.10.

The working and ultimate load capacity of the test-panels were also estimated on the basis of moment distribution under the load of 1 kN at the center, obtained from the elastic analysis of the equivalent grids with rigidities of cracked

TABLE 3.2 CRACKED SECTION MOMENT OF INERTIA, WORKING MOMENT AND ULTIMATE MOMENT CAPACITY OF RIBS BASED ON THE AREA AND LOCATION OF PROVIDED REINFORCEMENT

PANEL	RIB*	b (mm)	d (mm)	A_s (mm^2)	x** (mm)	I^{cr} ($10^4 mm^4$)	M_w (kN.m)	M_u (kN.m)
I_A	1	304.8	145.6	400	43.70	3818	8.68	22.60
	2	609.6	127.2	129	18.15	1217	2.59	6.72
	3	609.6	122.0	284	25.37	2218	5.34	13.96
	6	304.8	150.0	413	45.07	4174	9.23	24.03
	7	609.6	146.8	510	36.32	5416	11.38	29.77
I_B	1	304.8	141.6	329	39.65	2982	6.99	18.27
	2	609.6	137.6	200	23.14	2122	4.30	11.20
	3	609.6	139.9	284	27.38	2993	6.15	16.07
	6	304.8	152.0	568	51.68	5499	12.68	32.70
	7	609.6	157.0	200	24.92	2828	4.94	12.86
II	1	304.8	139.6	329	39.32	2990	6.89	17.99
	2	609.6	120.2	645	35.72	4196	11.57	30.13
	5	609.6	147.2	645	40.20	6570	14.29	37.34
III	1	304.8	149.6	329	40.93	3468	7.41	19.35
	2	609.6	144.6	200	23.78	2358	4.53	11.78
	3	609.6	145.2	258	26.57	2978	5.82	15.19
	6	304.8	146.2	645	53.06	5524	13.73	35.11

$$x = -\frac{1}{b}(n\,A_s) + \sqrt{\left[\frac{(n\,A_s)^2}{b^2} + 2d\,\frac{(n\,A_s)}{b}\right]}; \quad n = \frac{E_s}{E_c} = \frac{200{,}000\ \text{MPa}}{28{,}000\ \text{MPa}} = 7.14;$$

$$I^{cr} = \frac{b\,x^3}{3} + (n\,A_s)\,(d-x)^2;$$

(M in kN.mm, A_s in mm^2, b,d,x in mm and f in MPa)

$$M_w = \min\{A_s\,f_s^{all}(d-\tfrac{x}{3}),\ \tfrac{1}{2}\,f_c^{all}\,b\,x(d-\tfrac{x}{3})\};$$

$$f_c^{all} = 0.40\,f'_c = 0.40 \times 34.5 = 13.8\ \text{MPa} \quad ***$$

$$M_u = A_s\,f_y\left(d-0.59\,\frac{A_s}{b}\,\frac{f_y}{f'_c}\right)$$

$$f_s^{all} = 0.40\,f_y = 0.40 \times 414 = 165.6\ \text{MPa} \quad ***$$

* For the numbering of ribs see Fig. 3.7.

** Thickness of the top slab h_f = 38.10 mm

*** Ref: "Design of Highway Bridges" (CAN3-S6-M78, Section 8.5.2)

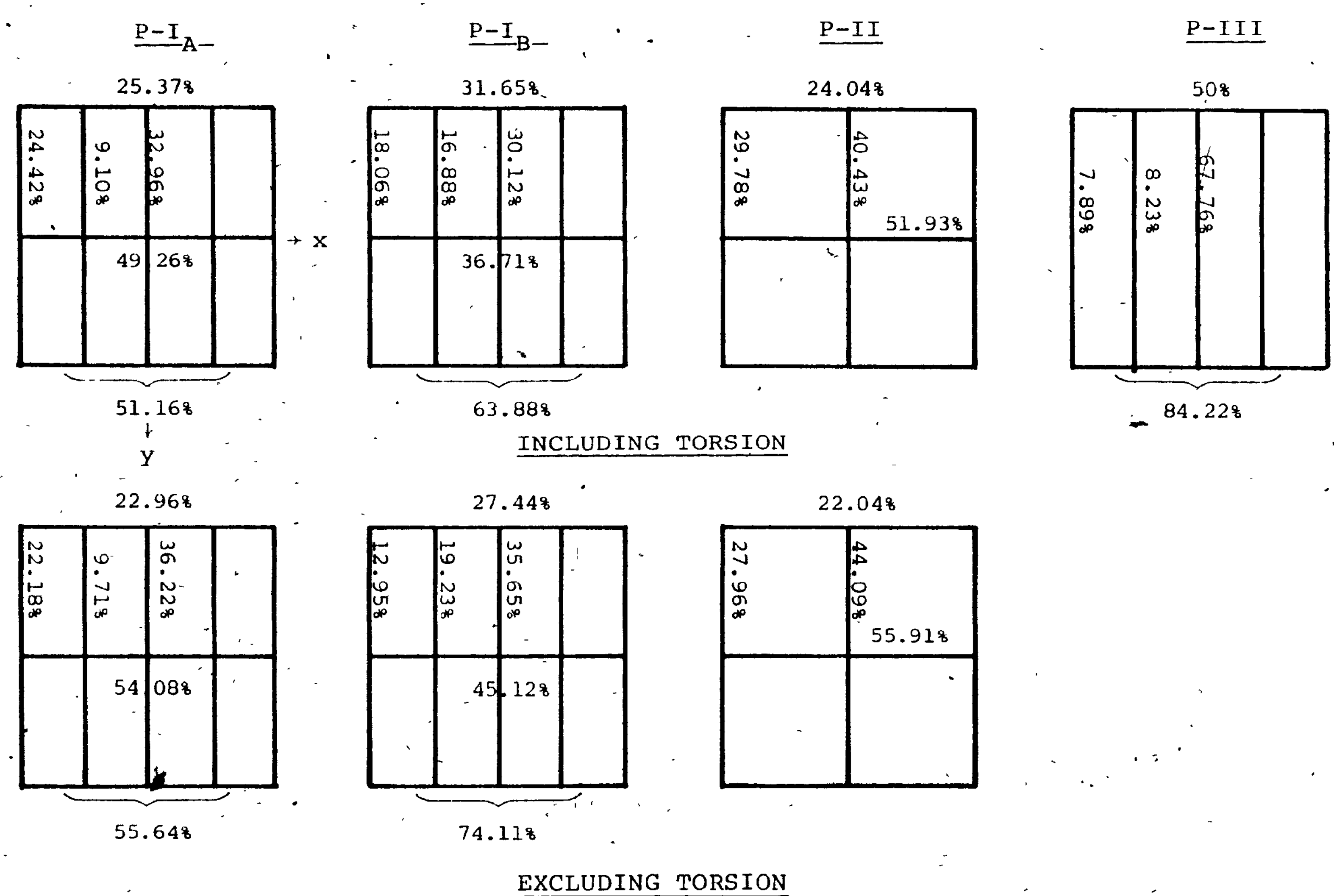

FIG. 3.9 DISTRIBUTION OF MOMENTS ACCORDING TO THE ELASTIC ANALYSIS BASED ON CRACKED TRANSFORMED SECTIONS

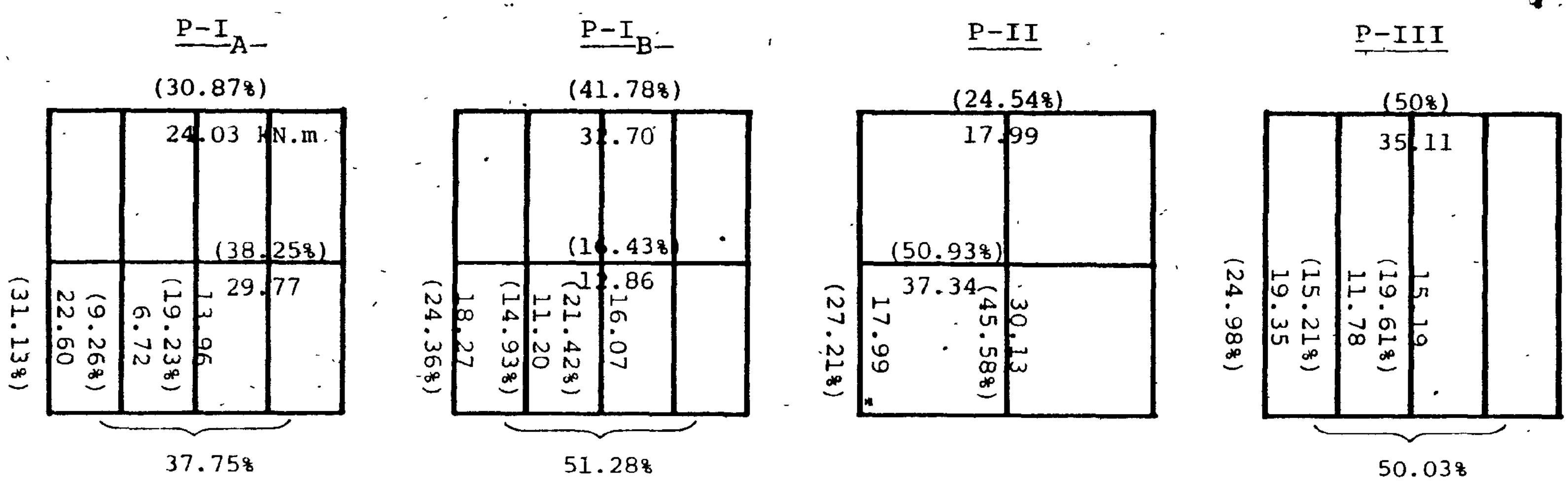

ULTIMATE MOMENT CAPACITY OF RIBS ACCORDING TO REINFORCEMENT PROVIDED

(FROM TABLE 3.2)

P-I_A	P-I_B	P-II	P-III
$\Sigma M_{x,u} = 77.83$ kN.m	$\Sigma M_{x,u} = 75.01$	$\Sigma M_{x,u} = 73.32$	$\Sigma M_{x,u} = 70.22$
$\Sigma M_{y,u} = 72.60$	$\Sigma M_{y,u} = 78.26$	$\Sigma M_{y,u} = 66.11$	$\Sigma M_{y,u} = 77.45$
$\Sigma M_{av} = 75.22$	$\Sigma M_{av} = 76.64$	$\Sigma M_{av} = 69.72$	$\Sigma M_{av} = 73.84$
$75.22/72.59 = 1.04$	$76.64/72.59 = 1.06$	$69.72/72.59 = 0.96$	$73.84/72.59 = 1.02$

OVERDESIGN FACTOR

FIG. 3.10 ULTIMATE MOMENT CAPACITY OF RIBS AND MOMENT PERCENTAGES transformed sections, and the corresponding working and ultimate moment capacity of the ribs. The derivation of these values is shown in Figures 3.11 and 3.12. The calculation was made on the assumption that the load limit is reached at the minimum applied load, for which the moment capacity, at least for one rib, has been attained.

The collapse load of the equivalent grids was estimated as well, on the basis of the ultimate moment capacity of individual ribs, by using limit analysis procedures. The upper and lower bound limit analysis techniques used and the results obtained, are presented in Appendix B.

Furthermore, the equilibrium method of limit design previously described in paragraph 2.4 was used to produce a typical example of refined design for the test-panels under the specified ultimate load of 119 kN, and is presented in Appendix C. From the broad spectrum of possible solutions, a simple case has been chosen, which gives the plastic moments as multiples of the elastic moments, with the same scale factor for all critical sections of each model. The scale factors were calculated from the limit equilibrium equations written for the collapse mechanisms of those systems with weak interior ribs and strong edge ribs, assuming that the collapse occurred precisely at the specified ultimate load. These collapse mechanisms are similar to those observed at failure of the test-panels.

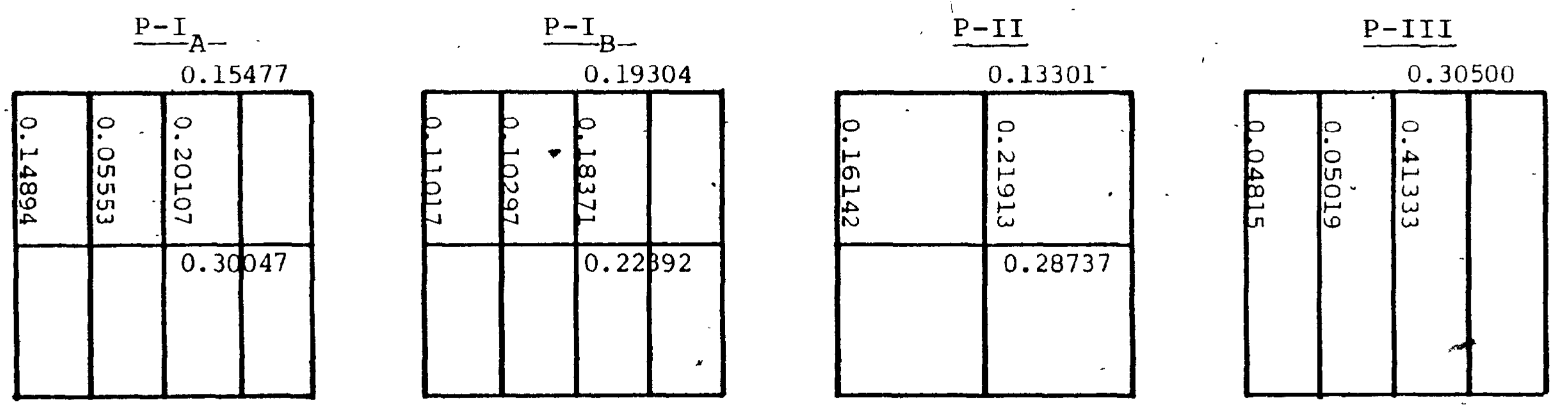

$(\Sigma M_x = \Sigma M_y = 0.61 \text{ kN.m})$

MOMENT DISTRIBUTION UNDER LOAD OF 1 kN (FROM FIG. 3.9)

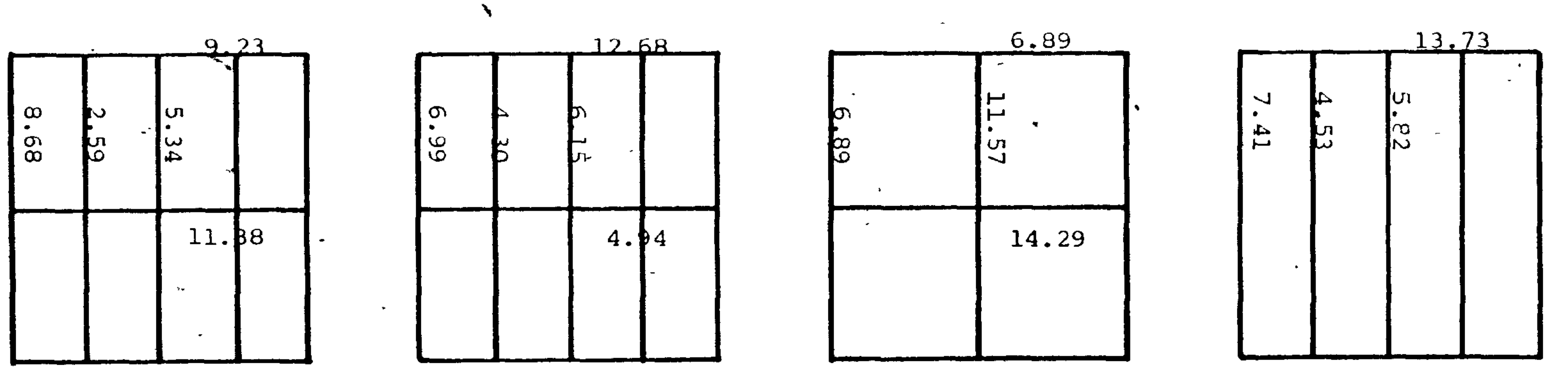

ALLOWABLE MOMENT CAPACITY OF RIBS (FROM TABLE 3.2)

$P_W = \frac{5.34}{0.20107} = 26.56$ kN $\quad P_W = \frac{4.94}{0.22392} = 22.06$ kN $\quad P_W = \frac{6.89}{0.16142} = 42.68$ kN $\quad P_W = \frac{5.82}{0.41333} = 14.08$ kN

FIG. 3.11 ESTIMATION OF WORKING LOAD CAPACITY OF THE TEST-PANELS AT THE MOMENT OF REACH OF ALLOWABLE STRESS IN WEAKEST RIB

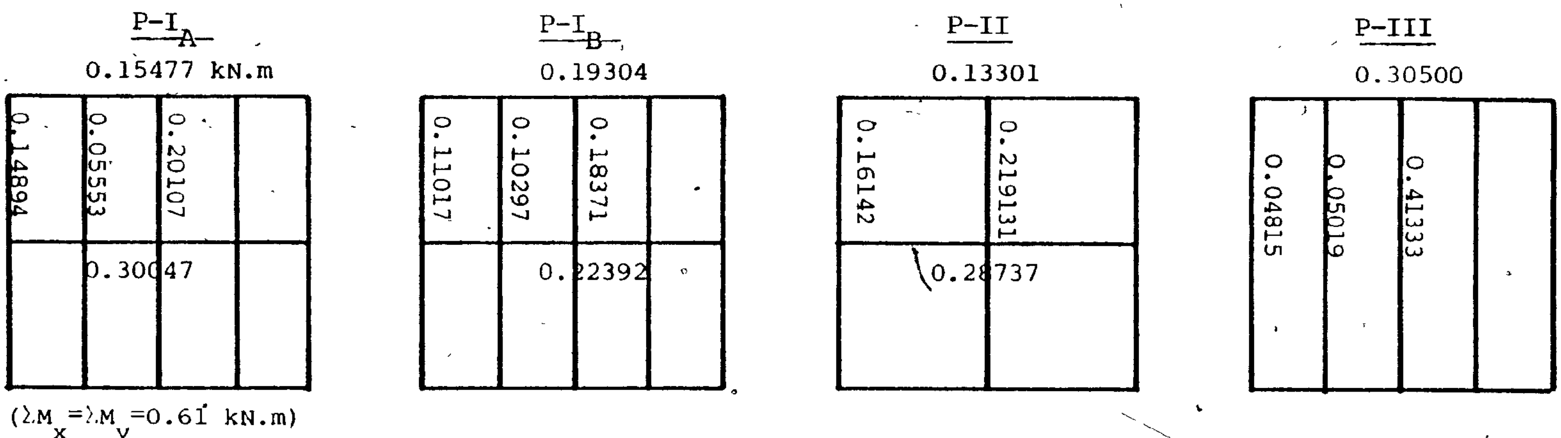

MOMENT DISTRIBUTION UNDER LOAD OF 1 kN (FROM FIG. 3.9)

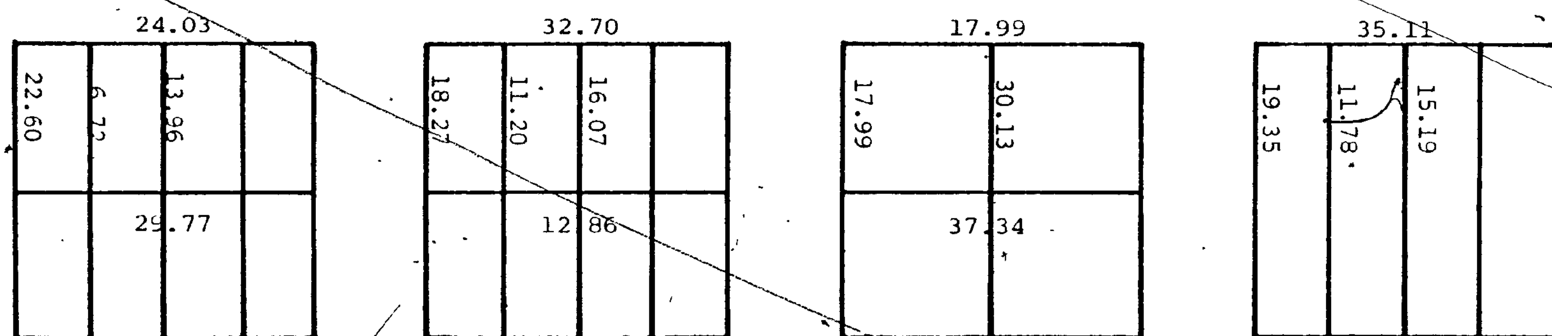

ULTIMATE MOMENT CAPACITY OF RIBS (FROM TABLE 3:2)

$P_u = \frac{13.96}{0.20107} = 69.43$ kN $P_u = \frac{12.86}{0.22392} = 57.43$ kN $P_u = \frac{17.99}{0.16142} = 111.45$ kN $P_u = \frac{15.19}{0.41333} = 36.75$ kN

FIG. 3.12 ESTIMATION OF ULTIMATE LOAD CAPACITY OF THE TEST-PANELS AT THE MOMENT OF YIELD OF WEAKEST RIB

The results of the limit design are shown in Figure 3.13, in comparison with the other cases of moment distribution considered in this study. The cases shown are, the assumed moment distribution and the corresponding actual moment distribution based on the reinforcement provided in the test-panels. In addition the moment distribution based on the elastic analysis of the equivalent grid with gross concrete sections is shown together with the corresponding proposed moment distribution based on the limit design of the equivalent joist floor models. The comparison shows the difference between the provided and required moment capacity in the ribs according to elastic grid analysis and plastic design.

3.4 CONSTRUCTION OF THE TEST-PANELS

The dome-shaped BEER-ZAZ plastic form pans were used for the construction of the test-panels. The pans were placed inside a shallow wooden box to form the ribbed side of the panels, the same way as in regular construction practice, except that wooden inserts were used to reduce the overall depth of the ribs to the model's scale.

The main reinforcement of the ribs was placed in the rib cavities, and a wire mesh was placed in the mid-depth of the slab, supported on top of the stirrups. The main reinforcement consisted of one or two deformed steel bars per rib, ranging in size from #4 (~10M) to #9 (~30M), as shown in Figure 3.7. Stirrups of smooth W4.5 wire (ϕ6mm) spaced 150 mm apart,

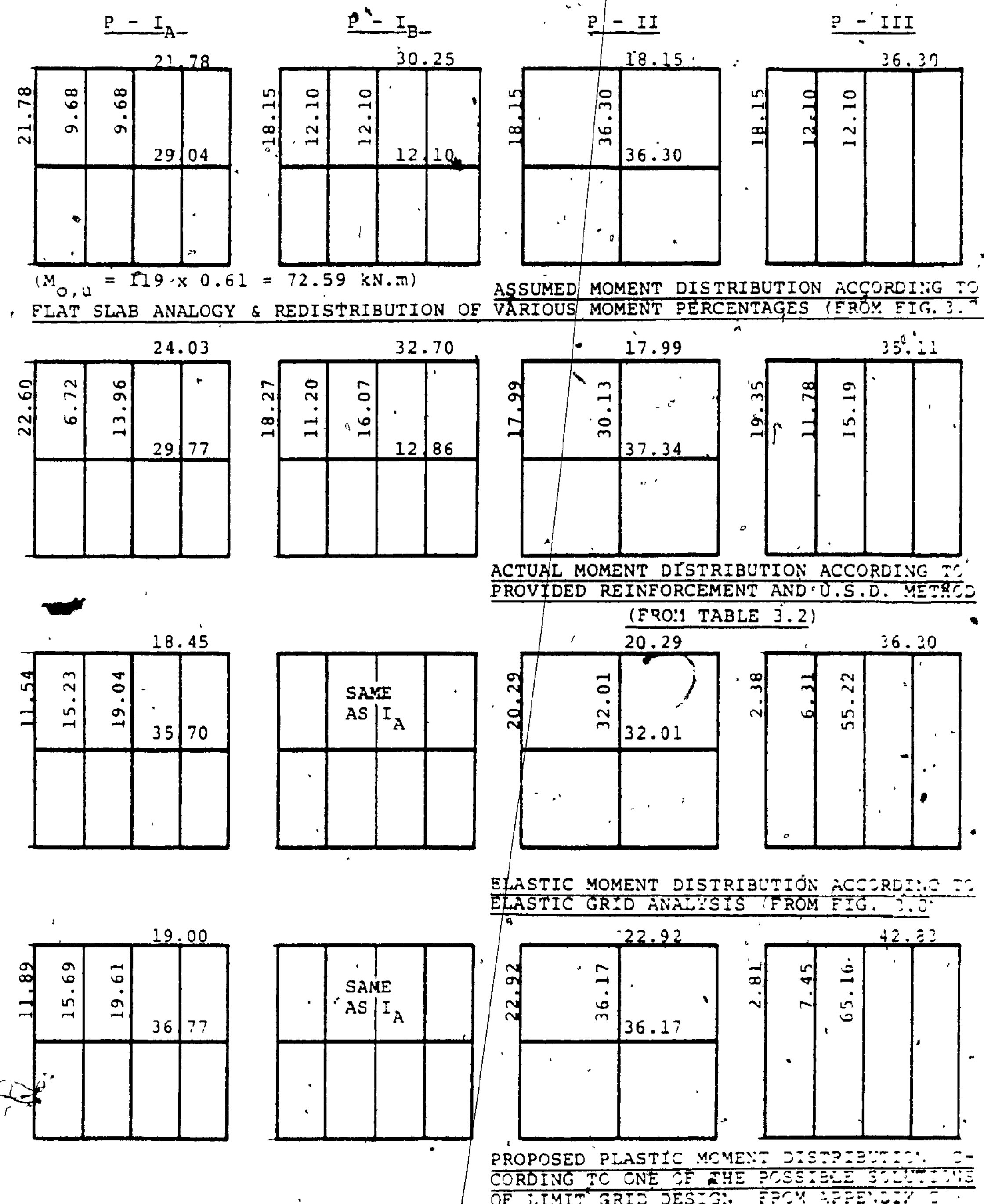

FIG. 3.13 MOMENT DISTRIBUTION UNDER SPECIFIED ULTIMATE LOAD

were used to hold the bars and the wire mesh. The wire mesh was WWF 6 × 6 – W1.4 × W1.4 (152 mm × 152 mm – ϕ3.4 mm × ϕ3.4 mm).

All four test panels and test cylinders were cast at the same time, using ready-mixed concrete. The formwork and reinforcement in place for panel I_A before concreting, is shown in Figure 3.14. A mixture of cement, sand, water and a liquid acrylic polymer additive was used for the smoothing of the flat face of the panels.

Electrical strain gages were installed on each bar of the main reinforcement at midlength and on selected locations of the concrete surface. The gages on the bars were covered with special coating for protection during concreting.

3.5 TEST ARRANGEMENT AND PROCEDURE

All models were tested in up-side-down position, supported from the top at the four corners and loaded from the bottom by a single load at the center. The loading frame and testing arrangement are shown in Figure 3.15.

The supports of the test-panels consisted of a system of steel plates and rollers which allowed free rotation and horizontal displacement under loading in the direction of the diagonals. The size of the supports was 140 mm × 140 mm, corresponding to the width of the panel edge ribs at the bottom.

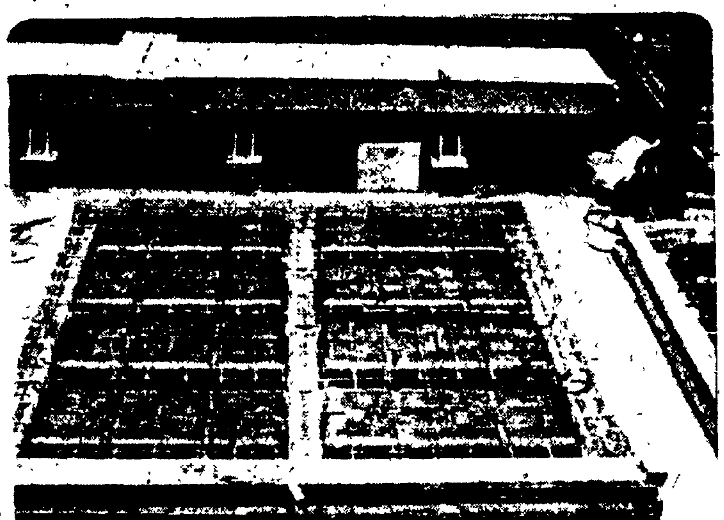

FIG. 3.14 MOULD AND REINFORCEMENT IN PLACE FOR THE TEST-PANEL I_A

FIG. 3.15 LOADING FRAME AND TESTING ARRANGEMENT
(FOR THE TEST-PANEL III)

Neoprene pads were placed between the supports and the concrete surface of the test-panels.

The load was applied to the panels by a hydraulic jack, through a steel plate and a neoprene pad of 300 mm × 300 mm. The applied load was measured by a load cell (transducer) placed between the jack and the steel plate, and connected to a calibrated strain indicator.

The strains were recorded and printed automatically for all loading stages by direct connection of the electric strain gages to a data-acquisition system. The deflections were also measured by means of dial gages to 0.001 in (0.025 mm) accuracy.

The load was applied in increments of about 10 kN. The strains and deflections were monitored and the cracks were observed and marked for each loading increment. Loading was increased continuously, up to failure. Failure was considered to occur when the deflection at the center of the panel increased rapidly, with little or no increase in the load.

CHAPTER 4

EXPERIMENTAL RESULTS

CHAPTER 4

EXPERIMENTAL RESULTS

4.1 GENERAL

The overall behavior and strength of two-way irregularly ribbed joist floors, subjected to a single concentrated load, investigated experimentally, is discussed in this Chapter. This investigation provides information on the elastic performance, the formation of the collapse mechanisms and the load carrying capacity of these floors. In addition, information is obtained on the contribution of each of the two major structural components of the rib-stiffened plate, the top slab and the rib grid.

The test models used, represent typical floor systems of orthogonal grid pattern with differently distributed and reinforced ribs. The reinforcement arrangements were chosen with the purpose of studying the effects of reinforcement distribution between the ribs and in particular, the influence of reinforcement transferring from the middle to the edge strips.

4.2 BEHAVIOR OF TEST-PANELS UNDER INCREASING LOAD

A classification of the various load capacity limits corresponding to the different loading stages, is presented in Table 4.1. This vocabulary for the load capacity limits will

TABLE 4.1 CLASSIFICATION OF LOAD CAPACITY LIMITS

LOADING STAGE		LOAD DERIVATION	
		ANALYTICAL	EXPERIMENTAL
1	REACH OF ALLOWABLE STRESS	WORKING (STRESS DESIGN) LOAD	ASSUMED SERVICE LOAD
2	REACH OF YIELD STRESS (FIRST PLASTIC HINGE)	a. SPECIFIED ULTIMATE (STRENGTH) DESIGN LOAD b. ULTIMATE DESIGN LOAD	- FIRST YIELD LOAD
3	FIRST STAGE OF GRID MECHAN-ISM COLLAPSE	a. SPECIFIED ULTI-MATE* LOAD b. "UNIQUE" COLLAPSE LOAD	ASSUMED FAILURE LOAD
4	SECOND STAGE OF GRID MECHAN-ISM COLLAPSE	"UPPER BOUND" COLLAPSE LOAD	GRID FINAL COLLAPSE LOAD
5	FINAL STAGE OF PANEL COLLAPSE		GENERAL COLLAPSE LOAD

* In this case the term "ULTIMATE" refers to a specific limit state.

<u>NOTE</u>: The same load of 119 kN was used in both cases 2a and 3a.

be used in the presentation of the experimental results.

The load capacity limits of specimens tested to failure, are given in Table 4.2, together with relevant analytical and experimental results. The collapse loads given in the table in column (8) correspond to the final state of formation of the first elementary collapse mechanism of the equivalent grid, which is the first stage of the incremental collapse of the panels. The collapse loads of column (9) correspond to the second stage of incremental collapse, developed in the unyielded part of the grid system in the perimeter of the previously collapsed part. This type of incremental collapse which is characteristic of joist floors under concentrated load, corresponds to a forced superposition of various elementary collapse mechanisms, and may be explained by the transfer of the load from the collapsed part to the adjacent unyielded part of the grid system by tensile membrane action of the top slab.

The values of column (8) can be considered to be the failure state of the test-panels, whereas the enhancement of the load capacity due to membrane action can be neglected for practical reasons, since it is usually associated with excessive deflections. Furthermore, the radius of the influence area of the concentrated load, where yielding of ribs can take place before a local failure occurs under the load-point, cannot be easily defined in practice depending on the tensile membrane capacity of the top slab. The assumed experimental failure

TABLE 4.2(1) SUMMARY OF ANALYTICAL AND EXPERIMENTAL RESULTS

TEST-PANEL	SPECIFIED ULTIMATE LOAD - kN	THEORETICAL LOAD CAPACITY - kN (EQUIVALENT GRID): ELASTIC ANALYSIS BASED ON WEAKEST RIB (CRACKED TRANSF. SECTIONS): WORKING STRESS DESIGN METHOD	THEORETICAL: ELASTIC ANALYSIS: ULTIMATE STRENGTH DESIGN METHOD	THEORETICAL: PLASTIC ANALYSIS (MECHANISM COLLAPSE): "UNIQUE" SOLUTION BASED ON STATIC AND KINEMATIC PRINCIPLES	THEORETICAL: PLASTIC ANALYSIS: "UPPER-BOUND" SOLUTION (YIELDING OF ALL RIBS)	EXPERIMENTAL LOAD CAPACITY - kN: AT FIRST REACH OF ALLOWABLE STRESS (ASSUMED SERVICE LOAD)	EXPERIMENTAL: AT FIRST REACH OF YIELD STRESS (FIRST YIELD LOAD)	EXPERIMENTAL: INCREMENTAL GRID MECHANISM COLLAPSE: FIRST ELEMENTARY MECHANISM COLLAPSE (ASSUMED FAILURE STATE)	EXPERIMENTAL: INCREMENTAL GRID MECHANISM COLLAPSE: SECOND STAGE OF GRID COLLAPSE (GRID FINAL COLLAPSE)	EXPERIMENTAL: GRID AND SLAB COLLAPSE: FINAL STAGE OF PANEL COLLAPSE (GENERAL COLLAPSE)	MODE OF FAILURE
	(1)	(2)	(3)	(4)	(5)	(6)	(7)	(8)	(9)	(10)	(11)
I_A	119	26.56	69.43	82.70	123.30	41	80	96	122	133.5	Collapse of interior ribs Tensile membrane action
I_B	119	22.06	57.43	65.79	125.63	30	53	91	143	144.5	Collapse of interior ribs Tensile membrane action
II*	119	42.68	111.45*	108.39	114.29	50	95	115	115	133.5	Overlapping of two collapse mechanisms. Tensile membrane action
III	119	14.08	36.75	34.56	121.04	32	60	60**	-	83.5	Local failure of one rib Compressive membrane action

* Design based on elastic analysis
** Rib collapse

TABLE 4.2(2) SUMMARY OF ANALYTICAL AND EXPERIMENTAL RESULTS

TEST-PANEL	RATIO OF ASSUMED SERVICE LOAD TO WORKING LOAD	RATIO OF FIRST YIELD LOAD TO ULTIMATE DESIGN LOAD	RATIO OF ASSUMED FAILURE LOAD TO "UNIQUE" COLLAPSE LOAD	EXPERIMENTAL COLLAPSE LOAD / THEOR. "UPPER-BOUND" COLL. LOAD		MAXIMUM DEFLECTION UNDER ASSUMED SERVICE LOAD – mm		INVERSE RATIO OF MAXIMUM EXPERIMENTAL DEFLECTION OVER SPAN ǂ
				GRID FINAL COLLAPSE	GENERAL COLLAPSE	ANALYTICAL	EXPERIMENTAL	
	(12) = (6)/(2)	(13) = (7)/(3)	(14) = (8)/(4)	(15) = (9)/(5)	(16) = (10)/(5)	(17)	(18)	(19) = (18)/L
I_A	1.54	1.15	1.16	0.99	1.08	6.58 (2.87)+	4.92	$\frac{1}{496}$
I_B	1.36	0.92	1.38	1.14	1.15	5.21 (2.10)+	3.34	$\frac{1}{731}$
II	1.17	0.85	1.06	1.01	1.01	7.70 (4.00)+	6.21	$\frac{1}{393}$
III	2.27	1.63	1.74	-	0.69	9.22 (4.48)+	4.22	$\frac{1}{578}$

+ Based on gross concrete sections.

ǂ Span L = 2440 mm

loads for the panels are compared with theoretical values based on plastic analysis, as shown in columns (14). As it can be seen from the given ratios, the assumed failure load was quite accurately predicted by the plastic theory for panel II, while it was found higher than the estimated value for the other panels.

The service loads given in column (6) were established graphically from the load-strain curves for the steel reinforcement, as the loads corresponding to the first attainment of allowable stress (see Figures 4.5 to 4.8). These values of service load were found to be more conservative than the values obtained from the experimental load-deflection curves, corresponding to the deflection limit of span/360, at the center of the panels (see Figures 4.3 and 4.4). Also, the service loads of column (6) are shown to be higher than the corresponding service loads given in column (2) based on allowable stress in the weakest rib of the grid, as shown in column (12).

The first yield loads reported in column (7) were obtained as the loads corresponding to the first recorded yielding in the reinforcement which marks the end of the elastic stage and the beginning of the formation of the grid collapse mechanism.

The ratio of the first yield loads to the ultimate design loads are given in column (13). It is shown that the yield stress was reached earlier than was anticipated in panel II and much later in panel III. These discrepancies in the estimation of first yield load show that the U.S.D. method cannot be used reliably for this purpose.

The general collapse loads of column (10) correspond to the final collapse stage of the test-panel, referred to as grid and slab collapse stage. The values of grid final collapse and of general collapse loads are compared with the theoretical "upper-bound" collapse load in columns (15) and (16). The comparison shows that both cases of experimental collapse loads are relatively close to each other and are in good agreement with the theoretical values (with the exception of panel III).

The deflections at the center of the panels under the assumed experimental service load, calculated by elastic analysis for both cases of gross concrete sections and cracked transformed sections, are given in column (17) and corresponding measured experimental values are given in column (18). The comparison shows that the deflections of the test-panels under the assumed experimental service load are smaller than the corresponding deflections of the equivalent analytical model, based on cracked transformed sections, but larger than the theoretical deflections based on gross concrete sections.

The inverse ratios of maximum deflections under the assumed experimental service load to the span of the ribbed panels are given in column (19).

A short description of the failure characteristics of the panels is also given in the same table, (column (11)). A more detailed description is given at the end of this Chapter.

4.3 LOAD-DEFLECTION CHARACTERISTICS

The central point deflections measured by dial gages for all four panels are shown in Figure 4.1, and compared with the theoretical deflections obtained from the analysis of equivalent elastic grids ~~using~~ rigidities based on both the gross concrete sections and the cracked transformed sections. A close relation can be observed between the deflections measured on the test panels and deflections calculated on the basis of those equivalent grids with transformed sections in the elastic range. This relationship can be seen clearly in Figure 4.2, where a superposition of the two sets of curves is made. It is also noticeable that panel I_A was stiffer than panel I_B and is of similar behavior to panel II.

Load-deflection curves for the midspan of the ribs of all panels tested, are shown in Figures 4.3 and 4.4. The relationships are nonlinear at low loads because of the progressive cracking of the concrete and at higher loads because of the progressive development of plastic hinges. The serviceability limits of $\ell/360$ and $\ell/180$ maximum allowable deflections, are also shown in the graphs. The loads corres-

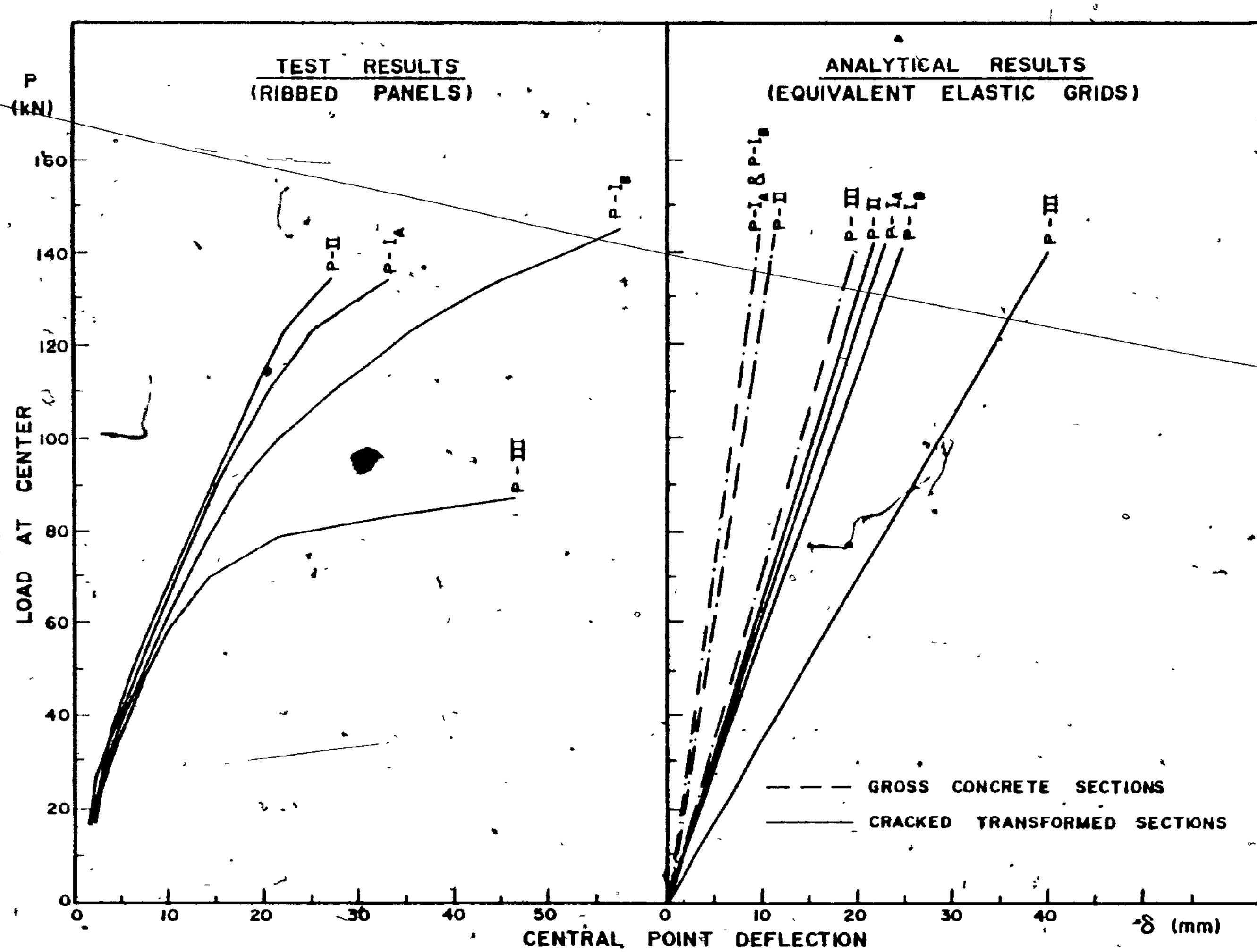

FIG. 4.1 LOAD-DEFLECTION RELATIONSHIP FOR THE CENTER-POINT OF EACH TEST-PANEL

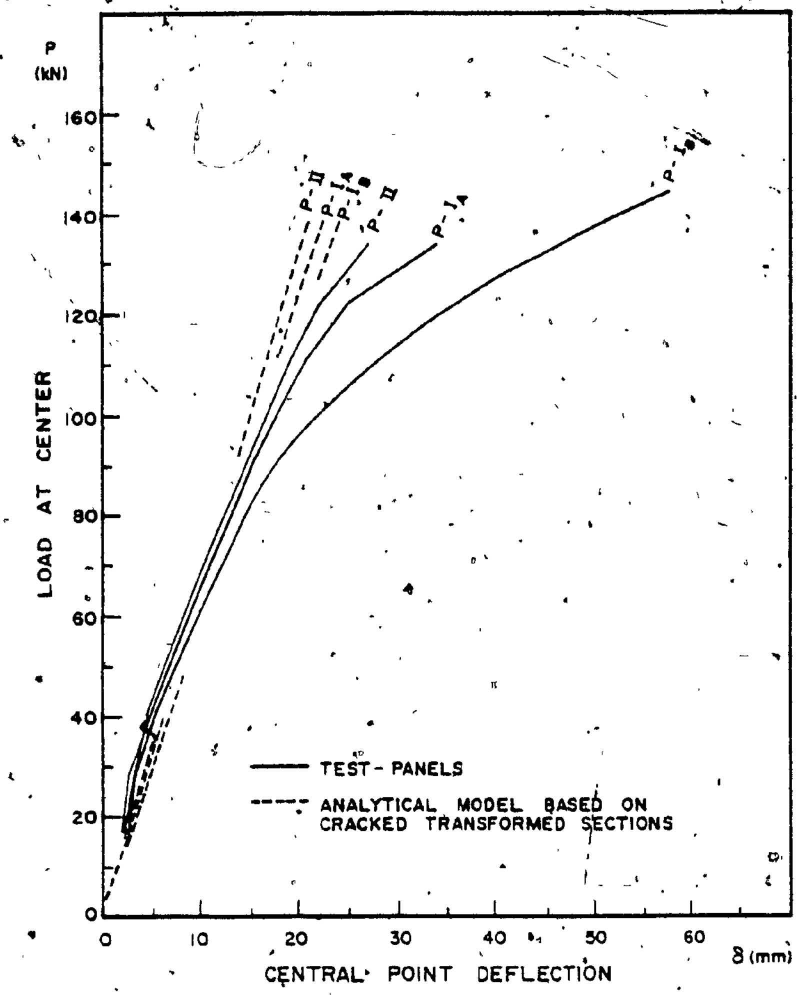

FIG. 4.2 COMPARISON BETWEEN CENTRAL POINT DEFLECTIONS OF TEST-PANELS AND CORRESPONDING ANALYTICAL MODELS

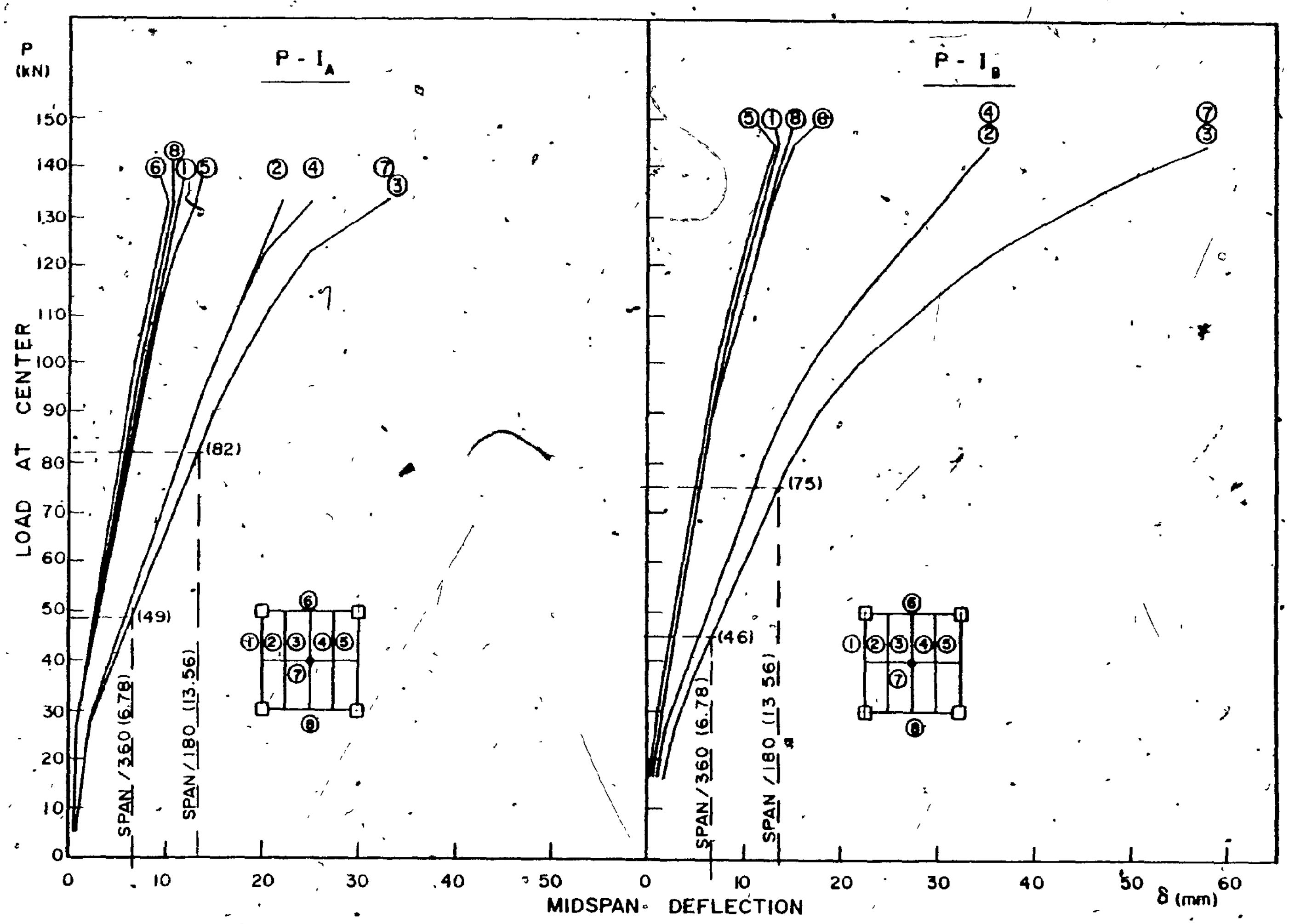

FIG. 4.3 LOAD-DEFLECTION RELATIONSHIP AT MIDSPAN OF EACH RIB OF THE TEST-PANELS I_A AND I_B

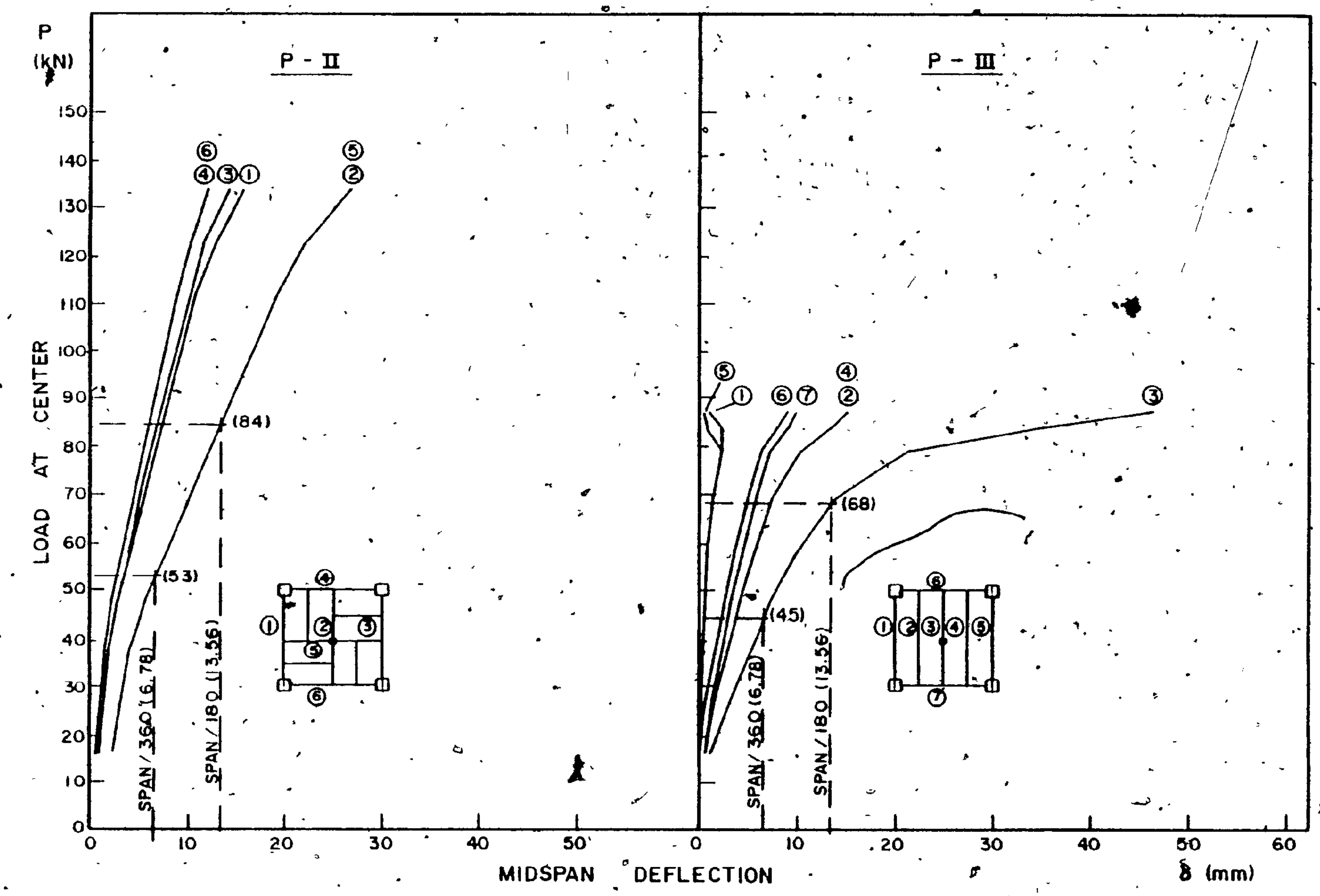

FIG. 4.4 LOAD-DEFLECTION RELATIONSHIP AT MIDSPAN OF EACH RIB OF THE TEST-PANELS II AND III

ponding to the first limit are found to be higher than the service loads based on allowable stresses. The loads corresponding to the second limit are comparable to the first yield loads.

The deflected shape of the panels under load during the early loading stages was approximately that of a parabola. As the load increased, the deflections in the center of the panels increased more rapidly than those elsewhere. As a result, the deflected shape of the panels became more marked, taking a triangular profile at failure. These characteristic deflected shapes in sections along the two center lines of the panels can be seen in the graphs of Figures 4.9 to 4.12. The triangular profile of the deflected shape at failure is an indication that the flexural resistance of the system has been exhausted and that the panel has been practically divided by the hinges into segments.

4.4 LOAD-MOMENT RELATIONSHIP

The stresses in the steel reinforcement and the corresponding bending moments in the ribs were calculated on the basis of tensile strains measured by electrical strain gages in the main reinforcement at midspan of each rib. The calculation of the moments was based on the equilibrium of internal forces in the cracked transformed sections, according to the linear stress distribution assumed in the working stress design method, for as long as the stresses in the steel remained below the assumed yield strength. At the assumed yield point of the steel reinforcement, the moments were calculated on the basis of inelastic stress distribution in the concrete compression zone, according to the ultimate strength design theory. When stresses in individual bars exceeded the assumed yield stress, the moment in the corresponding ribs was considered having constant value under increased load, and equal to the ultimate moment capacity of the ribs referred to as "plastic moment" according to the plastic theory.

The experimental load-strain relationship in the steel reinforcement and the corresponding load-moment relationship in the ribs were plotted for all test panels and they are presented in Figures 4.5 to 4.8. These graphs show the sequence of yielding of each individual bar, the rate of moment increase in each rib, and the various loading stages corresponding to the formation of plastic hinges. These graphs were also used in establishing the assumed experimental service load.

The distribution of the bending moments and the deflections across the center line of the panels in the x and y directions, for each load increment of 20 kN, is presented for all test panels in Figures 4.9 to 4.12. In these figures, the moment redistribution and the sequence in the formation of the collapse mechanism can be seen in the moment diagrams, as well as the successive deflected shapes of the panels and the triangular profile of the panels at the failure stage, in the deflection diagrams. Also, from the total one-way moment ratio

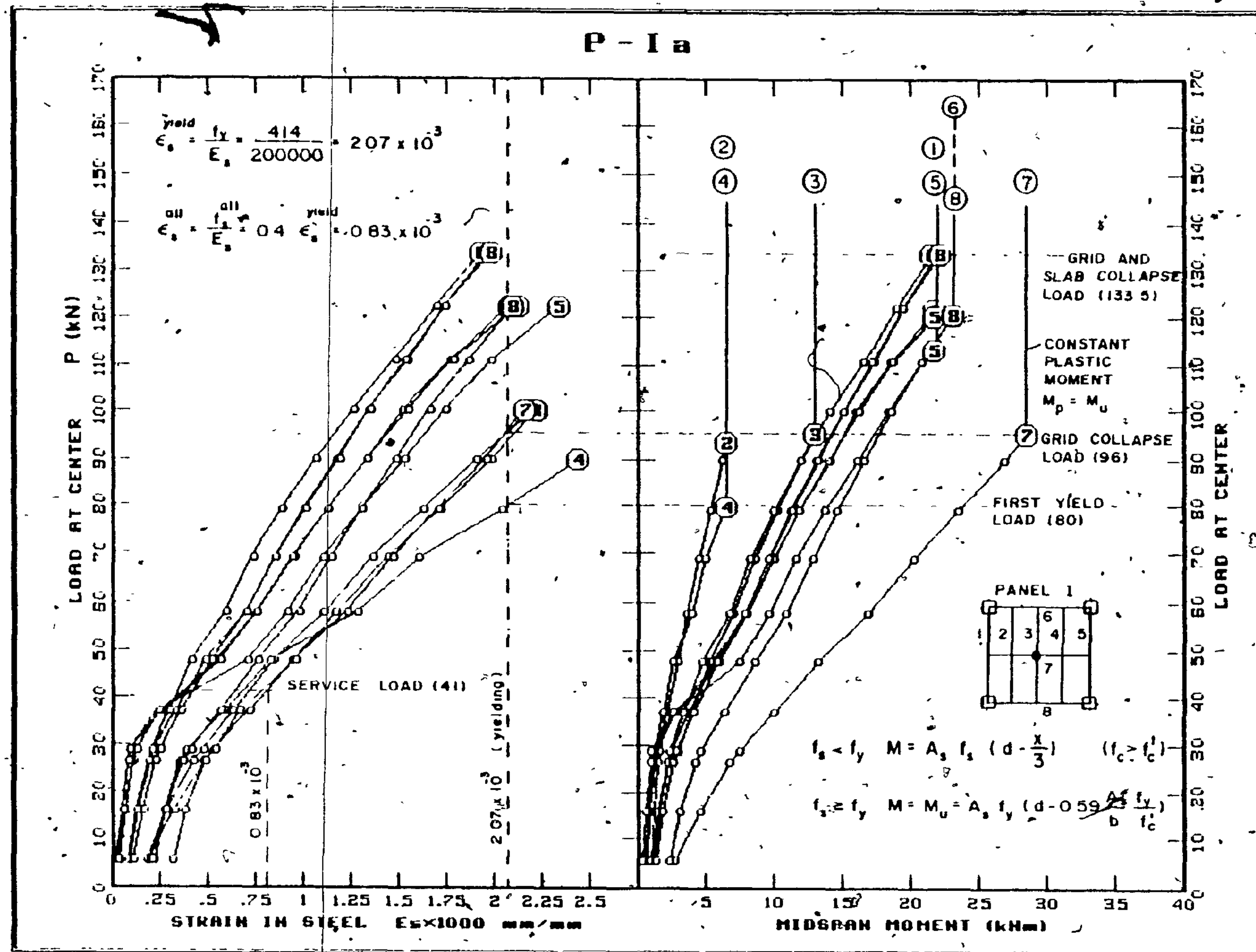

FIG. 4.5 LOAD-MOMENT RELATIONSHIP AT MIDSPAN OF EACH RIB OF THE TEST-PANEL I_A

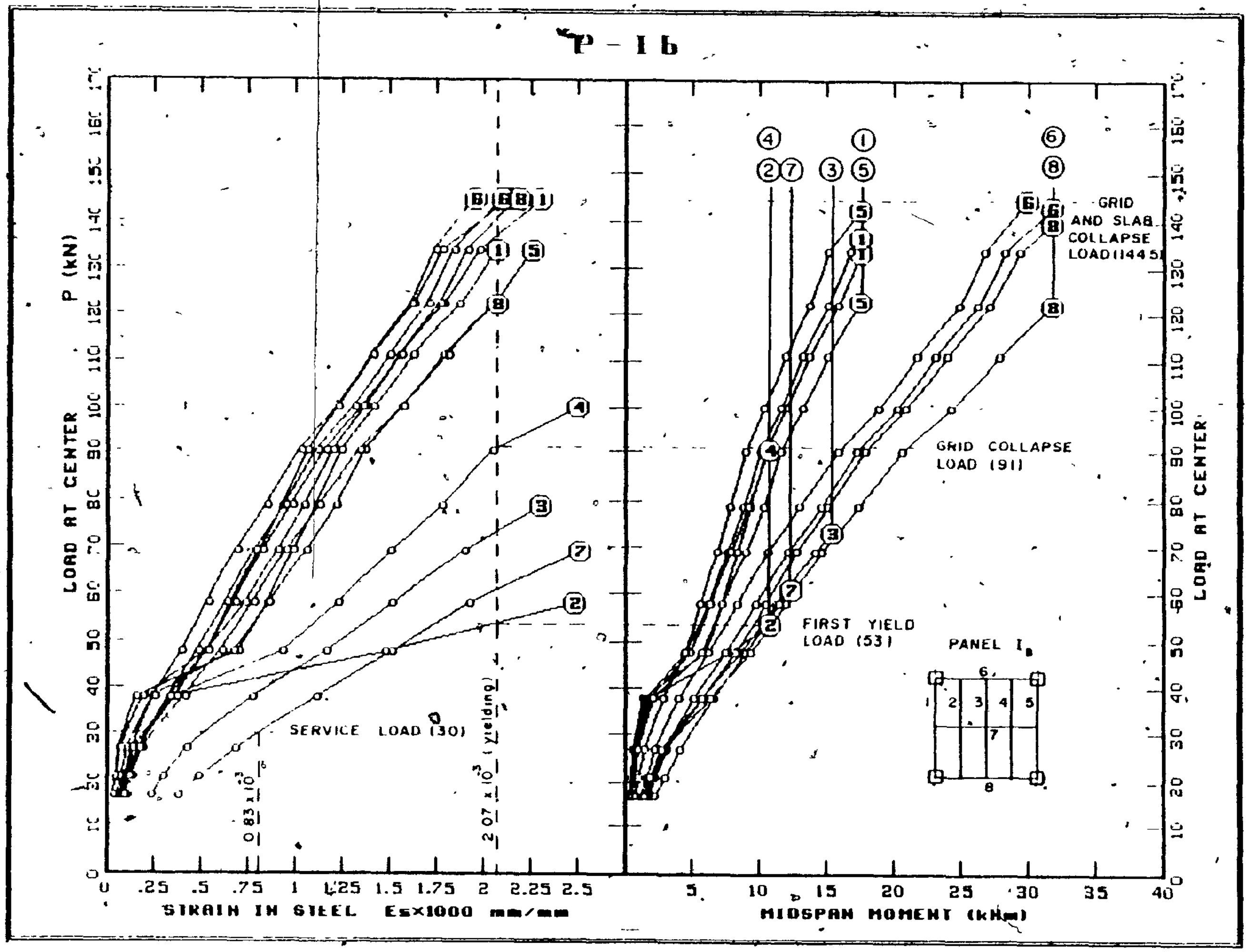

FIG. 4.6 LOAD-MOMENT RELATIONSHIP AT MIDSPAN OF EACH RIB OF THE TEST-PANEL I_B

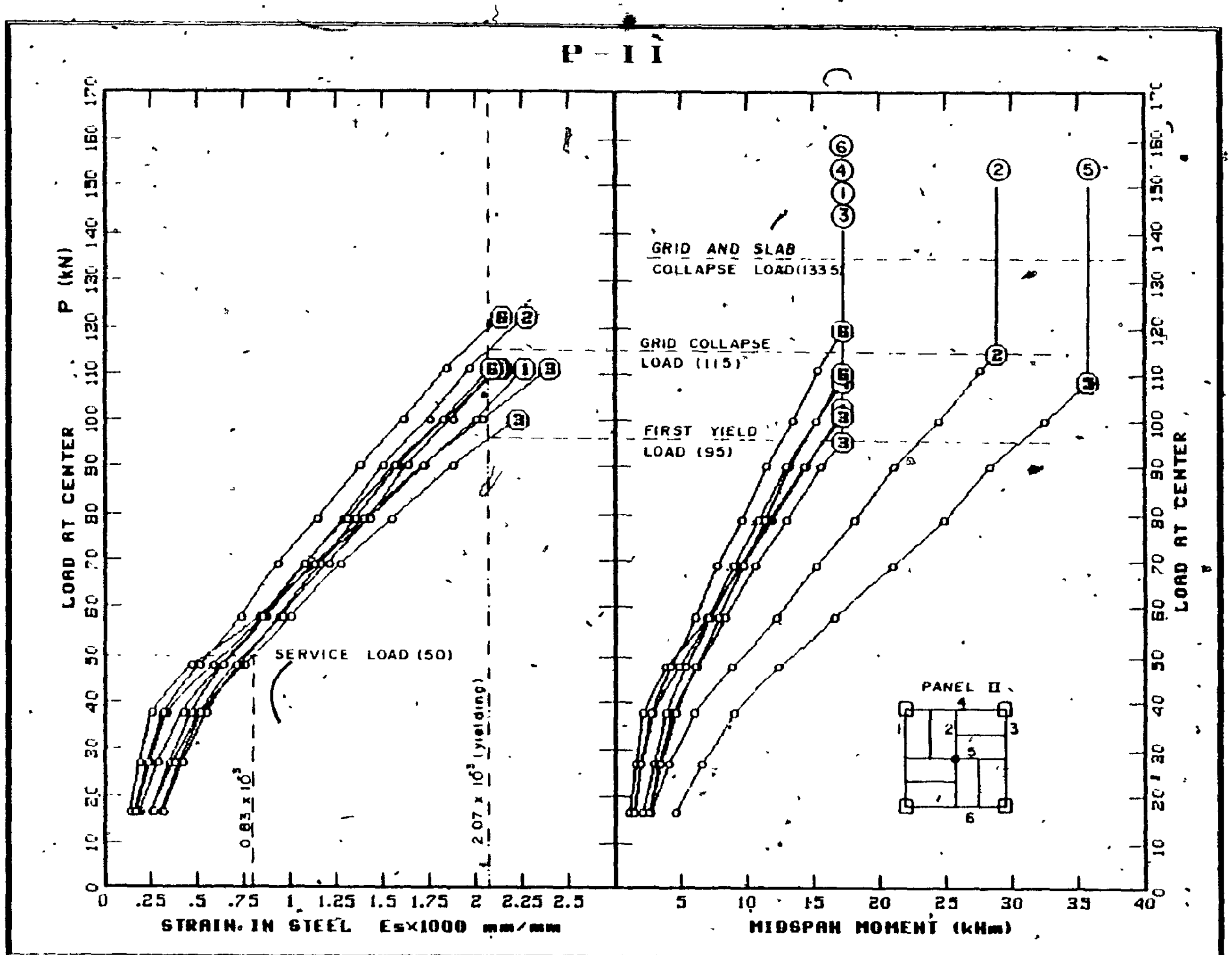

FIG. 4.7 LOAD-MOMENT RELATIONSHIP AT MIDSPAN OF EACH RIB OF THE TEST-PANEL II

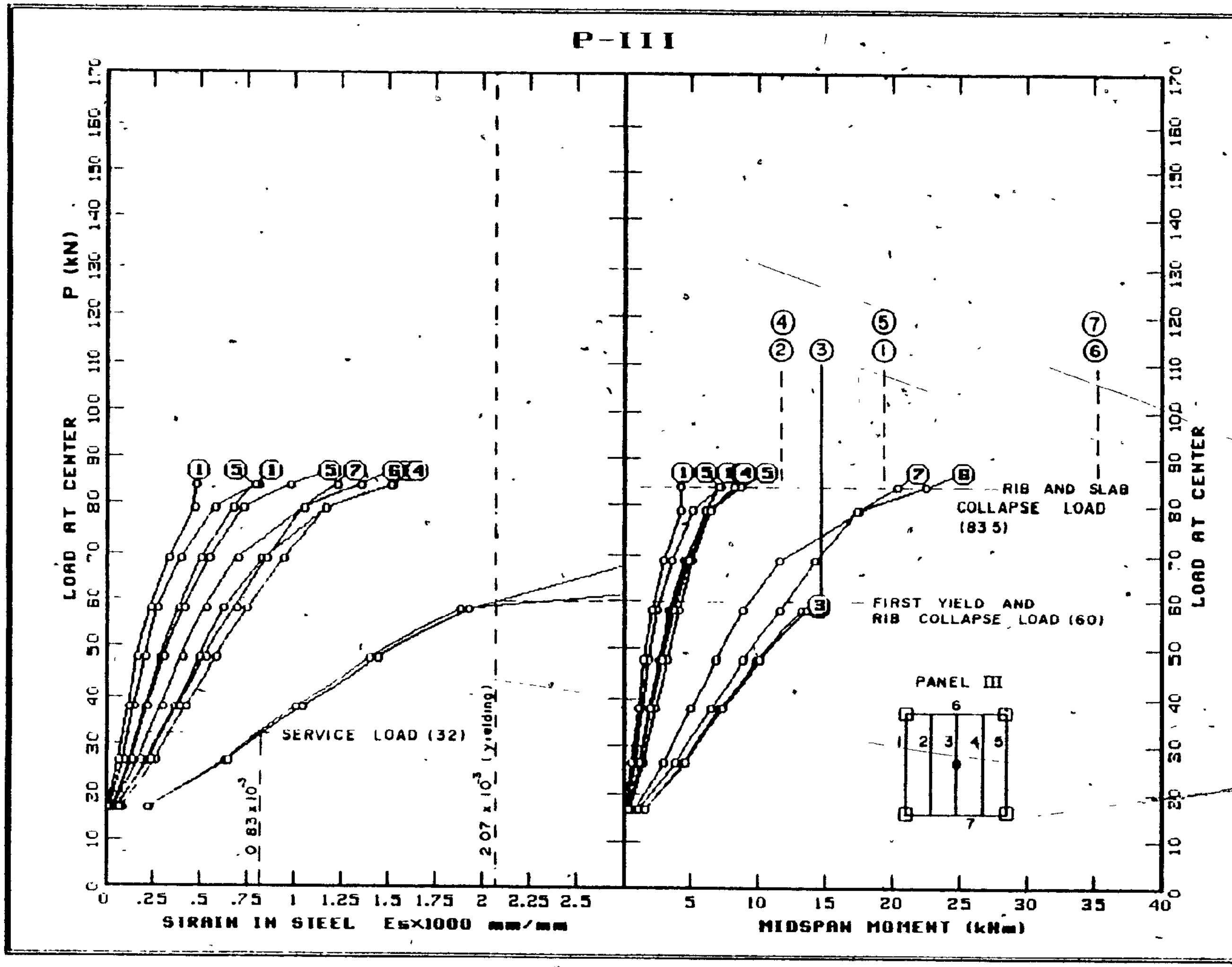

FIG. 4.8 LOAD-MOMENT RELATIONSHIP AT MIDSPAN OF EACH RIB OF THE TEST-PANEL III

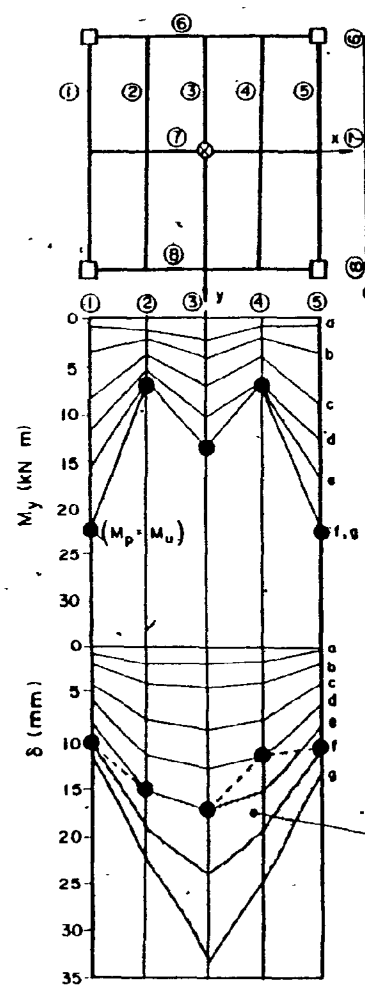

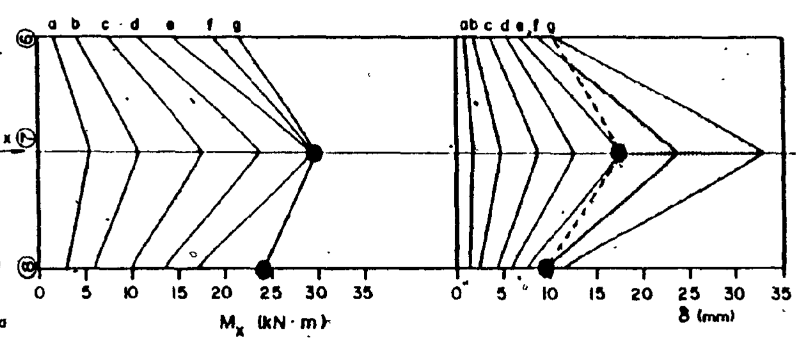

LOADING STEP	LOAD AT CENTER (kN)	TOTAL ONE-WAY MOMENT RATIO $\Sigma M_x/M_o$	$\Sigma M_y/M_o$
a	20	0.835	0.509
b.	40	0.852	0,670
	(41)*		
c	60	0.954	0.900
d	80	0.980	0.978
	(96)**		
e	100	1.003	0.996
f	120	0.991	0.992
g	133.5		

RIB NO.	(1) & (5)	(2) & (4)	(3)	(6) & (8)	(7)
M_u (kN.m)	22.60	6.72	13.96	24.03	29.77
A_s (cm^2)	4.00	1.29	2.84	4.13	5.10
M_u/A_s (kN/m x 10^4)	5.65	5.21	4.92	5.82	5.84

$M_o = PL/4 = 0.61\ P$

*SERVICE LOAD
**GRID COLLAPSE LOAD

NOTE: The black points represent plastic moments of constant value.

After the successive yielding of ribs and the formation of the grid collapse mechanism the panel continues to sustain load by membrane action.

FIG. 4.9 MOMENTS AND DEFLECTIONS ACROSS THE CENTER LINES OF THE TEST-PANEL I_A UNDER INCREASING LOAD

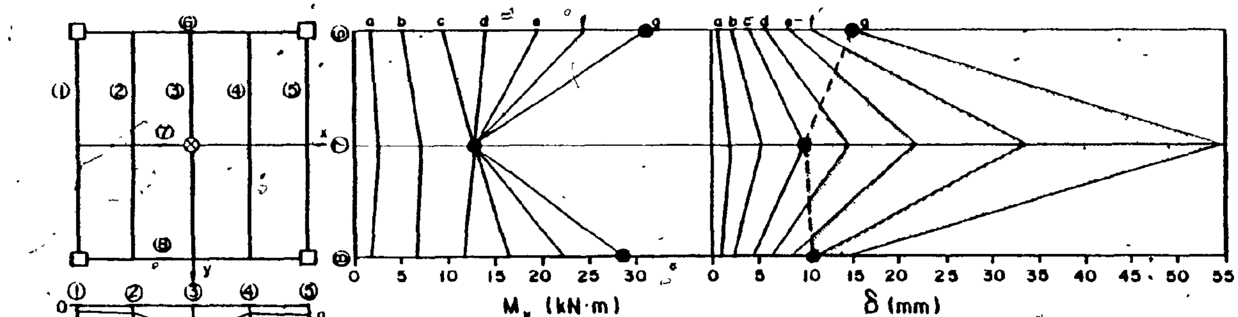

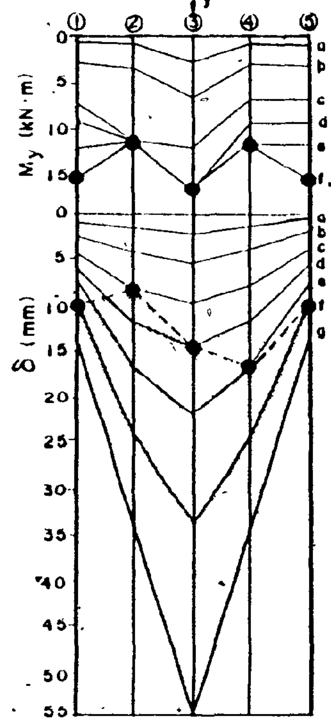

LOADING STEP	LOAD AT CENTER (kN)	TOTAL ONE-WAY MOMENT RATIO $\Sigma M_x/M_o$	$\Sigma M_y/M_o$
a	20	0.528	0.363
	(30)*		
b	40	0.775	0.715
c	60	0.933	1.188
d	80	0.892	1.131
	(91)**		
e	100	0.901	1.018
f	120	0.913	0.939
g	144.5		

RIB NO.	(1) & (5)	(2) & (4)	(3)	(6) & (8)	(7)
M_u (kN.m)	18.27	11.20	16.07	32.70	12.86
A_s (cm^2)	3.29	2.00	2.84	5.68	2.00
M_u/A_s (kN/m x 10^4)	5.55	5.60	5.66	5.76	6.43

*SERVICE LOAD
**GRID COLLAPSE LOAD

FIG. 4.10 MOMENTS AND DEFLECTIONS ACROSS THE CENTER LINES OF THE TEST-PANEL I_B UNDER INCREASING LOAD

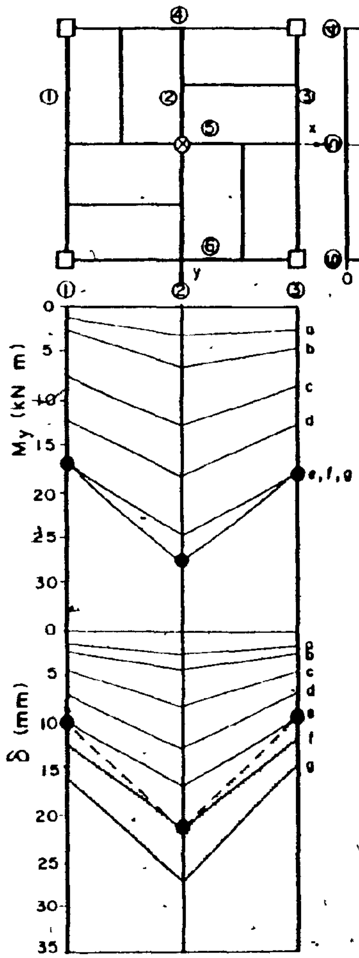

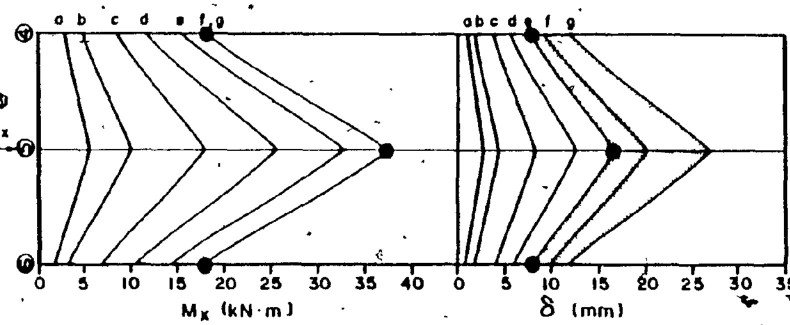

LOADING STEP	LOAD AT CENTER (kN)	TOTAL ONE-WAY MOMENT RATIO $\Sigma M_x/M_o$	TOTAL ONE-WAY MOMENT RATIO $\Sigma M_y/M_o$
a	20	0.807	0.590
b	40	0.732	0.561
	(50)*		
c	60	0.894	0.786
d	80	0.965	0.884
e	100	1.019	0.971
	(115)**		
f	120		
g	133.5		

	RIB NO. (1), (3), (4) & (6)	RIB NO. (2)	RIB NO. (5)	
M_u (kN.m)	17.99	30.13	37.34	
A_s (cm^2)	3.29	6.45	6.45	
M_u/A_s (kN/m x 10^4)	5.47	4.67	5.79	

*SERVICE LOAD
**GRID COLLAPSE LOAD

FIG. 4.11 MOMENTS AND DEFLECTIONS ACROSS THE CENTER LINES OF THE TEST-PANEL II UNDER INCREASING LOAD

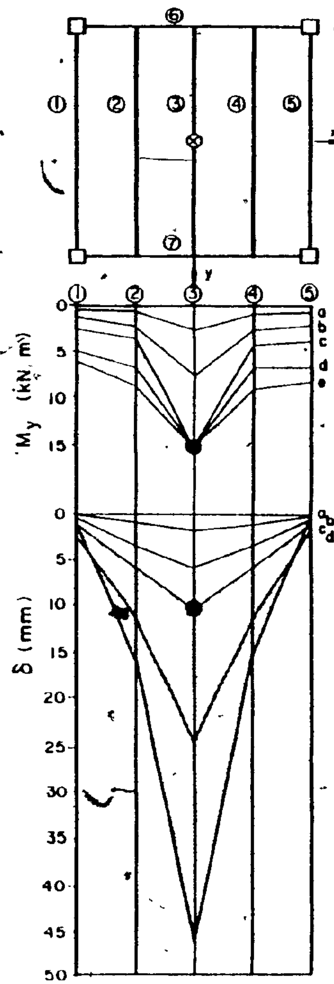

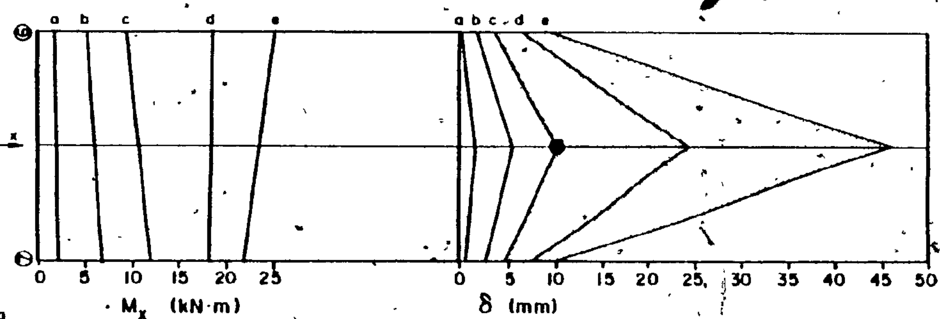

LOADING STEP	LOAD AT CENTER (kN)	TOTAL ONE-WAY MOMENT RATIO $\Sigma M_x/M_o$	TOTAL ONE-WAY MOMENT RATIO $\Sigma M_y/M_o$
a	20	0.301	0.414
	(32)*		
b	40	0.507	0.654
c	(60)**	0.588	0.806
d	80	0.753	0.831
e	87	0.887	0.895

	RIB NO. (1) & (5)	(2) & (4)	(3)	(6) & (7)	
M_p (kN.m)	19.35	11.78	15.19	35.11	
A_s (cm^2)	3.29	2.00	2.58	6.45	
M_p/A_s (kN/m x 10^4)	5.88	5.89	5.89	5.44	

*SERVICE LOAD
**RIB COLLAPSE LOAD

FIG. 4.12 MOMENTS AND DEFLECTIONS ACROSS THE CENTER LINES OF THE TEST-PANEL III UNDER INCREASING LOAD given in tabular form, in the same figures, it can be observed that the ratio of the sum of the moments in the ribs to the total static moment in each direction is less than one and increases with the load, approaching unity at the state of formation of the first plastic hinge. This may be attributed to the inadequacy of the assumption of the linear stress distribution of the W.S.D. method, in describing the actual stress distribution in reinforced concrete sections, in the loading range where progressive cracking occurs (There is a small underestimation of the moment carried by the sections).

The total one-way moment-to-the load relationship in both principal directions of all test panels is presented in Figure 4.13, where the discrepancies of the estimated total one-way moments from the theoretical total one-way static moment of the equivalent beam are clearly shown.

4.5 IN-PLANE STRESSES

The higher collapse loads recorded in the test at the second stage of incremental collapse, compared with the collapse loads at the first elementary mechanism collapse, as well as the still higher recorded loads corresponding to the general collapse of the system of grid and top slab, can be attributed partly to the membrane action in the top slab. Generally, a flexural T-beam action generates some precompression within the slab. These membrane stresses are additional to the compressive stresses created by an arching action, which

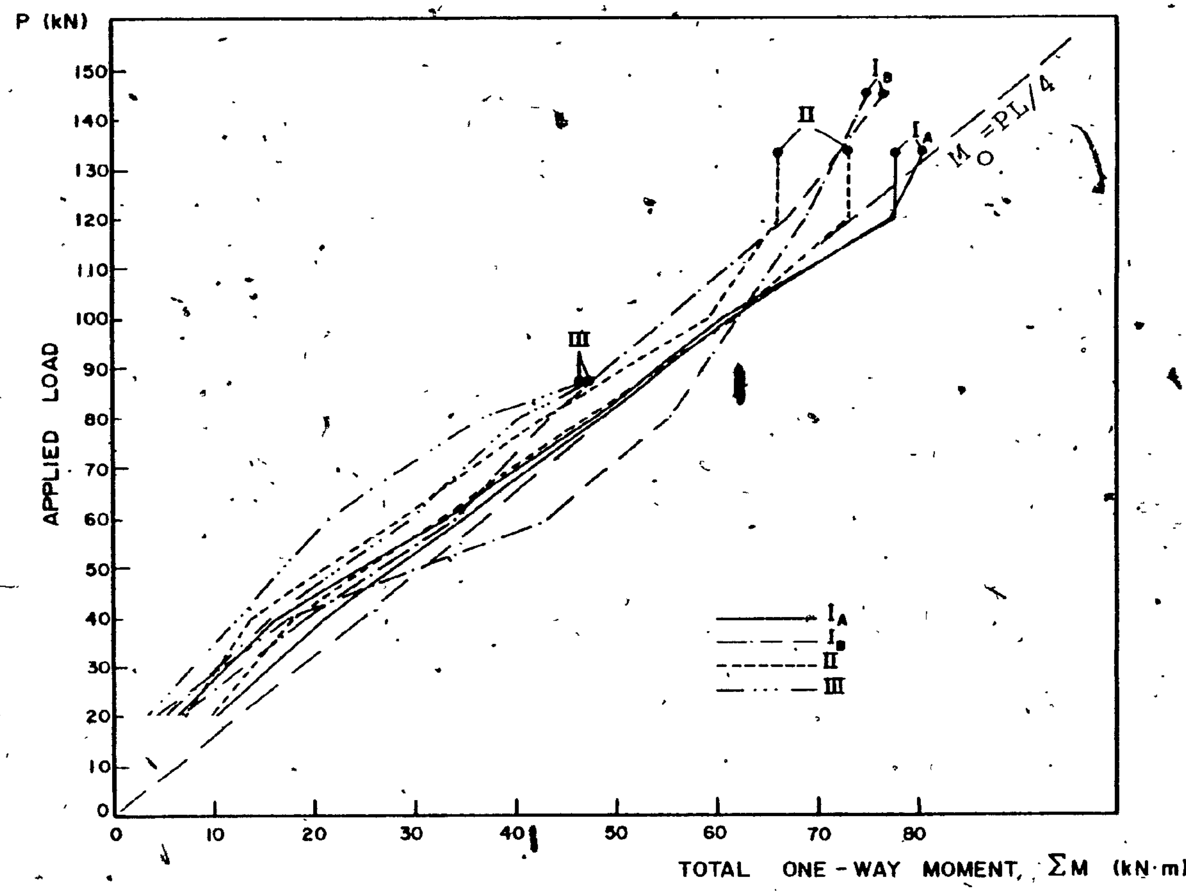

FIG. 4.13 LOAD-TOTAL ONE-WAY MOMENT RELATIONSHIP FOR BOTH DIRECTIONS OF ALL TEST-PANELS

may occur within the depth of the ribs, resulting from possible restraint to the outward movement of the bottom edges of the interior ribs. The outward movement may be restricted by the torsional rigidity of the edge ribs. This torsional rigidity is usually secured by the addition of reinforcement tying the edge ribs together at the corners of the panel. These compressive membrane stresses can be created at any loading stage, depending on the degree of torsional rigidity of the edge ribs. At large deflections, the edges of the panels tend to move inwards. This lateral movement may be partially restricted by the resistance of the edge ribs in lateral bowing, thus creating tensile membrane stresses. At still larger deflections, a central area of tensile membrane stresses may be created. These tensile stresses are resisted by the formation of an outer compression ring in the perimeter region of the top slab of the panels. Such tensile stresses may develop throughout the depth of the ribbed slab in the central area and cracks may penetrate to the top of the panel. All these developments can result in an enhancement of the carrying capacity of the panels in the various loading stages.

The development of membrane stresses in various circumstances is a recognized phenomenon and has been documented for solid slab and slab-beam systems with edges free to permit lateral movements. These stresses are discussed in detail by Hayes (1968) [32] for tensile membrane action and by Datta and Ramesh (1975) [33] for compressive membrane action.

The in-plane strains in the top slab of the test panels were monitored by strain gages placed in selected locations on the concrete surface, on the ribbed side of the panels. The location of the strain gages and the corresponding load-strain curves are shown in Figure 4.14, for the panels I_A and I_B, and in Figure 4.15, for the panels II and III. The sign of the membrane stresses at the loading stages of the first stage grid collapse, and the grid and slab system collapse for all four panels is illustrated in Figure 4.16. As the graphs show, tensile stresses were recorded by the majority of gages in the test panels, with the exception of panel III. This confirms the hypothesis made earlier, that in joist floor systems, the compressive zone is limited to a part of the flange area, and that the whole web of the T-beam is subjected to tension.

However, compressive stresses were recorded in the vicinity of some of the edge ribs, which indicates that a compression ring was formed in this area. After the first stage grid collapse, the tensile forces at the center of the panels started decreasing, which can probably be explained as a convex arch effect. In panel III, where large deflections were recorded, the geometry of the deformations may also have created such an arch effect since in-plane compressive stresses dominated the behavior of the central portion of the slab. Similar behavior was demonstrated by the panel I_B, which also had relatively large deflections.

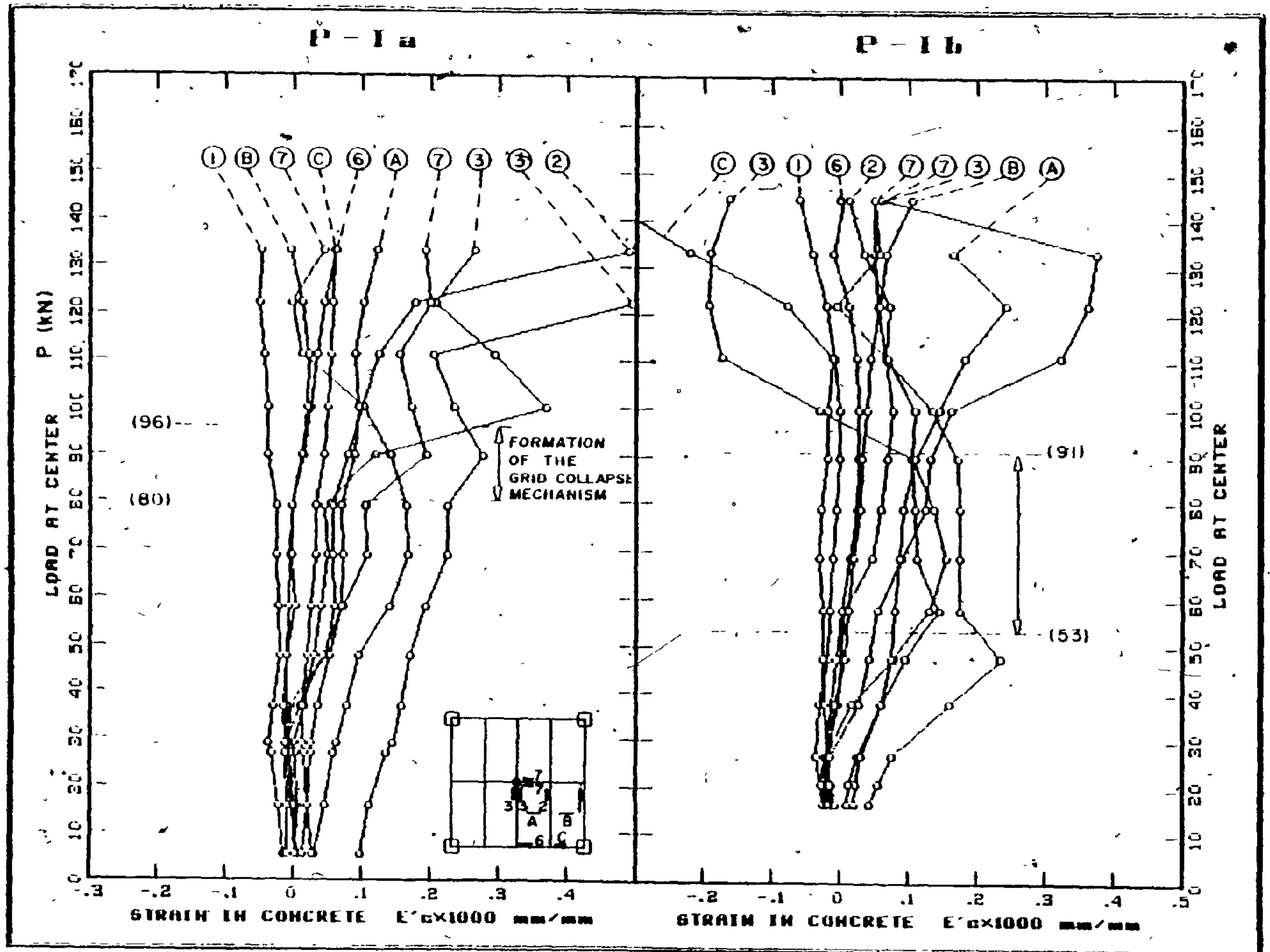

FIG. 4.14 LOAD-STRAIN RELATIONSHIP AT SELECTED LOCATIONS ON THE TOP SLAB OF THE TEST-PANELS I_A AND I_B

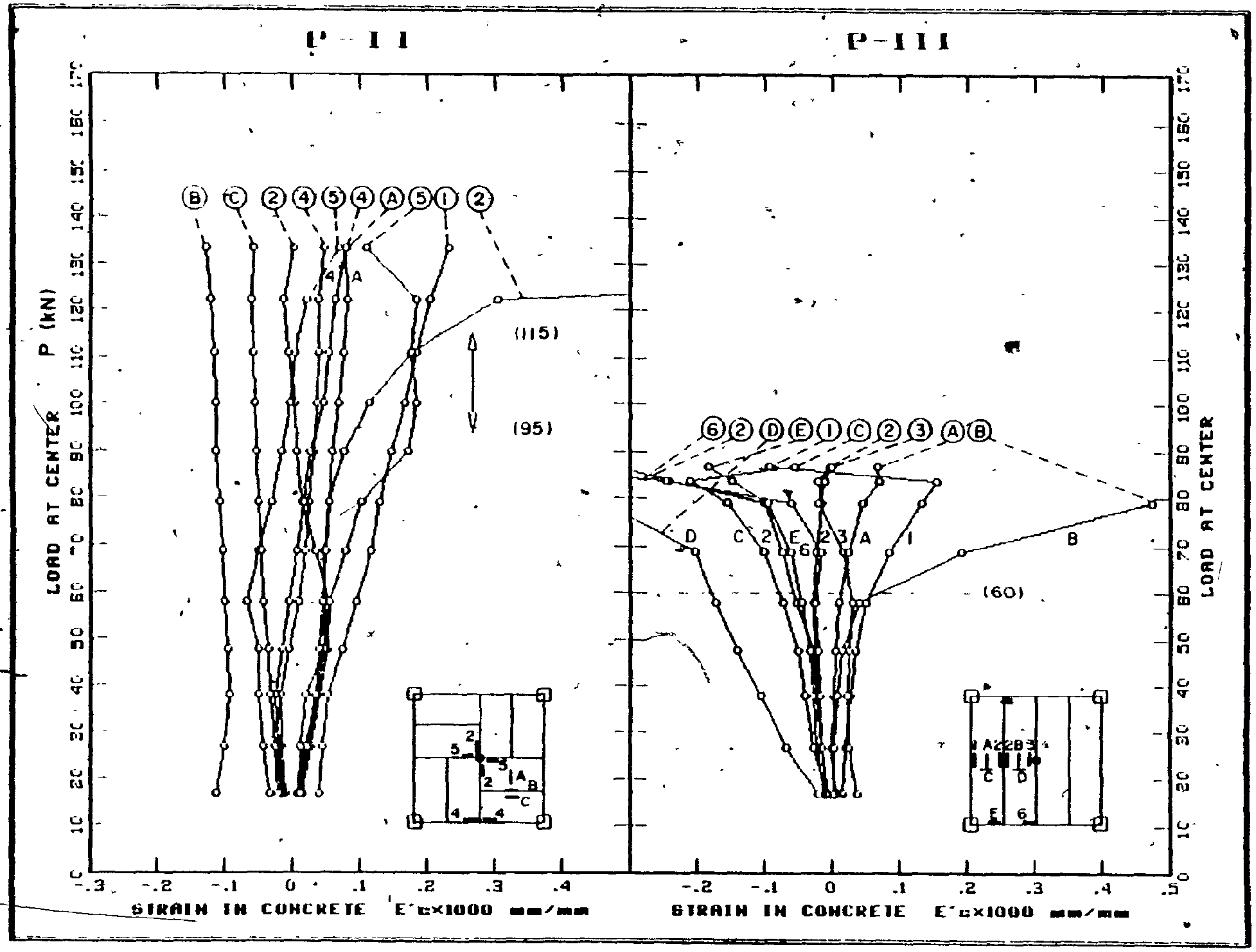

FIG. 4.15 LOAD-STRAIN RELATIONSHIP AT SELECTED LOCATIONS ON THE TOP SLAB OF THE TEST-PANELS II AND III

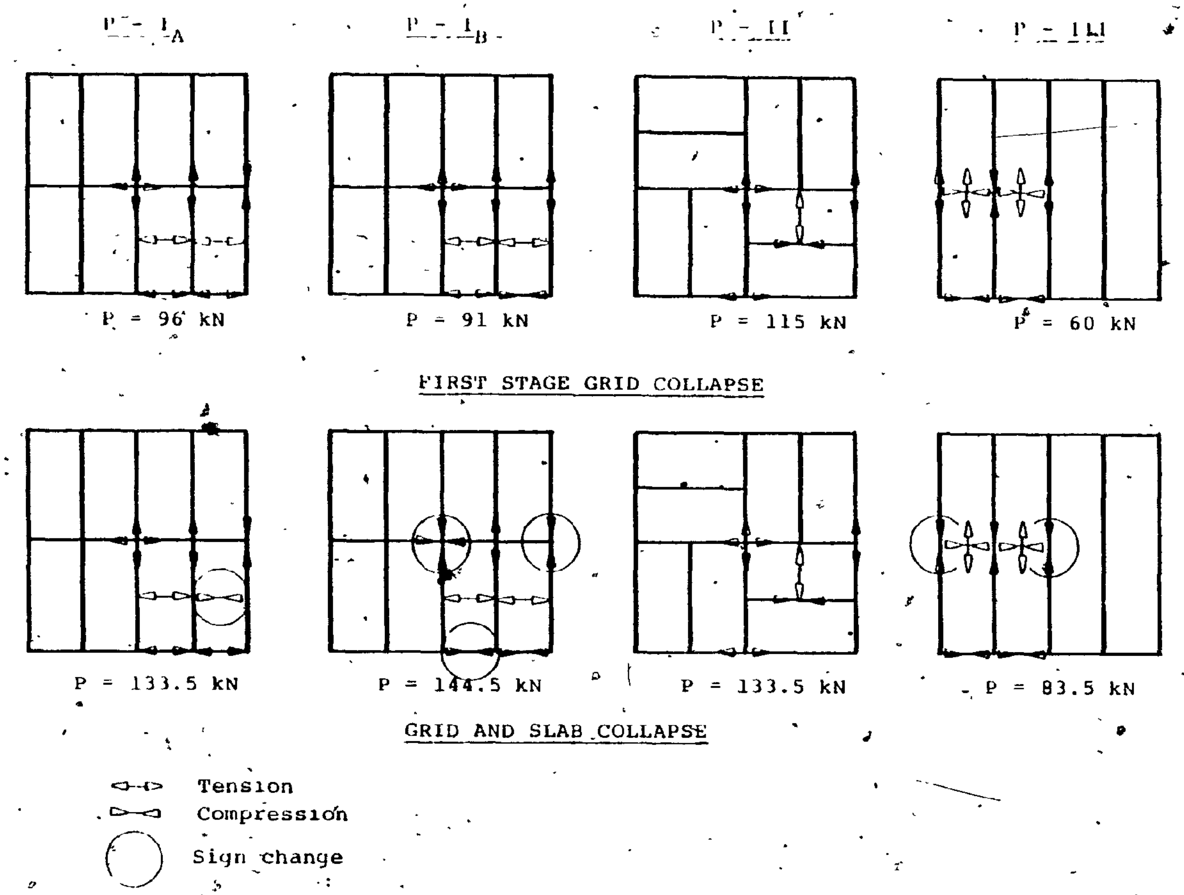

FIG. 4.16 MEMBRANE STRESSES AT RESPECTIVE LOADINGS OF FIRST STAGE GRID COLLAPSE AND GRID AND SLAB COLLAPSE

4.6 CRACKING PATTERNS AND COLLAPSE MECHANISMS

The observation and recording of cracking patterns under increasing loads was undertaken to examine the overall behavior and the redistribution of those bending moments in the test-panels.

The recorded crack patterns developed during the loading of the test-panels within the elastic range are illustrated in Figure 4.17. It is shown that the cracks were confined mainly to the web of the T-beams and were distributed almost uniformly along all the ribs, which confirms the two-way action and a similarity in the behavior of all four panels.

In the subsequent loading stages until failure, cracks also developed in the top slab, in association with the formation of the flexural hinges in the ribs and the overall collapse mechanism. These cracks are shown in Figure 4.18, for all panels.

Pictures of the test panels after failure are shown in Figure 4.19 and a close view for one of the panels (I_B) is shown in Figure 4.20, where the deflected shape and cracking can be observed.

The grid collapse mechanisms established from the load-moment relationship graphs, based on steel strain measurements, are generally in good agreement with the results of the plastic

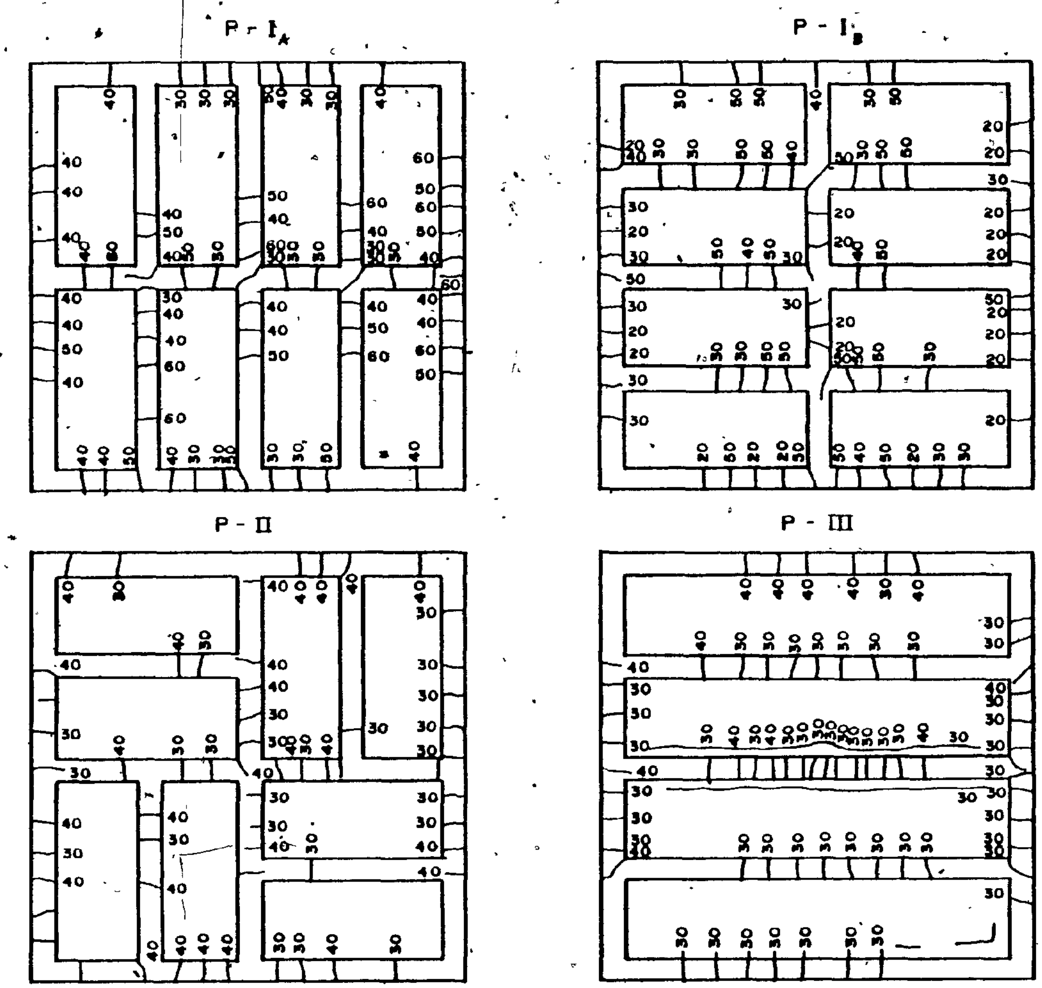

FIG. 4.17 CRACK PATTERN IN THE RIBS OF THE TEST-PANELS

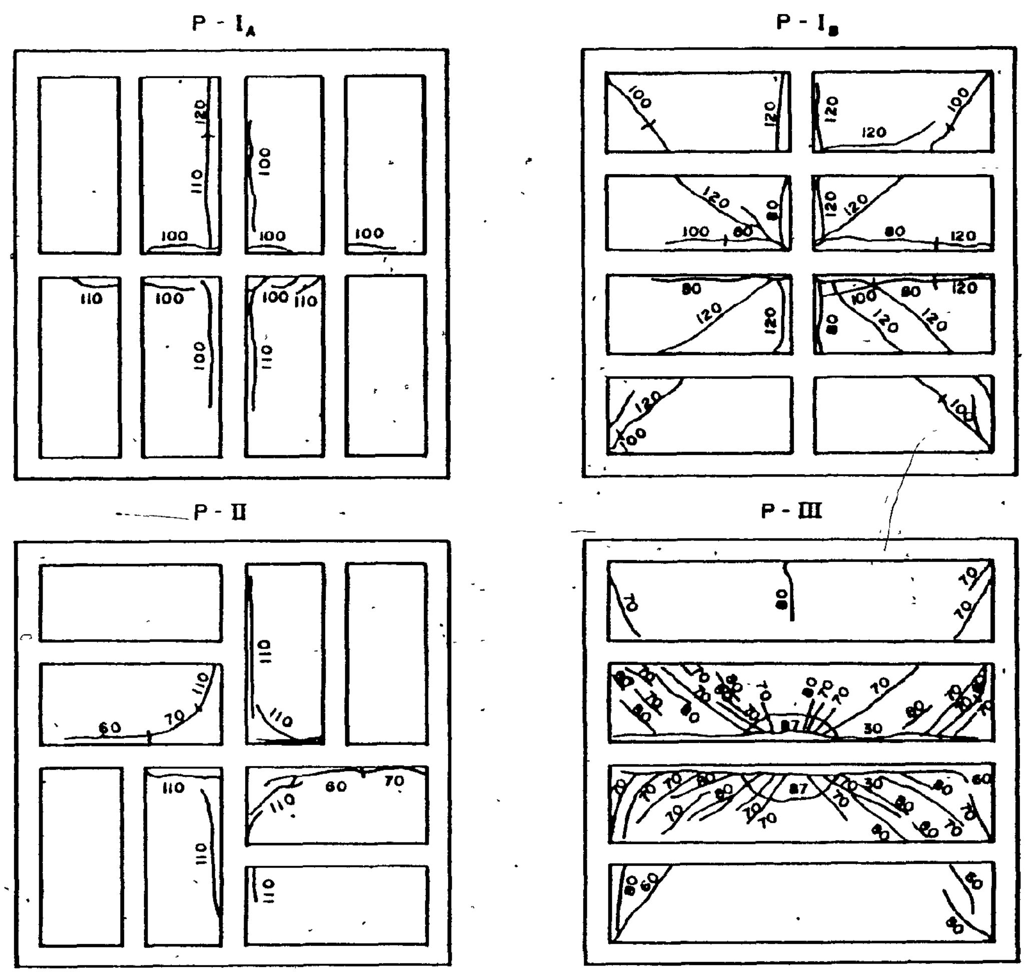

FIG. 4.18 CRACK PATTERN IN THE TOP SLAB OF THE TEST-PANELS

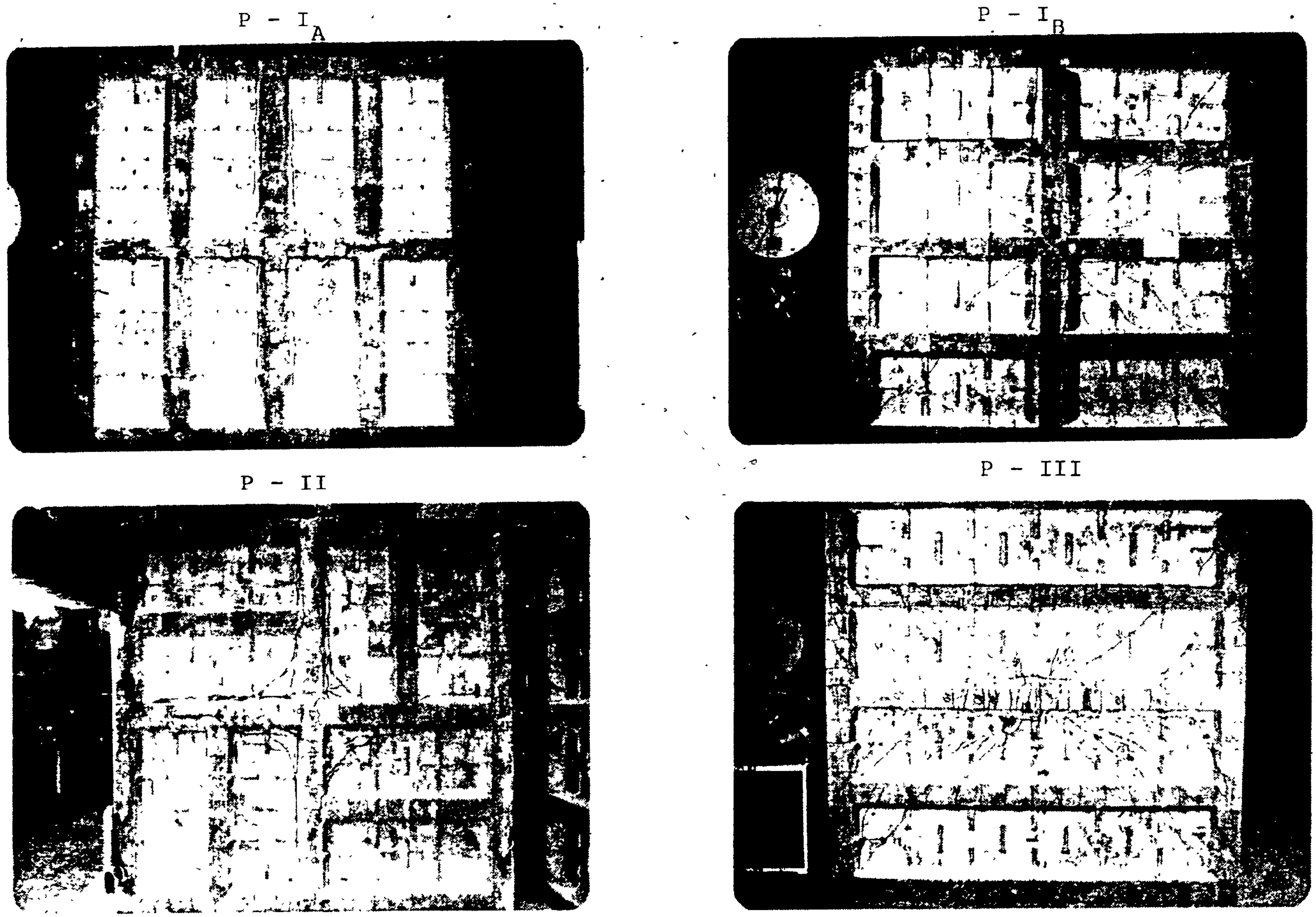

FIG. 4.19 TEST-PANELS AFTER FAILURE

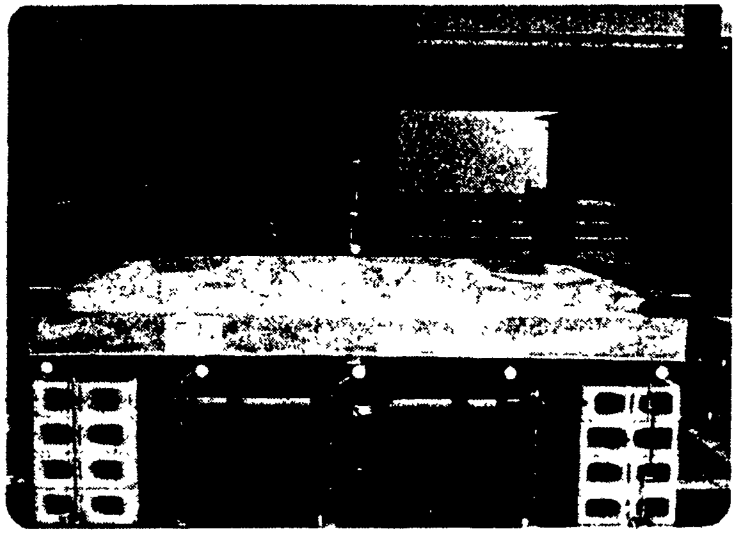

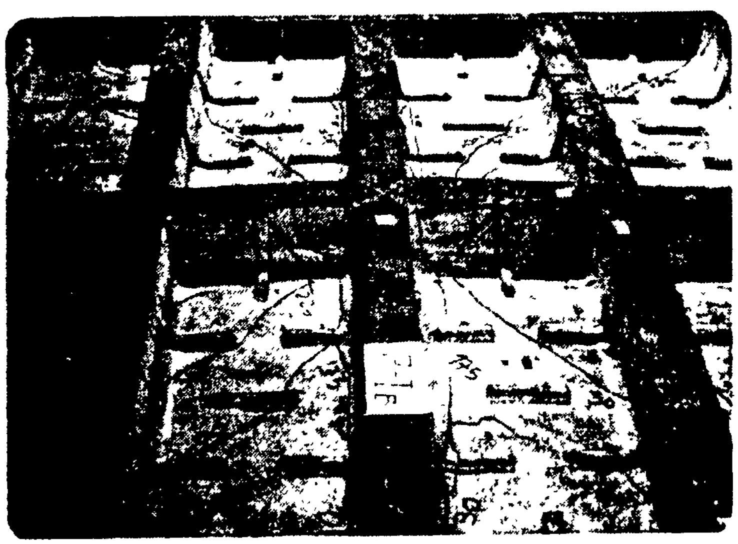

FIG. 4.20 DEFORMED SHAPE AND CRACKS OF THE TEST-PANEL I_B

analysis given in Appendix B. All those panels tested failed by flexure. The failure occurred after the full development of the predicted collapse mechanisms, with the exception of panel III, as was anticipated.

The failure behavior of the panels can be described in more detail, as follows.

4.6.1 Test-Panel I_A

In this panel, all the interior ribs failed after the reinforcement reached yield strength within the loading range of 80 to 96 kN, according to the predicted "unique" solution of limit analysis associated with mechanism (5) shown in Appendix B, and in agreement with the predicted collapse load. This load was estimated at 82.70 kN, which value is close to the beginning of the mechanism formation stage.

Under further loading and with the help of tensile membrane action at deflections beyond the $\ell/180$ serviceability limit, the failure of the edge ribs followed as the load increased from 113 to 123 kN. This was considered as the second stage of incremental collapse of the grid system, taking place according to the predicted "upper bound" solution associated with mechanism (3), under the collapse load of 123.30 kN. After that, the panel continued to resist additional load by tensile membrane action until it collapsed at a load of 133.5 kN. This high level of tensile resistance by the top slab seems to result from the presence of wire-mesh reinforcement provided at the mid-depth of the slab. (The tensile yield capacity of the wire-mesh alone was 25 kN per meter width.)

4.6.2 Test-Panel I_B

This panel exhibited more ductile behavior and much larger deflections than panel I_A. The panel failed with the predicted collapse mechanism (5) which was the same as that in panel I_A. All the interior ribs failed by yielding of reinforcement within the loading range of 53 to 91 kN, while the predicted collapse load was 65.79 kN, somewhere in the middle of the mechanism formation stage.

The panel continued to carry load with the help of tensile membrane action, which led to the failure of the edge ribs between the loads of 123 and 143 kN. The predicted collapse load for this collapse stage was 125.63 kN corresponding to the collapse mechanism (3). The general collapse of the panel followed immediately after at the load of 144.5 kN.

4.6.3 Test-Panel II

In this panel, there was an overlapping between the two stages of incremental collapse. Both, the mechanism (1) with a predicted collapse load of 108.38 kN, and the mechanism (3) with a predicted collapse load of 114.29 kN, were formed within the loading range of 95 to 115 kN.

The panel continued to carry load with the help of the tensile membrane action until the general collapse at the load of 133.5 kN.

4.6.4 Test-Panel III

Panel III failed early by a local failure of the central rib, which carried the load without sufficient help from the cross-ribs. This rib showed large deflections from the beginning and was almost separated from the rest of the panel by cracking in the top slab along the sides of the rib. The separation and out-of-plane movement of the rib caused the stretching out in a cross-direction of the wire mesh, as well as the shear and moment at the edges of the cracks in the top slab. The rest of the panel resisted the out-of-plane movement by in-plane action demonstrated by compressive stresses in the slab outside the cracking perimeter of the tensile central zone, as was recorded by the strain gages.

The arching action associated with the large deflections allowed the panel to continue supporting the increasing load from the stage of failure of the central rib, at 60 kN, until the ultimate failure at 83.5 kN by a circular punching shear crack around the loading jack.

A mode of failure, similar to the one of mechanism (3) having a collapse load of 121.04 kN, had been initiated but was not completed, due to the local failure.

CHAPTER 5

DISCUSSION AND RECOMMENDATIONS

CHAPTER 5

DISCUSSION AND RECOMMENDATIONS

5.1 GENERAL

Most of the statically indeterminate reinforced concrete structures, including the regular two-way ribbed floors, are currently designed by determining their internal forces from an elastic analysis and by proportioning the sections, using ultimate strength criteria. This procedure does not provide the means for a realistic evaluation of the actual factor of safety in complex structures such as the irregularly ribbed joist floors. In structures whose deformation capacity is large enough to permit a mechanism collapse, an equilibrium limit design method, formulated in terms of member strength, can be used. In this manner the members are proportioned for serviceability and safety against local failure and overall structural collapse.

The design criteria of such a limit design method may also be used to assess the serviceability and safety of those grid structures designed by the method of ultimate strength design, with or without reinforcement transfer. Using this procedure, the experimental results from the test-panels can be interpreted and the influence of the reinforcement transfer can thus be evaluated.

The tests performed in this research program were limited to a single bay center point loaded slab, however, some of the observations and conclusions of this investigation can be valid in the analysis of the behavior of continuous floor systems. For example, the comparison of the distribution of elastic bending moments in a single and a multi-bay floor system is shown in Figure 5.1. This comparison shows close similarities in the moment distribution patterns for both cases. The only significant difference is that the reference axis (axis of zero moment), is shifted upwards in the continuous floor model, corresponding to the negative moment developed over the supporting strips.

5.2 INTERPRETATION USING LIMIT DESIGN CRITERIA

The test-panels were reinforced on the basis of the total one-way static moment, due to the ultimate design load of 119 kN (see paragraph 3.2), which was distributed between the individual ribs by assumed distribution percentages, such as the ones conventionally used for flat slab structures, and subsequent transfer of various moment percentages between strips. A comparison of the resulting moments, with the moments obtained by the elastic analysis of the equivalent grids of the T-beams, based on gross concrete sections (Figures 3.7 and 3.8), shows a shifting of moment from the ribs of the middle strips (interior ribs) to the ribs of the column strips (edge ribs). The reinforcement provided in the test-panels, based on the

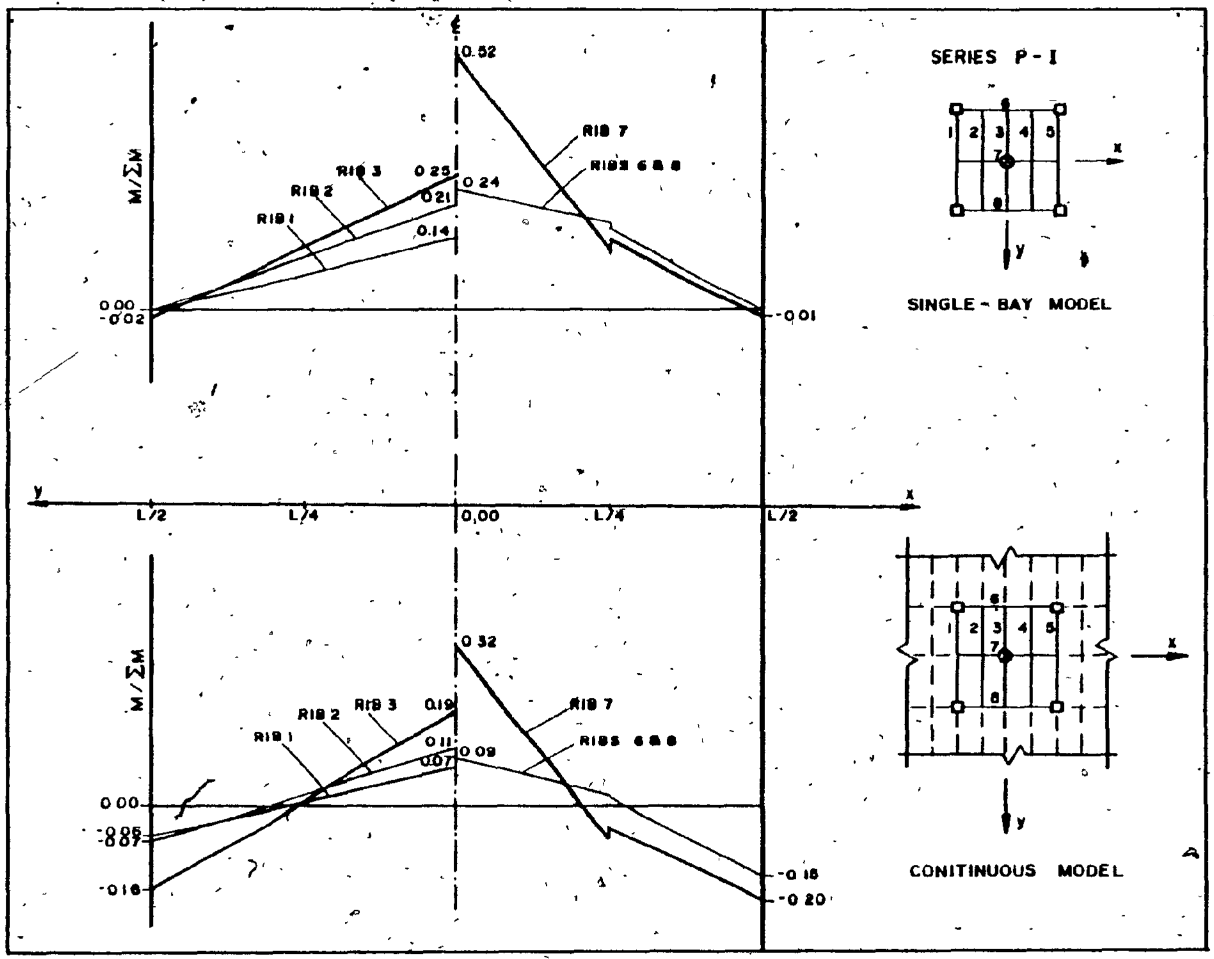

FIG. 5.1 DISTRIBUTION OF MOMENTS IN A SINGLE-BAY AND A CONTINUOUS MODEL ACCORDING TO THE ELASTIC ANALYSIS

assumed distribution of moments, in comparison with the reinforcement corresponding to an elastic distribution of moments, is similarly affected by a transfer from the middle to the edge strips. The average reinforcement transfer between the two directions of each panel previously discussed in paragraph 3.3 constitutes a parameter of this investigation and its influence is examined.

The behavior of the test-panels and the influence of reinforcement transfer were assessed by such limit design criteria as the overall load factor, the first yield load factor and the percentage of elastic moment redistribution. The above limit design criteria previously mentioned in the "equilibrium (serviceability)" methods of limit design were evaluated on the basis of the experimentally obtained load capacity limits of the test-panels. The values of the limit design criteria are calculated in Table 5.1, for all four panels, first on the basis of the assumed experimental service loads for each panel, then on the basis of the assumed experimental service load of panel II, for the purpose of comparison since this panel corresponds to the case of zero reinforcement transfer. The results show that in the case of panel II, the first yield load factor or factor of safety against local section failure (λ_1) is equal to 1.90, the largest value between all panels, which is larger than the lower limit of 1.2 suggested by Cohn in his draft code provisions [31]. The serviceability index (x_i) is equal to 0.83 which means that a 17% moment redistribution takes place.

TABLE 5.1 LIMIT DESIGN CRITERIA FOR THE TEST-PANELS

PANEL	I_A	I_B	II	III
Percentage of reinforcement transfer	~20	~25%	~ 0%	~40%
Assumed experimental service load (W) *	41** (50)***	30 (50)	50 (50)	32 (50)
Assumed experimental failure load (W_u)+	96	91	115	60
Experimental first yield load (W_1)±	80	53	95	60
Overall load factor ($_C = W_u/W$)	2.34 (1.92)	3.03 (1.82)	2.30 (2.30)	1.88 (1.20)
First yield load factor ($\cdot_1 = W_1/W$)	1.95 (1.60)	1.76 (1.06)	1.90 (1.90)	1.88 (1.20)
Service-ability index ($x_1 = W_1/W_u$)	0.83	0.58	0.83	1.00
Percentage of elastic moment redistribution ($Y_1 = 1 - x_1$)	17% (0.17)	42%	17%	0

* From Table 4.2, column (6).
** Experimental service load of each panel.
*** Experimental service load of panel II.
\+ From Table 4.2, column (8).
± From Table 4.2, column (7).

This percentage is close to 15% limit suggested in the 1972 CEB recommendations and below the 20% limit suggested in the American Standards (ACI 318-77), for continuous beams or equivalent structures and for negligible dead load, as explained by Cohn [31]. A comparison of the behavior of panel II with the other panels shows that an increase in the percentage of reinforcement transfer causes proportional decrease in the service and collapse load, a similar decrease in the factor of safety, and a decrease in the first yield load factor. The decreased first yield load factor of panel I_B was 1.06, below the minimum value of 1.2, and this resulted in the large deflections recorded in the experiments and a large percentage of elastic moment redistribution of 42%. This percentage is still below the limit of 67% suggested by the Danish Standard, (DS, 411-49), but above the 20% suggested in the American Standard. Considering the overall poor performance of panel I_B, it seems that a percentage of reinforcement transfer of 20% may be the practical limit for these types of structures.

5.3 THE EFFECTS OF REINFORCEMENT TRANSFER

A parametric investigation of the various types of equivalent models has been undertaken in order to explain the influence of reinforcement transfer on the load-carrying capacity and structural safety. The various series of models studied are shown in Appendix E, where the ultimate load capacity of the models is calculated on the basis of the first stage grid collapsed mechanisms similar to the ones observed in the test-panels. Each series of models consists of various cases, produced by a progressive reduction in the average percentage of the middle strip reinforcement of the two directions.

The results of this study are summarized graphically in Figure 5.2, which shows that the load capacity of the models is reduced linearly with respect to the increase in the percentage of the reinforcement transfer. This is explained by the fact that the ultimate load is always a linear function of the moment capacity of the individual ribs. The slope of the linear relationship is the same for the isotropic model II and for the model I, in the case that the reinforcement transfer occurs in the stronger direction. In cases where the reinforcement transfer in model I is shared between the two directions, then the line of the relationship falls within the shadowed area shown in the graph. The same graph also shows that the ultimate load capacity of a grid model is reduced when the number of ribs is reduced. Thus, the strongest of all grid models is the model I and the weakest, model III. The slope of the linear relationship for model III is different than in the other models because the load is actually carried by the interior ribs in the one direction only.

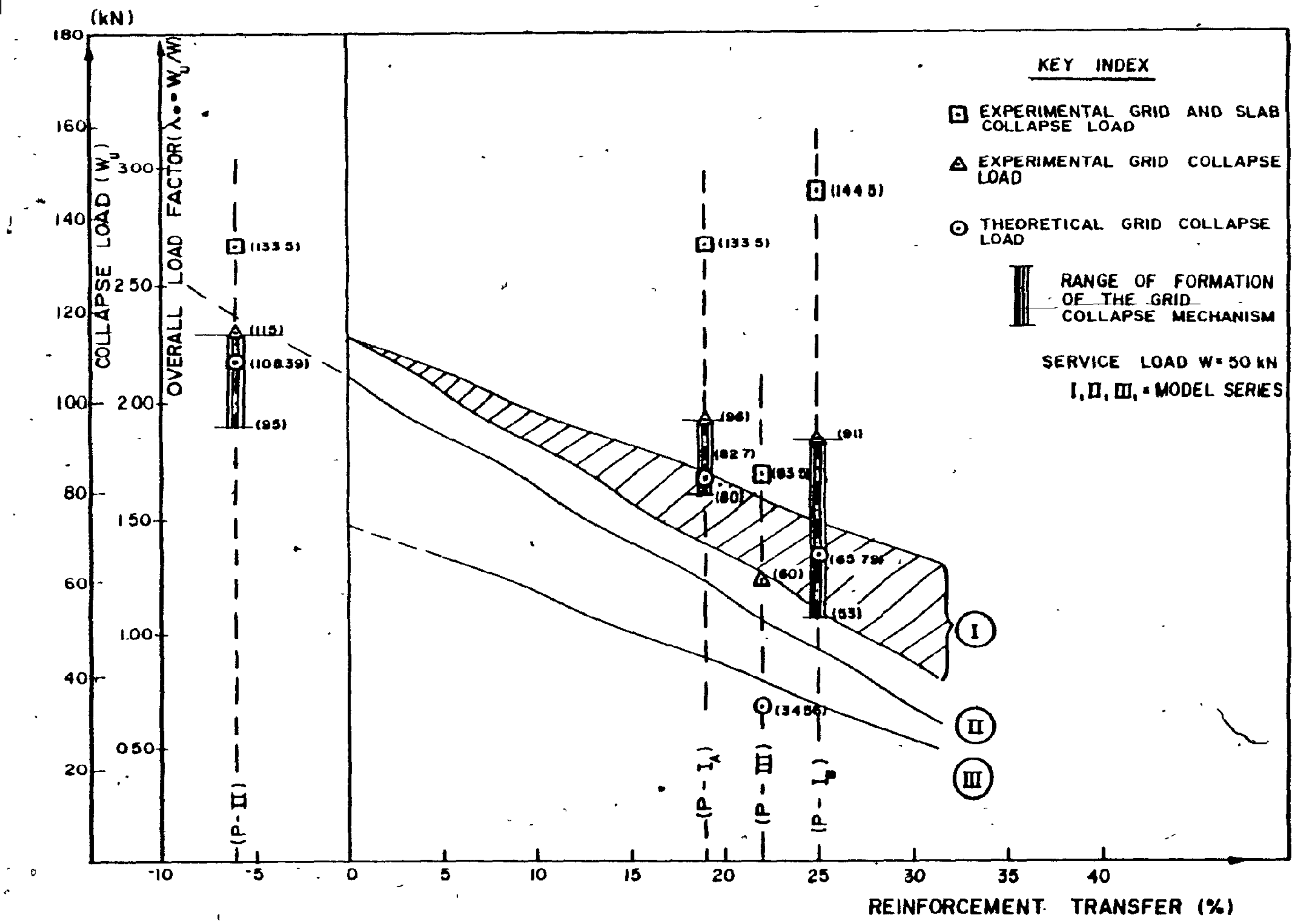

FIG. 5.2 EFFECT OF REINFORCEMENT TRANSFER ON THE ULTIMATE LOAD CAPACITY OF THE MODELS

The theoretical and experimental collapse loads for the test-panels are also shown in Figures 5.2, in relation to the ultimate load of the various models. It is shown that the first stage grid collapse load of the test-panels is close to the corresponding values of the linear ultimate load-reinforcement transfer relationships for the models.

The same graph is also used to express the factor of safety-to-the reinforcement transfer relationship, for the assumed service load of 50 kN.

5.4 OBSERVATIONS AND RECOMMENDATIONS

On the basis of the results of the investigation of corner-supported ribbed panels subjected to a single concentrated load, as described earlier, several observations can be made concerning the general behavior of the panels in the elastic and elastoplastic range, the advantages of a design based on an elastic analysis, and the consequences of transferring of reinforcement between ribs.

5.4.1 Overall Behavior

1. In joist floor systems where a good two-way action exists, the amount of reinforcement transferred between strips and in general the way that reinforcement is distributed between ribs does not effect substantially the general collapse load, which remains always above the specified ultimate load (Note: the

percentage of reinforcement transfer was kept within limits).

5.4.2 Elastic Behavior

1. The elastic analysis of an open grid equivalent model with rigidities based on cracked transformed sections gives a good approximation of the actual behavior (deflections, moment distribution) of the joist floor systems in the elastic range.

5.4.3 Elasto-Plastic Behavior

1. In general, the overall behavior of the joist floor systems in the elasto-plastic range depends on the amount and distribution of the reinforcement.

2. Plastic deformations may start early in weak ribs, resulting in moment redistribution and reduction of the elastic range, or in extreme cases, in local failures and premature collapse.

3. The collapse mechanism in joist floor systems can be considered as a combination of an incremental grid failure mechanism associated with in-plane membrane action of the top slab enhancing the ultimate carrying capacity of the floors beyond the grid collapse stages.

4. Local failure in a particular rib may be associated with cracking in the top slab and out-of-plane movement of the separated rib under the load.

5.4.4 Design Based on Elastic Analysis (The Case of Test-Panel II)

A design, based on elastic analysis, seems to be advantageous for the following reasons:

1. It gives the largest elastic range (maximum assumed experimental service load).

2. It gives the highest first-stage grid collapse load (assumed failure load).

3. It gives the highest structural safety for the same service load (overall load factor).

4. It gives the highest factor of safety against local section failure (first-yield load factor).

5. It results in the minimum elastic moment redistribution and maximum serviceability (in respect to cracks and deflections).

5.4.5 Design With Reinforcement Transfer (The Case of Test-Panels I_A and I_B)

An increase in the percentage of reinforcement transferred between the rib zones, which can be accepted to a limited degree only, may result in the following:

1. The reduction of the elastic range.
2. The reduction of the first-stage grid collapse strength.
3. The reduction of structural safety.
4. The reduction of yield safety.
5. The reduction in the flexural rigidity of the interior strips, resulting in larger deflections.

5.4.6 Recommendations

The following recommendations are proposed for the design of two-way irregular joist floors subjected to a single concentrated load, based on the results of this investigation:

1. A trial-and-error limit design procedure can be used in the design practice, for example, as the one presented in Chapter 2.
2. The deflection calculations should be based on cracked, transformed concrete sections.
3. The estimation of collapse load can be based on the first stage grid collapse mechanism ignoring the enhancement of the in-plane action.
4. The precentage of reinforcement transfer from the middle to the edge strips or supporting zones, should be limited to assure satisfactory serviceability and

to avoid local failures. The allowable percentage established at 20% in this investigation may be verified in the design process by checking the load factors and deflections.

5. The tentative minimum values for the various limit design criterion, proposed by Cohn in his draft code provisions for continuous beams or equivalent structures, may be used in the proposed trial-and-error limit design procedure, until further studies justify a change.

5.4.7 Further Research

The equilibrium methods of limit design allow the control of serviceability and of the elastic moment redistribution, through the yield safety parameters (x_j) and the corresponding yield load factors (λ_{ij}). The maximum acceptable values of these parameters have to be established experimentally for each class of structures. Some draft code provisions have been suggested by Cohn for continuous beams and one-storey frames. Similar provisions can be developed for certain regular and irregular grid-type structures, based on suitable testing programs.

By establishing realistic load factors, a direct limit equilibrium design procedure may be acceptable for some standard forms of grid-type structures. On the other hand, if a trial-and-error procedure, which may be laborious at times, is to be further developed, a computer program may be written on the basis of the flowchart given in Chapter 2 to allow some automation in the design process.

In the present study, the dead load has been disregarded having relatively small influence, compared to the effect of the concentrated live load. The combined effects of uniformly distributed and concentrated load have to be further studied.

The present series of experiments showed that unless a local failure occurs, the general collapse load is always higher than the specified ultimate load. This phenomenon of reserve strength due to membrane action in the top slab, which allows freedom in the rib arrangement and reinforcement distribution, should be further explored. For this purpose, suitable limit analysis techniques should be employed to count in a deterministic fashion this extra capacity of joist floors.

Also, more tests are needed for a precise evaluation of the effects and the importance of redistribution of reinforcement, from the distribution determined by elastic analysis, as in the case of reinforcement transfer between zones.

CHAPTER 6

SUMMARY AND CONCLUSIONS

CHAPTER 6

SUMMARY AND CONCLUSIONS

6.1 GENERAL OUTLINE OF THE INVESTIGATION

The study presented deals with the behavior and strength of reinforced concrete two-way irregular joist floors subjected to a single concentrated load at the center, and the subsequent development of an appropriate design methodology.

A classification of two-way ribbed floors and the definition of irregular joist floors is introduced. The discussion that follows establishes the usefulness of irregular joist floors and their range of applicability. Some principles for the selection of rib pattern is also discussed. The introduction of a new formwork system facilitating their construction is reported. The concept of an equivalent grid for the analysis of joist floor systems is presented, and the reinforcement distribution as the basic parameter in their structural performance is examined.

A review of previous studies includes developments on the elastic and limit analysis and design of regular two-way ribbed flat floor systems. The conclusion from the evaluation of this information was that these studies do not provide a complete treatment for the full elasto-plastic range, neither do they consider the case of a single concentrated load. The search for analytical solutions led to the following considerations:

1. For the elastic analysis of grillages, several computer programs are commercially available and can be used.

2. For the limit analysis of grillages, a variety of techniques and procedures presently available, can provide the necessary information for the cases of regular and irregular grid-type structures under different loading conditions.

3. The "equilibrium (serviceability)" methods of limit design for concrete frames appear to be the most appropriate of the available methods to be used as a basis for the development of a trial-and-error limit design procedure for the proportioning of grid-type structures. Such a procedure developed for the design of irregularly ribbed joist floors, is proposed in this study.

A series of models is studied analytically and experimentally, in order to verify the assumptions and procedures considered. The experimental program consists of the testing of four ribbed panels, which are 1/3-scale models of actual single-bay, square, four-corner supported, two-way irregular joist floors. The design of the test-panels was based on the total one-way static moment of an equivalent simply-supported beam under a specified ultimate load at the center. This moment was distributed between the ribs by assuming conventional distribution percentages, similar to the ones used in flat slabs (panel I_A) and redistribution in such a way that the total static moment in each direction remained the same. The panels were reinforced according to the resulting moment distribution. On the basis of the provided reinforcement and by using appropriate analytical techniques, the elastic and elasto-plastic behavior of the test-panels was derived analytically.

The test allowed the study of the elastic and elasto-plastic behavior of the test-panels, the evaluation of the various load capacity limits and the sequence and duration in the formation of the collapse mechanisms.

A limit design of the test-panels shows quantitatively the difference between the required and provided ultimate moment capacity in the ribs. The behavior of the test-panels is assessed by limit design criteria which are evaluated on the basis of the experimental load capacity limits. A parametric study on the influence of reinforcement transfer between strips on the ultimate load capacity of the equivalent models is made to provide the background for the assessment of the collapse behavior of the test-panels.

6.2 GENERAL CONCLUSIONS CONCERNING TWO-WAY IRREGULAR JOIST FLOORS

The following conclusions based on the study of single-bay ribbed panels are believed to be applicable to any type of two-way irregular joist floor system under any type of transverse loading. These conclusions are also proposed to be used as basic design guidelines, in dealing with two-way irregular joist floors.

1. The concept of equivalent grid of T-beams can be used for the analysis and design of two-way joist floors.

2. Elastic analysis of the equivalent grid with rigidities based on cracked-transformed sections, gives a good approximation of the behavior of two-way joist floors in the elastic range.

3. Plastic analysis allows an accurate prediction of the mode of failure and a close estimation of the assumed failure load (first-stage grid collapse load) on the basis of geometry and ultimate moment capacity of ribs, whereas the in-plane membrane action of the top slab conservatively can be neglected.

4. Two-way joist floors with a reasonably dense rib pattern, sufficient to assure an acceptable two-way action, can be designed on the basis of the elastic analysis of

the equivalent grid with rigidities those of gross concrete sections, and of the ultimate strength design method for the proportioning of ribs. The calculated reinforcement may then be distributed between ribs with some flexibility, but excessive redistribution should be avoided.

5. A limit design procedure offers a rational estimation of the factors of safety, and it may result in a more economic design. The trial-and-error limit design procedure proposed in this study seems to be suitable for a conceptual design of irregular joist floors.

6. A design based on the elastic analysis will give the best elastic performance and the highest factors of safety.

7. A limited reinforcement transfer from the middle to the edge strips or supporting zones, may result in proportional reduction of elastic performance and factors of safety. The maximum suggested percentage of such reinforcement transfer, taking an average for the two directions, should not exceed 20%. However, further studies are recommended in order to establish the extent of allowable reinforcement transfer between strips.

REFERENCES

REFERENCES

[1] Zielinski, Z.A. and Nicolopoulos, A., "Development and Application of Shell Type Plastic Forms for Concrete Construction," Proceedings of the IASS Symposium on Wood, Ferrocement and Plastics in Shells and Spatial Structures, Oulu, Finland, (June 1980), pp. 543-556.

[2] Lightfoot, E. and Sawko, F., "The Analysis of Grid Frameworks and Floor Systems by the Electronic Computer," The Structural Engineer, Vol.38, No.3, (March 1960), pp. 79-87.

[3] Ray, K.C. "Analysis of Grid Floors," Indian Concrete Journal, Vol.34, No.6, (June 1960), pp. 227-232.

[4] Mase, P.T. and Jain, L.K., "Analysis of Building Grid Floors," Journal Institution of Engineers (India), Civil Engineering Division, Vol.50, No.7, PT C14, (March 1970), pp. 184-187.

[5] Harris, P.J., "The Analysis of Rectangular Grillages," Engineering Journal (Canada), Vol.55, No.9, (Sept. 1972), EIC Trans. I-VII.

[6] Reiss, M., Socal, J., "Design of Ribbed Flat Slabs," The Structural Engineer, Vol.50, No.8, (August 1972), pp. 303-307.

[7] Goldberg, M., Tatsa, E.Z., and Levy, M., "Behavior of Anisotropic Skew Ribbed Slabs," Israel Journal of Technology, Vol.15, No.6, (1977), pp. 340-350.

[8] Gilardi, J., "Calcul automatique des planchers à nervures croisées sous charges uniformement reparties," Annales de l'Institut Technique du Batiment et des Travaux Publics, Vol.31, No.365, (October 1978), pp. 107-116.

[9] Tebbett, I.E., and Harrop, J., "Analytical Design of Ribbed Flat Slabs," The Structural Engineer, Vol. 57A, No.7, (July 1979), pp. 223-230.

[10] Kennedy, J.B., and Bali, S.K., "Rigidities of Concrete Waffle-Type Slab Structures," Canadian Journal of Civil Engineering, Vol.6, No.1, (March 1979), pp. 65-74.

[11] Moreira da Rocha, A., "Le dimensionnement idéal des ponts en grille de béton armé," Proceedings, 7th Congress International Association for Bridge and Structural Engineering, Rio de Janeiro, Brazil, Preliminary Publication, Vol.1, (1964), pp. 221-230.

[12] Das, M., "Design of Reinforced Concrete Grid Floors by Collapse-Load Method," Journal Institution of Engineers (India), Vol.46, Part Cl, No.11, (July 1966), pp. 557-568.

[13] Petcu, V., "Plastic Design of Reinforced Concrete Grid Floors," Revue Roumaine des Sciences Techniques - Serie de Mecanique Appliquée, Vol.13, No.5, (1968), pp. 951-971.

[14] Pillai, S.U., and Lash, S.D., "Ultimate Strength of Reinforced Concrete Grid and Slab Bridges," First International Symposium on Concrete Bridge Design, SP-23, American Concrete Institute, Detroit, (1969), pp. 361-384.

[15] Heyman, J., "The Limit Design of a Transversely Loaded Square Grid," Journal of Applied Mechanics, American Society of Mechanical Engineers, Vol.19, No.2, (June 1952), pp. 153-158.

[16] Reddy, D.V., and Hendry, A.W., "Elasto-Plastic Analysis of an Interconnected Beam System," Publication of International Association for Bridge and Structural Engineering, Vol.20, (1960), pp. 299-318.

[17] Reddy, D.V. and Hendry, A.W., "A Moment Distribution Method for the Elasto-Plastic Analysis of Grid Frameworks," Civil Engineering and Public Works Review, Vol.56, No.661, (August 1961), pp. 1051-1054.

[18] Shaw, F.S. "Limit Analysis of Grid Frameworks," Journal of the Structural Division, ASCE, Vol.89, No.ST5, (October 1963), pp. 1-14.

[19] Sawko, F. "Analysis of Grillages in the Elasto-Plastic Range," Civil Engineering and Public Works Review, Vol.59, No.695 (June 1964), pp. 737-739 and No.696, (July 1964), pp. 866-869.

[20] Hongladaromp, T., Rossow, E.C. and Lee, S.L., "Analysis of Elastic-Plastic Grid Systems," Journal of the Engineering Mechanics Division, ASCE, Vol.94, No.EM1, (February 1968), pp. 241-269.

[21] Wah, T. "Elasto-Plastic Analysis of Uniform Grillages Under Lateral Load," Journal of Ship Research, (June 1969), pp. 103-110.

[22] Snonoda, K., and Kurata, M., "A Numerical Method for the Limit Analysis of Grillages, Girders and Plates," Proceedings of the Japan Society for Civil Engineering, No.182, (October 1970), pp. 93-114.

[23] Walsh, P.F. "Limit Analysis of Grids Including Torsion," Institution of Engineers, Australia, Civil Engineering Transactions, Vol. CE12,No.1, (April 1970), pp. 90-93.

[24] Askari, M.R. "Limit Analysis of Grid Frameworks, Excluding Torsional Effect," Annales de l'Institute Technique du Batiment et des Travaux Publics, Vol.29, No.337, (Mars 1976), pp. 86-91.

[25] Marsh, C. "Collapse of Point Supported Square Grillages," Journal of the Structural Division, ASCE, Vol.103, No.ST9, (September 1977), pp. 1703-1712.

[26] Grigorian, M. "Limit Design of Corner Supported, Regular Rectangular, Gridworks Under Uniform Loading," Proceeding of the Institution of Civil Engineers, Vol.55, No.286, (1973), pp.285-290.

[27] Grigorian, M. "Limit Analysis of Simply-Supported Grids Under Point Loading," Iranian Journal of Science and Technology," Vol.6, No.1, Pergamon Press (1977), pp. 39-43.

[28] Massonnet, C., and Save, M. "Dimensionnement limite des grillages de poutres," Construction Metallique, Vol.17, No.2, (June 1980), pp. 11-14.

[29] ACI-ASCE Committee 428."Progress Report on Code Clauses for "Limit Design"", Journal of the American Concrete Institute, Vol.65, No.9, (September 1968), pp. 713-719.

[30] Cohn, M.Z. "Equilibrium (Serviceability) Methods of Limit Design for Concrete Frames," Proceedings of the Institution of Civil Engineers, Paper 7514 S, Supplement XIV, (1972), pp. 263-275.

[31] Cohn, M.Z. "Inelasticity of Reinforced Concrete and Structural Standards," Journal of the Structural Division, ASCE, Vol.105, No.ST11, (November 1979), pp. 2221-2241.

[32] Hayes, B. "Allowing for Membrane Action in the Plastic Analysis of Rectangular Reinforced Concrete Slabs," Magazine of Concrete Research, Vol.20, No.65, (December 1968), pp. 205-212.

[33] Datta, T.K., and Ramesh, C.K. "Some Experimental Studies on a Reinforced Concrete Slab-Beam System, Magazine of Concrete Research, Vol.27, No.91, (June 1975), pp. 111-120.

APPENDIX A

TYPICAL ELASTIC ANALYSIS OF GRILLAGES

APPENDIX A

TYPICAL ELASTIC ANALYSIS OF GRILLAGES

ANALYSIS OF A SQUARE, CORNER-SUPPORTED WAFFLE PANEL USING THE "STRESS" COMPUTER PROGRAM

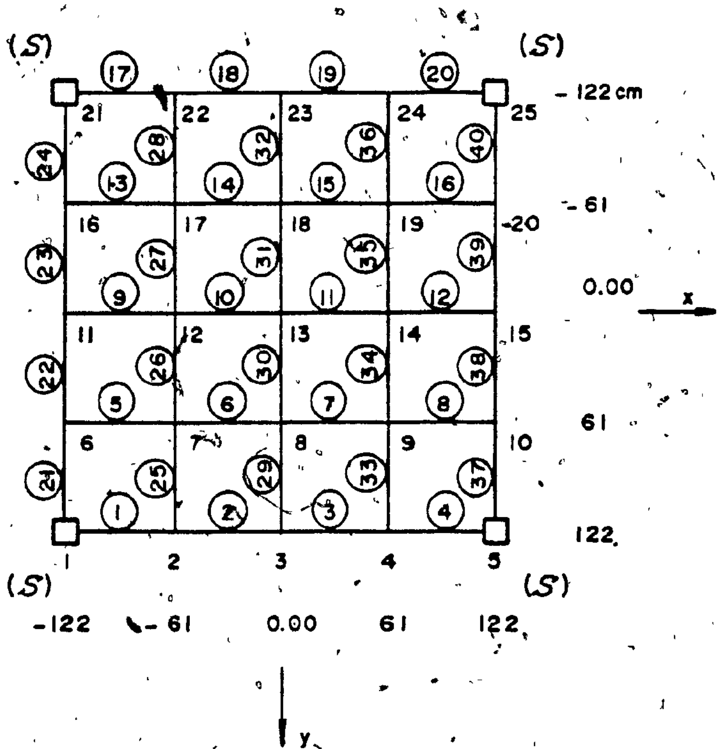

ANALYTICAL MODEL*

UNITS		MEMBER PROPERTIES	MODULUS OF ELASTICITY
LENGTH:	cm	IY = MOMENT OF INERTIA	$E_c = 2,800\ kN/cm^2$
FORCE:	kN	IX = TORSIONAL CONSTANT	

* NOTE: The same analytical model was used for the analysis of all test-panels by varying the member properties.

COMPUTER OUTPUT - DATA ECHO AND RESULTS

```
PROGRAMME S T R E S S
=====================================================================

STRUCTURE WAFFLE FLOOR PANEL
*
TYPE PLANE GRID
NUMBER OF JOINTS 25
NUMBER OF MEMBER 40
NUMBER OF SUPPORTS 4
NUMBER OF LOADING 1
* UNITS: CM,KN.
JOINT COORD
1 -122. 122. S
2 -61. 122.
3 0. 122.
4 61. 122.
5 122. 122. S
6 -122. 61.
7 -61. 61.
8 0. 61.
9 61. 61.
10 122. 61.
11 -122. 0.
12 -61. 0.
13 0. 0.
14 61. 0.
15 122. 0.
16 -122. -61.
17 -61. -61.
18 0. -61.
19 61. -61.
20 122. -61.
21 -122. -122. S
22 -61. -122.
23 0. -122.
24 61. -122.
25 122. -122. S
MEMBER INCIDENCES
1 1 2
2 2 3
3 3 4
4 4 5
5 6 7
6 7 8
7 8 9
8 9 10
9 11 12
10 12 13
11 13 14
12 14 15
13 16 17
14 17 18
15 18 19
16 19 20
17 21 22
18 22 23
19 23 24
20 24 25
21 1 6
```

```
22 6 11
23 11 16
24 16 21
25 2 7
26 7 12
27 12 17
28 17 22
29 3 8
30 8 13
31 13 18
32 18 23
33 4 9
34 9 14
35 14 19
36 19 24
37 5 10
38 10 15
39 15 20
40 20 25
JOINT RELEASES
1 MOMENT X Y
5 MOMENT X Y
21 MOMENT X Y
25 MOMENT X Y
MEMB PROP PRIS IX 10000.
1 THRU 4 IY 8339.
5 THRU 8 IY 10557.
9 THRU 12 IY 10557.
13 THRU 16 IY 10557.
17 THRU 20 IY 8339.
21 THRU 24 IY 8339.
25 THRU 28 IY 10557.
29 THRU 32 IY 10557.
33 THRU 36 IY 10557.
37 THRU 40 IY 8339.
CONSTANT E 2800. ALL
TABULATE ALL
LOADING 1
JOINT LOAD
13 FORCE Z 1.
SOLVE
```

INFERÍEURE

STRUCTURE WAFFLE FLOOR PANEL

LOADING 1

MEMBER FORCES

MEMBER	JOINT	SHEAR FORCE	TORSION MOMENT	BENDING MOMENT
1	1	-0.125	-0.479	0.48
1	2	0.125	0.479	7.15
2	2	-0.029	-0.120	-7.02
2	3	0.029	0.120	8.78
3	3	0.029	0.120	-8.78
3	4	-0.029	-0.120	7.02
4	4	0.125	0.479	-7.15
4	5	-0.125	-0.479	-0.48
5	6	-0.096	-0.128	-0.36
5	7	0.096	0.128	6.23
6	7	-0.096	0.371	-6.73
6	8	0.096	-0.371	12.59
7	8	0.096	-0.371	-12.59
7	9	-0.096	0.371	6.73
8	9	0.096	0.128	-6.23
8	10	-0.096	-0.128	0.36
9	11	-0.058	0.000	-0.24
9	12	0.058	0.000	3.75
10	12	-0.250	0.000	-3.01
10	13	0.250	0.000	18.26
11	13	0.250	0.000	-18.26
11	14	-0.250	0.000	3.01
12	14	0.058	0.000	-3.75
12	15	-0.058	0.000	0.24
13	16	-0.096	0.128	-0.36
13	17	0.096	-0.128	6.23
14	17	-0.096	-0.371	-6.73
14	18	0.096	0.371	12.59
15	18	0.096	0.371	-12.59
15	19	-0.096	-0.371	6.73
16	19	0.096	-0.128	-6.23
16	20	-0.096	0.128	0.36
17	21	-0.125	0.479	0.48
17	22	0.125	-0.479	7.15
18	22	-0.029	0.120	-7.02
18	23	0.029	-0.120	8.78
19	23	0.029	-0.120	-8.78
19	24	-0.029	0.120	7.02
20	24	0.125	-0.479	-7.15
20	25	-0.125	-0.479	-0.48
21	1	-0.125	0.479	0.48
21	6	0.125	-0.479	7.15
22	6	-0.029	0.120	-7.02
22	11	0.029	-0.120	8.78

23	11	0.029	-0.120	-8.78
23	16	-0.029	0.120	7.02
24	16	0.125	-0.479	-7.15
24	21	-0.125	0.479	-0.48
25	2	-0.096	0.128	-0.36
25	7	0.096	-0.128	6.23
26	7	-0.096	-0.371	-6.73
26	12	0.096	0.371	12.59
27	12	0.096	0.371	-12.59
27	17	-0.096	-0.371	6.73
28	17	0.096	-0.128	-6.23
28	22	-0.096	0.128	0.36
29	3	-0.058	0.000	-0.24
29	8	0.058	0.000	3.75
30	8	-0.250	0.000	-3.01
30	13	-0.250	0.000	18.26
31	13	0.250	0.000	-18.26
31	18	-0.250	0.000	3.01
32	18	0.058	0.000	-3.75
32	23	-0.058	0.000	0.24
33	4	-0.096	-0.128	-0.36
33	9	0.096	0.128	6.23
34	9	-0.096	0.371	-6.73
34	14	0.096	-0.371	12.59
35	14	0.096	-0.371	-12.59
35	19	-0.096	0.371	6.73
36	19	0.096	0.128	-6.23
36	24	-0.096	-0.128	0.36
37	5	-0.125	-0.479	0.48
37	10	0.125	0.479	7.15
38	10	-0.029	-0.120	-7.02
38	15	0.029	0.120	8.78
39	15	0.029	0.120	-8.78
39	20	-0.029	-0.120	7.02
40	20	0.125	0.479	-7.15
40	25	-0.125	-0.479	-0.48

APPLIED JOINT LOADS, FREE JOINTS

JOINT	FORCE Z	MOMENT X	MOMENT Y
2	0.000	0.000	-0.00
3	0.000	0.000	0.00
4	0.000	0.000	0.00
6	0.000	0.000	0.00
7	0.000	0.000	0.00
8	0.000	0.000	0.00
9	0.000	0.000	0.00
10	0.000	0.000	0.00
11	0.000	0.000	0.00
12	0.000	0.000	0.00
13	1.000	0.000	0.00
14	0.000	0.000	0.00
15	0.000	0.000	0.00
16	0.000	0.000	0.00
17	0.000	0.000	0.00
18	0.000	0.000	0.00
19	0.000	0.000	0.00
20	0.000	0.000	0.00
22	0.000	0.000	0.00
23	0.000	0.000	0.00
24	0.000	0.000	0.00

REACTIONS,APPLIED LOADS SUPPORT JOINTS

JOINT	FORCE Z	MOMENT X	MOMENT Y
1	-0.250	0.000	0.00
5	-0.250	0.000	0.00
21	-0.250	0.000	0.00
25	-0.250	0.000	0.00

FREE JOINT DISPLACEMENTS

JOINT	Z-DISPLACEMENT	X-ROTATION	Y-ROTATION
2	0.0016	0.0000	0.0000
3	0.0023	0.0000	0.0000
4	0.0016	0.0000	0.0000
6	0.0016	0.0000	0.0000
7	0.0031	0.0000	0.0000
8	0.0038	0.0000	0.0000
9	0.0031	0.0000	0.0000
10	0.0016	0.0000	0.0000
11	0.0023	0.0000	0.0000
12	0.0038	0.0000	0.0000
13	0.0046	0.0000	0.0000
14	0.0038	0.0000	0.0000
15	0.0023	0.0000	0.0000
16	0.0016	0.0000	0.0000
17	0.0031	0.0000	0.0000
18	0.0038	0.0000	0.0000
19	0.0031	0.0000	0.0000
20	0.0016	0.0000	0.0000
22	0.0016	0.0000	0.0000
23	0.0023	0.0000	0.0000
24	0.0016	0.0000	0.0000

SUPPORT JOINT DISPLACEMENTS

JOINT	Z-DISPLACEMENT	X-ROTATION	Y-ROTATION
1	0.0000	0.0000	0.0000
5	0.0000	0.0000	0.0000
21	0.0000	0.0000	0.0000
25	0.0000	0.0000	0.0000

APPENDIX B

LIMIT ANALYSIS OF THE TEST-PANELS

APPENDIX B

LIMIT ANALYSIS OF THE TEST-PANELS

PANEL I_A

A. CALCULATION OF THE UPPER BOUND COLLAPSE LOADS

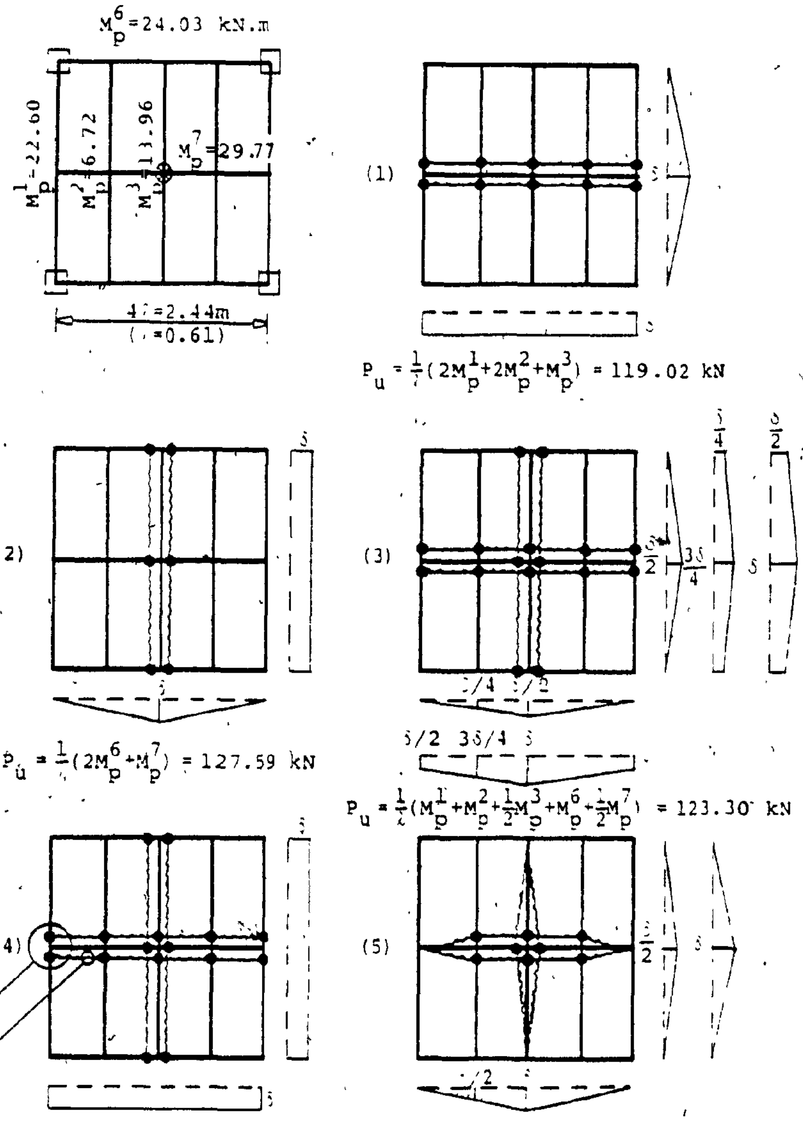

(1) $P_u = \frac{1}{\ell}(2M_p^1+2M_p^2+M_p^3) = 119.02$ kN

(2) $P_u = \frac{1}{\ell}(2M_p^6+M_p^7) = 127.59$ kN

(3) $P_u = \frac{1}{\ell}(M_p^1+M_p^2+\frac{1}{2}M_p^3+M_p^6+\frac{1}{2}M_p^7) = 123.30$ kN

(4) $P_u = \frac{1}{\ell}(2M_p^1+2M_p^2+M_p^3+2M_p^6+M_p^7) = 246.61$ kN

(5) $P_u = \frac{1}{\ell}(M_p^2+M_p^3+M_p^7) = \underline{\underline{82.70}}$ kN

The energy dissipated in the yield lines of the top slab is not taken into account.

The two dots shown at the position of flexural plastic hinges, represent certain lengths along the member of equal distance in both sides of the knot, over which inelastic curvatures occur.

The symmetry conditions require two hinges, but even replacing them by one does not affect the equations of plastic equilibrium.

B. CALCULATION OF THE LOWER BOUND COLLAPSE LOAD

(REF.: F.S. Shaw, Journal of Struct. Div.
ASCE, Oct. 1963)

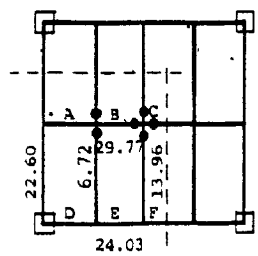

JOINT C:

$$\frac{2\times 13.96}{2\times 0.61} + \frac{2\times 29.77}{0.61} - \frac{2\times M_{BC}}{0.61} = 82.70$$

$$M_{BC} = \frac{13.96}{2} + 29.77 - 82.70 \times \frac{0.61}{2} = 11.53$$

JOINT B:

$$\frac{2\times M_{BE}}{2\times 0.61} + \frac{2\times 11.53}{0.61} - \frac{29.77}{0.61} = 0 \rightarrow M_{BE} = 29.77 - 2\times 11.53 = 6.71$$

JOINT A:

$$\frac{2\times M_{AD}}{2\times 0.61} - \frac{11.53}{0.61} = 0 \rightarrow M_{AD} = \underline{11.53 < 22.60} \quad \text{o.k.}$$

JOINT E:

$$\frac{2\times M_{EF}}{0.61} - \frac{6.72}{2\times 0.61} = 0 \rightarrow M_{EF} = \frac{6.72}{4} = 1.68$$

JOINT F:

$$\frac{2\times M_{FE}}{0.61} - \frac{13.96}{2\times 0.61} - \frac{2\times 1.68}{0.61} = 0 \rightarrow M_{FE} = \frac{13.96}{4} + 1.68 = \underline{5.17 < 24.03} \text{ o.k.}$$

∴ The statically admissible collapse mode is the No. (5).

JOINT C:

$$P_u = \frac{2\times 13.96}{2\times 0.61} + \frac{2\times 29.77}{0.61} - \frac{2\times 11.53}{0.61} = \underline{82.69} \text{ kN}$$

∴ The true collapse load is $P_u = 82.70$ kN.

PANEL I_B

A. CALCULATION OF THE UPPER BOUND COLLAPSE LOADS

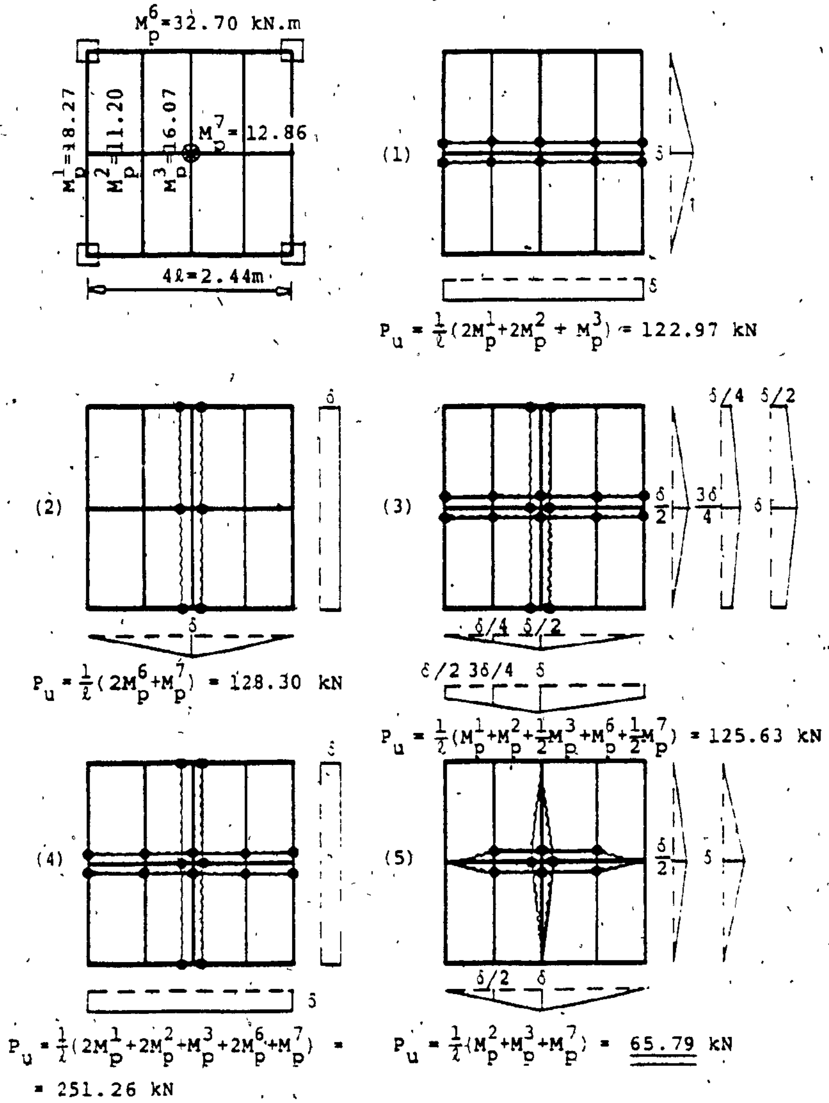

(6)

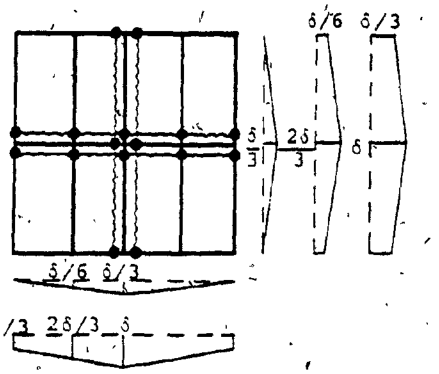

$$P_u = \frac{2}{3\ell}\left(M_p^1 + \frac{3}{2}M_p^2 + M_p^3 + M_p^6 + M_p^7\right) = 105.68 \text{ kN}$$

(7)

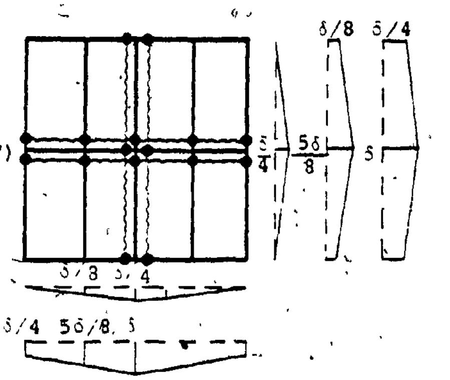

$$P_u = \frac{1}{\ell}\left(\frac{1}{2}M_p^1 + M_p^2 + \frac{3}{4}M_p^3 + \frac{1}{2}M_p^6 + \frac{3}{4}M_p^7\right) = 95.71 \text{ kN}$$

B. CALCULATION OF THE LOWER BOUND COLLAPSE LOAD

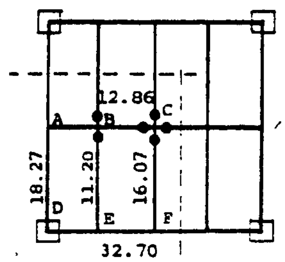

JOINT C:

$$\frac{2 \times 12.86}{0.61} + \frac{2 \times 16.07}{2 \times 0.61} - \frac{2M_{BC}}{0.61} = 65.79 \text{ kN}$$

$$M_{BC} = 12.86 + \frac{16.07}{2} - 65.79 \times \frac{0.61}{2} = 0.83$$

JOINT B:

$$\frac{2 \times M_{BE}}{2 \times 0.61} + \frac{2 \times 0.83}{0.61} - \frac{12.86}{0.61} = 0 \rightarrow M_{BE} =$$

$$12.86 - 2 \times 0.83 = 11.20$$

JOINT A:

$$\frac{2 \times M_{AD}}{2 \times 0.61} - \frac{0.83}{0.61} = 0 \rightarrow M_{AD} = \underline{0.83 < 18.27} \quad \text{o.k.}$$

JOINT E:

$$\frac{2 \times M_{EF}}{0.61} - \frac{11.20}{2 \times 0.61} = 0 \rightarrow M_{EF} = \frac{11.20}{4} = 2.80$$

JOINT F:

$$\frac{2 \times M_{FE}}{0.61} - \frac{16.07}{2 \times 0.61} - \frac{2 \times 2.80}{0.61} = 0 \rightarrow M_{FE} = \frac{16.07}{4} + 2.80 = \underline{6.82 < 32.70} \quad \text{o.k.}$$

∴ The statically admissible collapse mode is the No. (5).

JOINT C:

$$P_u = \frac{2 \times 12.86}{0.61} + \frac{2 \times 16.07}{2 \times 0.61} - \frac{2 \times 0.83}{0.61} = \underline{\underline{65.79}}$$

∴ The true collapse load is $P_u = 65.79$ kN.

PANEL II

A. CALCULATION OF THE UPPER BOUND COLLAPSE LOADS

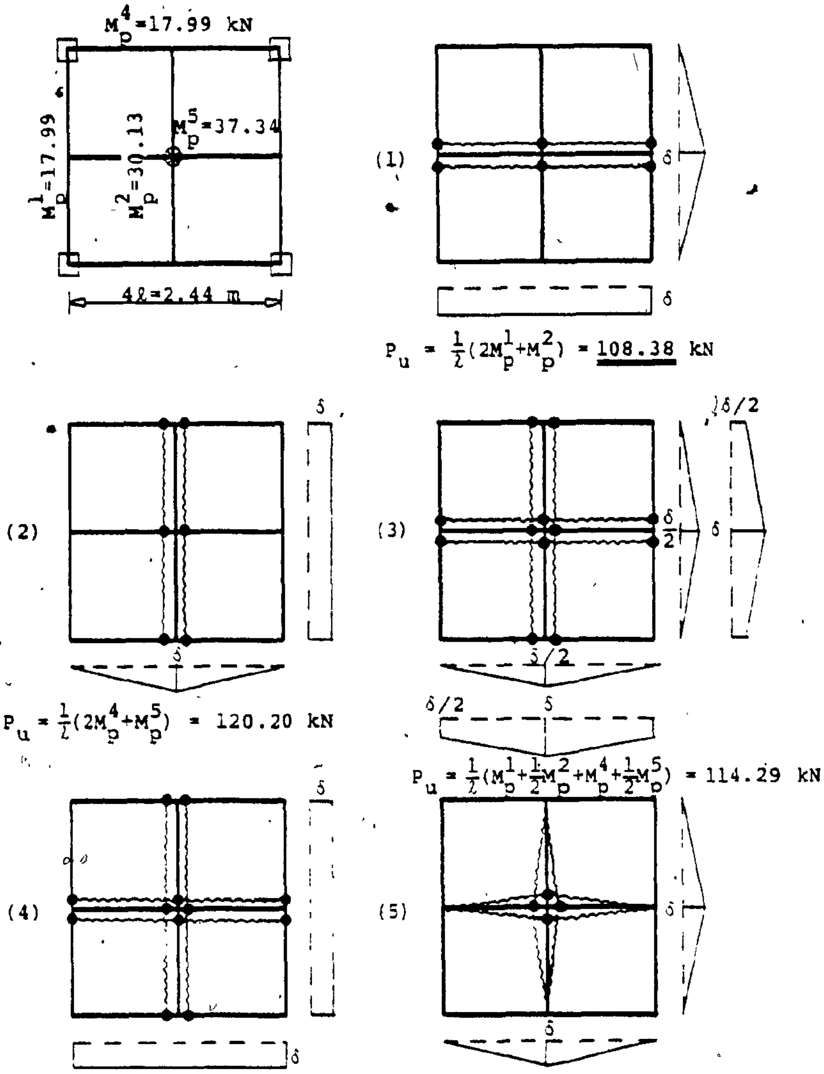

(1) $P_u = \frac{1}{\ell}(2M_p^1 + M_p^2) = \underline{108.38}$ kN

(2) $P_u = \frac{1}{\ell}(2M_p^4 + M_p^5) = 120.20$ kN

(3) $P_u = \frac{1}{\ell}(M_p^1 + \frac{1}{2}M_p^2 + M_p^4 + \frac{1}{2}M_p^5) = 114.29$ kN

(4) $P_u = \frac{1}{\ell}(2M_p^1 + M_p^2 + 2M_p^4 + M_p^5) = 228.57$ kN

(5) $P_u = \frac{1}{\ell}(M_p^2 + M_p^5) = 110.61$ kN

B. CALCULATION OF THE LOWER BOUND COLLAPSE LOAD

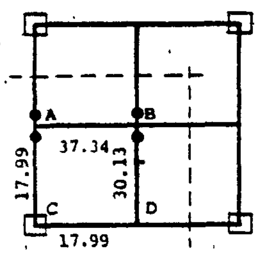

JOINT B:

$$\frac{2\times M_{BA}}{2\times 0.61} + \frac{2\times 30.13}{2\times 0.61} = 108.38 \rightarrow M_{BA} = 108.38\times 0.61 - 30.13 =$$

$$= \underline{35.98 < 37.34} \quad \text{o.k.}$$

JOINT A:

$$\frac{2\times M_{AC}}{2\times 0.61} - \frac{35.98}{2\times 0.61} = 0 \rightarrow M_{AC} = \frac{35.98}{2} = 17.99 \quad \text{o.k.}$$

JOINT D:

$$\frac{2\times M_{DC}}{2\times 0.61} - \frac{30.13}{2\times 0.61} = 0 \rightarrow M_{DC} = \frac{30.13}{2} = \underline{15.07 < 17.99} \quad \text{o.k.}$$

JOINT B:

$$P_u = \frac{2\times 35.98}{2\times 0.61} + \frac{2\times 30.13}{2\times 0.61} = \underline{\underline{108.39}} \quad \text{kN}$$

PANEL III

A. CALCULATION OF THE UPPER BOUND COLLAPSE LOADS

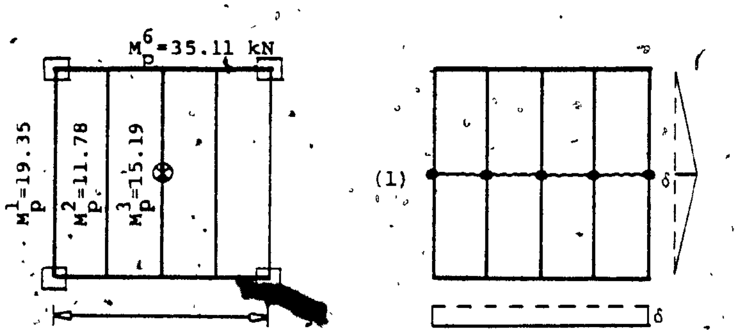

$P_u = \frac{1}{\ell}(2M_p^1+2M_p^2+M_p^3) = 126.97$ kN

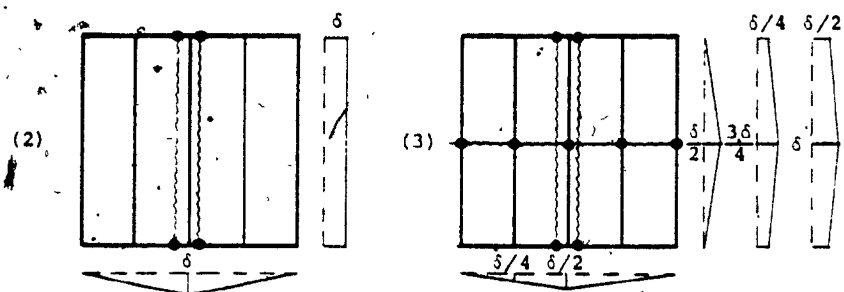

$P_u = \frac{1}{\ell}(2M_p^6) = 115.11$ kN $P_u = \frac{1}{\ell}(M_p^1+M_p^2+\frac{1}{2}M_p^3+M_p^6) = 121.04$ kN

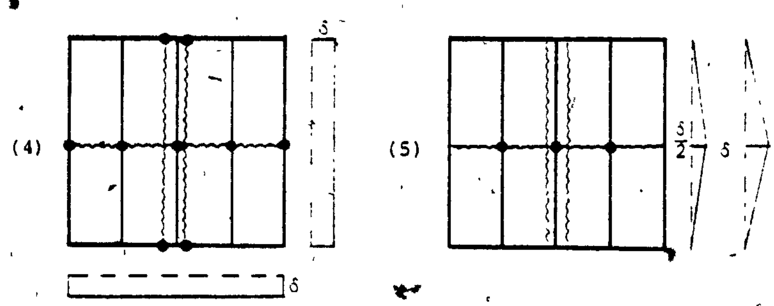

$P_u = \frac{1}{\ell}(2M_p^1+2M_p^2+M_p^3+2M_p^6) =$
$= 242.08$ kN

$P_u = \frac{1}{\ell}(M_p^2+M_p^3) = \underline{\underline{44.21}}$ kN

NFÉRIEURE

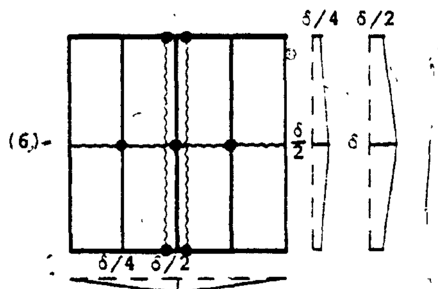

$$P_u = \frac{1}{\ell}\left(\frac{1}{2}M_p^2 + \frac{1}{2}M_p^3 + M_p^6\right) = 79.66 \quad kN$$

B. CALCULATION OF THE LOWER BOUND COLLAPSE LOAD

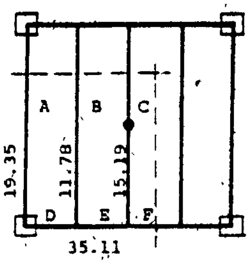

JOIST C:

$$\frac{2\times 15.19}{2\times 0.61} = P_u = \underline{\underline{24.90}} < 44.21$$

JOIST F:

$$\frac{2\times M_{FE}}{0.61} - \frac{15.19}{2\times 0.61} = 0 \rightarrow M_{FE} = \frac{15.19}{4} =$$

$$= \underline{3.80 < 35.11}$$

∴ The collapse load is assumed to be the average of the upper and the lower bound collapse load:

$$P_u = \frac{44.21+24.90}{2} = \underline{\underline{34.56}}\ \text{kN}$$

APPENDIX C

LIMIT DESIGN OF THE EQUIVALENT MODELS

APPENDIX C

LIMIT DESIGN OF THE EQUIVALENT MODELS

A. "EQUILIBRIUM (SERVICEABILITY)" METHOD OF LIMIT DESIGN (REF.: M.Z. Cohn, I.C.E. Proceedings, Supl. XIV-7514S, 1972).

DESIGN CRITERIA:

1. Design Service Load

$$W = 70 \text{ kN}$$

2. Overall Load Factor

$$\lambda_o = 1.7$$

(Ultimate Load: $W_u = \lambda_o W = 1.7 \times 70 = 119$ kN)

3. First Yield Load Factor

$$\lambda_1 = 1.2 \quad \text{(for good serviceability)}$$

4. Yield Safety Parameters (scale factors)

$$\min x_j = \lambda_1 / \lambda_o = 1.2/1.7 = 0.70$$

$$\therefore \quad 1.0 \geq x_j \geq 0.70$$ (It can be larger than 1.0 for grillages)

5. Net Reinforcement Index:

$$q = \frac{A_s}{b\ d} \frac{f_y}{f'_c} \leq 0.3$$

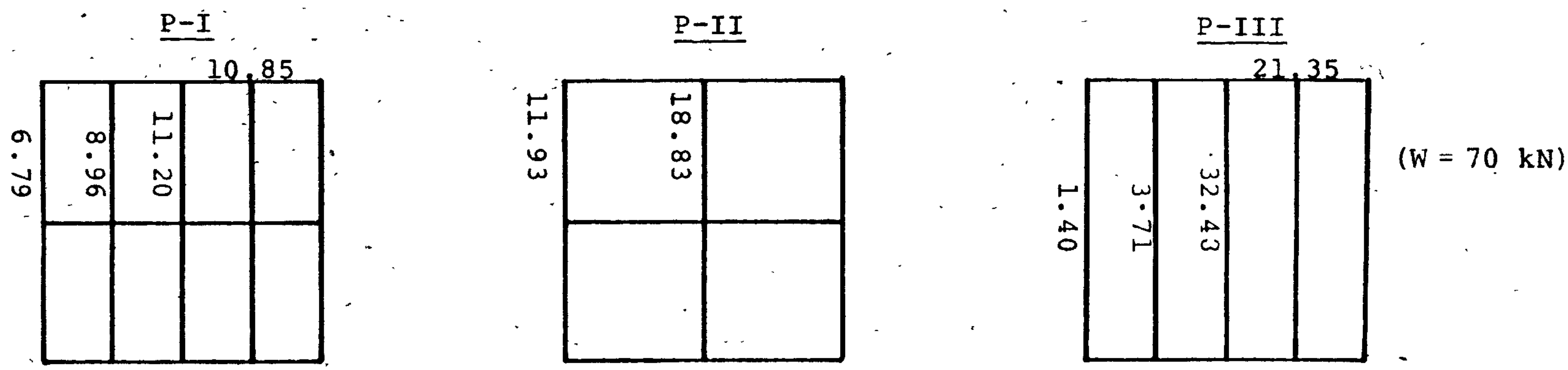

($\Sigma M_x = \Sigma M_y = 0.61 \times 70 = 42.7$ kN.m)

ELASTIC MOMENTS DUE TO DESIGN SERVICE LOAD (M_j)   (FROM FIG. 3.9)

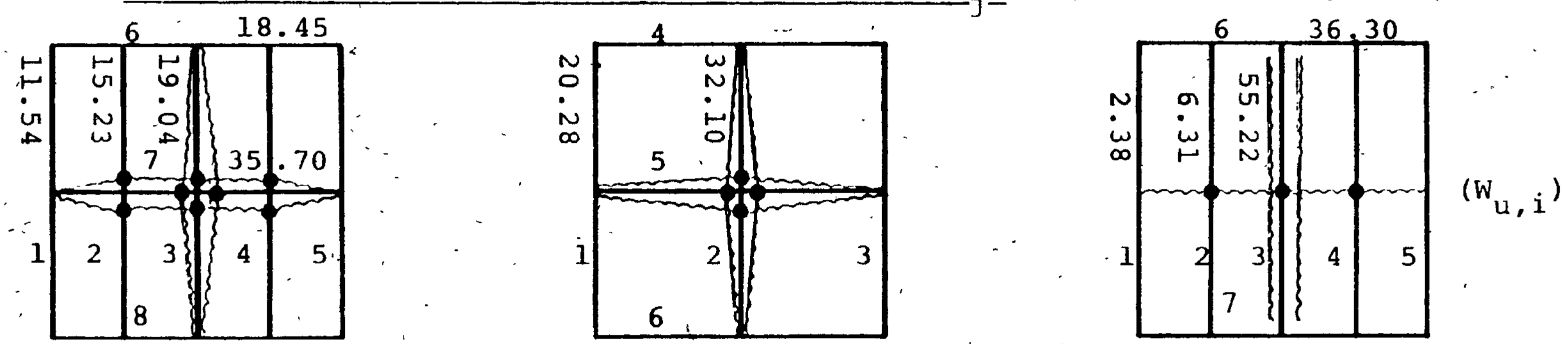

$W_{u,i} = \frac{1}{\ell}(M_p^2+M_p^3+M_p^7)$ $W_{u,i} = \frac{1}{\ell}(M_p^2+M_p^5)$ $W_{u,i} = \frac{1}{\ell}(M_p^2+M_p^3)$

FACTORED ELASTIC MOMENTS ($\overline{M}_j = \lambda_o M_j$)

LIMIT EQUILIBRIUM EQUATIONS

(Corresponding to the collapse mechanisms shown, which are assumed to take place under the specified ultimate load).

PANEL I

$$15.23\,x^2 + 19.04\,x^3 + 35.70\,x^7 = 119 \times 0.61 = 72.59$$

PANEL II

$$32.01(x^2+x^5) = 72.59$$

PANEL III

$$6.31\,x^2 + 55.22\,x^3 = 72.59$$

BALANCED YIELD SAFETY PARAMETER

$\bar{x}_i = x^2 = x^3 = x^7 = 1.04$ $\bar{x}_i = x^2 = x^5 = 1.13$ $\bar{x}_i = x^2 = x^3 = 1.18$

SCALE FACTORS

$x_j = \bar{x}_i = 1.04$ $x_j = 1.13$ $x_j = 1.18$

(**NOTE**: The above considered collapse mechanisms give the largest scale factor).

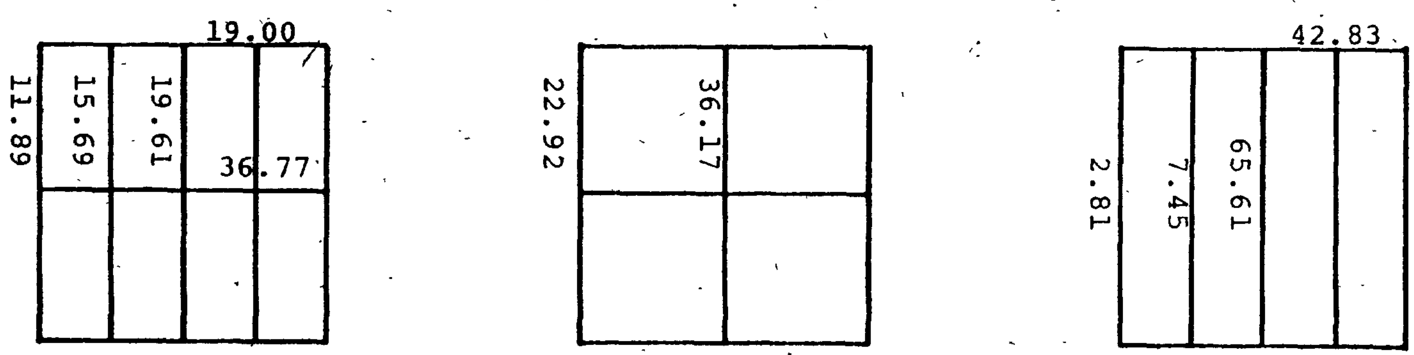

($W_u = 119$ kN)

DESIGN PLASTIC MOMENTS ($M_{pj} = x_j\,\bar{M}_j$)

APPENDIX D

LIMIT DESIGN OF THE TEST-PANEL I_A

APPENDIX D

LIMIT DESIGN OF THE TEST-PANEL I_A

PROPOSED TRIAL-AND-ERROR LIMIT DESIGN PROCEDURE

DATA: $W = 70$ kN, $J^g = 10{,}000$ cm^4, $h = 171.5$ mm, $d_{av} = 140$ mm

$f'_c = 34.5$ MPa, $E_c = 28{,}000$ MPa $= 2{,}800$ kN/cm^2

$f_y = 414$ MPa, $E_s = 200{,}000$ MPa

$\lambda_1 = 1.2$, $\lambda_o = 1.7$, min $x_j^{all} = 0.70$

$\delta^{all} = L/360 = 2440/360 = 6.78$ mm

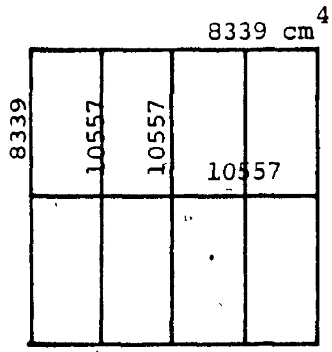

(I^g) - (FROM APP.A)

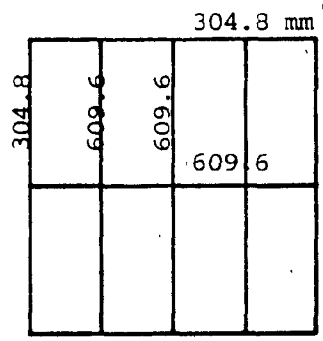

(b) - (FROM TABLE 3.2)

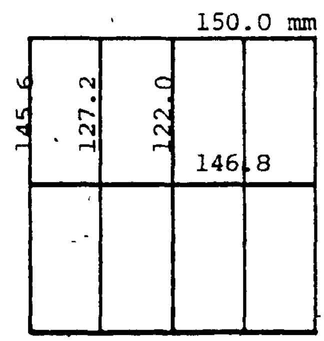

(d) - (FROM TABLE 3.2)

DESIGN PROCEDURE

$\lambda_o^g = \lambda_o = 1.7, W_u^g = \lambda_o . W = 1.7 \times 70 = 119$ kN, $M_{o,u} = 119 \times 0.61 = 72.59$ kN.m

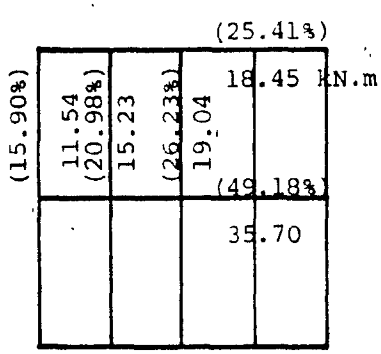

(M_{pj}^g) - (FROM FIG.3.8)

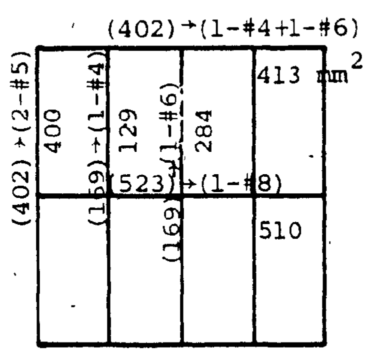

(A_s) - (FROM TABLE 3.2)

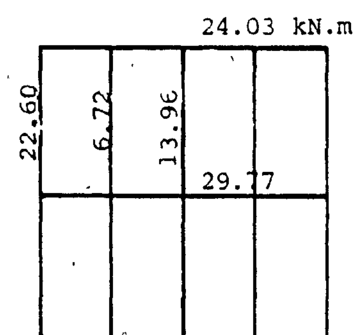

($M_{pj}^{cr} = M_u$) - (FROM TABLE 3.2)

$M_{o,w} = 70 \times 0.61 = 42.7$ kN.m

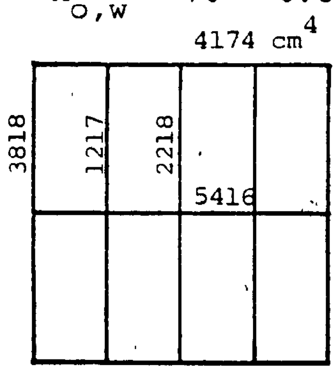

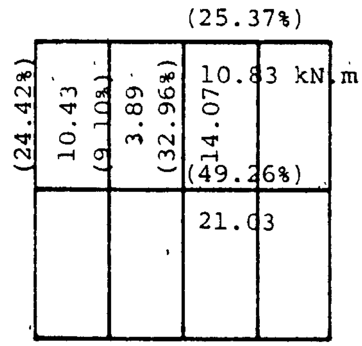

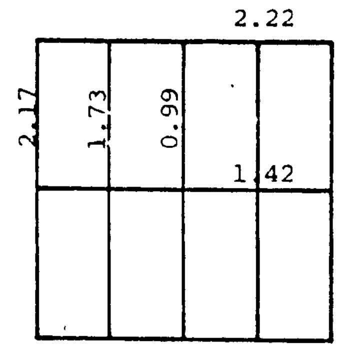

(I^{cr}) - (FROM TABLE 3.2) (M_j^{cr})-(FROM FIG.3.9) $(\lambda_{1j}^{cr} = M_{pj}^{cr}/M_j^{cr})$

$\lambda_1^{cr} = \min \lambda_{1j}^{cr} = 0.99 < \lambda_1 = 1.2$ (NOT ACCEPTABLE)

Assuming that the first yield load factor is acceptable the design procedure is allowed to continue for the purpose of demonstration.

$W_u^{cr} = \min W_{u,i}^{cr} = 87.70$ kN (FROM APPENDIX B)

$\lambda_o^{cr} = W_u^{cr}/W = 87.70/70 = 1.25 < 1.7$ (NOT ACCEPTABLE)

$x_i^{cr} = \lambda_1^{cr}/\lambda_o^{cr} = 0.99/1.25 = 0.79 > 0.70$ O.K.

$\delta^{cr} \simeq 11.0$ mm (FROM FIG. 4.1) $> \delta^{all} = 6.78$ (NOT ACCEPTABLE)

etc.

FIRST ITERATION

$\lambda_o^g = \lambda_o^g + 0.05 = 1.70 + 0.05 = 1.75$

$W_u^g = 1.75 \times 70 = 122.5$ kN

$M_{o,u} = 122.5 \times 0.61 = 74.73$ kN.m

etc.

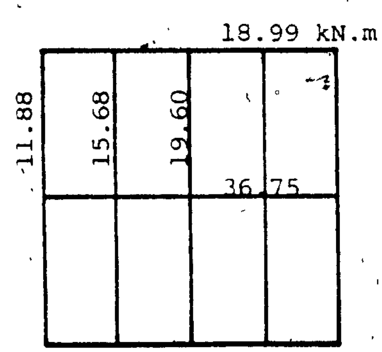

(M_{pj}^g)

APPENDIX E

PARAMETRIC STUDY OF THE EQUIVALENT MODELS

APPENDIX E

PARAMETRIC STUDY OF THE EQUIVALENT MODELS

SERIES I

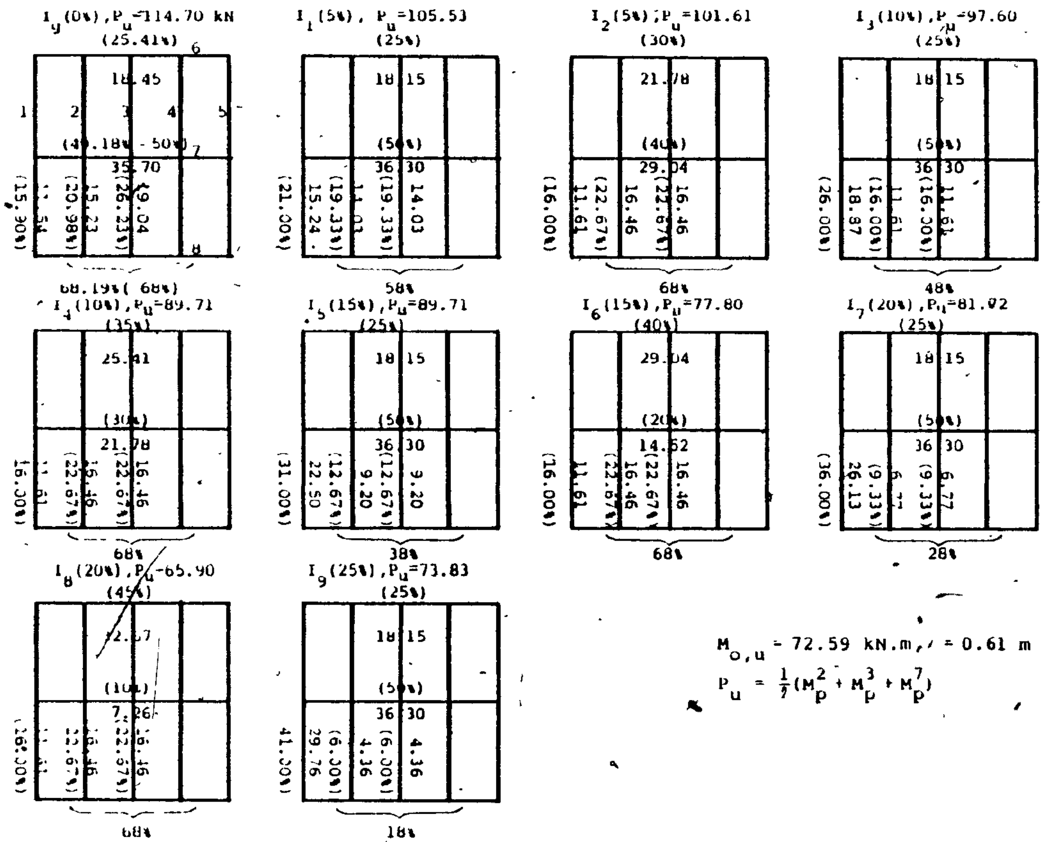

$M_{o,u}$ = 72.59 kN.m, ℓ = 0.61 m

$P_u = \frac{1}{\ell}(M_p^2 + M_p^3 + M_p^7)$

SERIES II

$II_0(0\%)$, $P_u=104.95$ kN

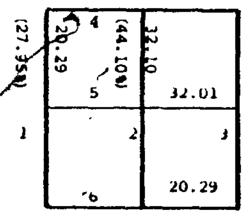

$II_1(5\%)$, $P_u=93.05$ kN

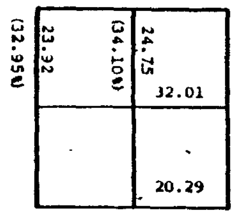

$II_2(10\%)$, $P_u=81.15$ kN

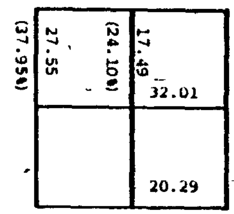

$II_3(15\%)$, $P_u=69.26$ kN

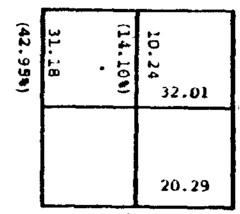

$II_4(20\%)$, $P_u=57.36$ kN

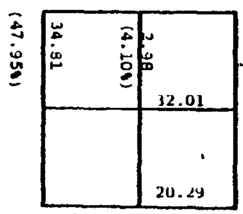

$M_{o,u} = 72.59$ kN.m, $\ell = 0.61$ m

$P_u = \frac{1}{\ell}(M_p^2+M_p^5)$

SERIES III

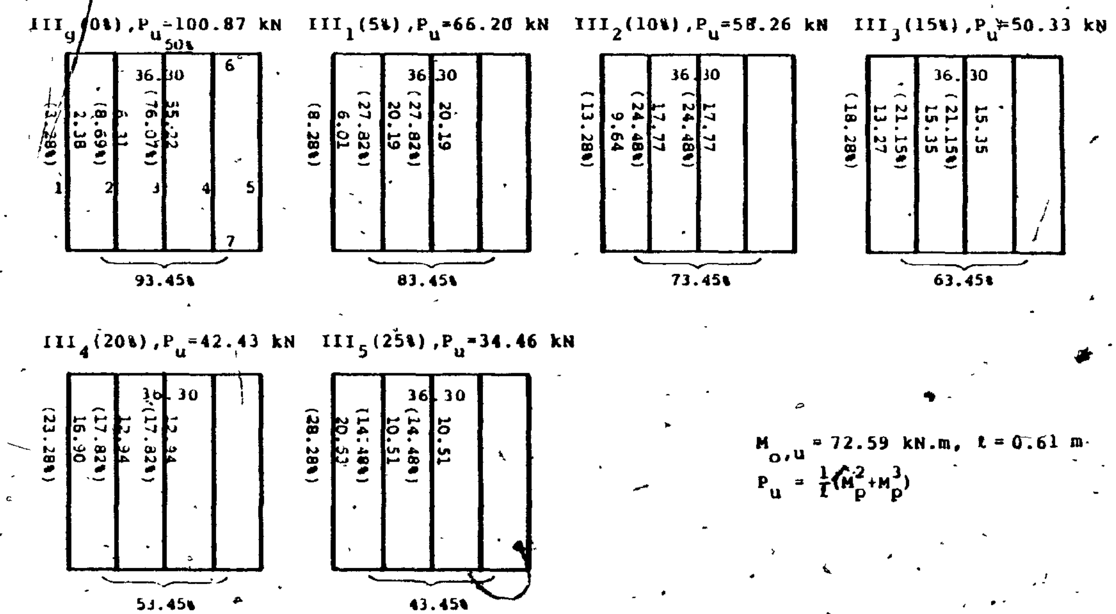

$M_{o,u} = 72.59$ kN.m, $\ell = 0.61$ m

$P_u = \frac{1}{\ell}(M_p^2 + M_p^3)$